Development of Thermal Model of Three Phase Induction Motor of a given frame

A

Thesis

By

Pravin Kumar

Registration No.: 154016 of 2020-21

Examination Roll No.: M4ELE22026B

submitted in partial fulfilment of the requirements for the award of the degree

MASTER OF ENGINEERING

in Electrical Engineering

(Specialization: *Electrical Machines*)

Under the guidance of

1. Prof. Suparna Kar Chowdhury
2. Prof. Arindam Kumar Sil
3. Prof. Dipten Maiti

DEPARTMENT OF ELECTRICAL ENGINEERING

FACULTY OF ENGINEERING AND TECHNOLOGY, JADAVPUR

JADAVPUR UNIVERSITY

KOLKATA-700 032

AUGUST 2022

CERTIFICATE

I/We hereby forward the thesis entitled "***Development of Thermal Model of Three Phase Induction Motor of a given frame***" submitted by **Pravin Kumar,** Examination Roll No. **M4ELE22026B**, Registration No. **154016 of 2020-21**, year 2020 under my/our guidance and supervision in partial fulfilment of the requirements for the award of the degree of **Master of Engineering in Electrical Engineering** (Specialization: **Electrical Machines**) from this department during the current academic session. To the best of my/our knowledge this work has not been submitted elsewhere for a degree.

……..

Prof. Suparna Kar Chowdhury
Professor
Department of Electrical Engineering
Jadavpur University
Kolkata, 700032

……

Prof. Arindam Kumar Sil
Professor
Department of Electrical Engineering
Jadavpur University
Kolkata, 700032

……

Prof. Dipten Maiti
Professor
Department of Electrical Engineering
Jadavpur University
Kolkata, 700032

……

Dean of Faculty Council of
Engineering and Technology
Jadavpur University
Kolkata, 700032

……

Prof. (Dr.) Saswati Mazumdar
Head of the Department of
Electrical Engineering
Jadavpur University
Kolkata, 700032

DECLARATION BY THE CANDIDATE

I certify that to the best of my knowledge

i) The work contained in the progress report is original and has been done by myself under the general supervision of my supervisors.

ii) I have conformed to the norms and guidelines given in the Ethical Code of Conduct of the University.

iii) Whenever I have used materials (data, theoretical analysis and text) from other sources, I have given due credit to them by citing them in the text of the report and giving their details in the references.

iv) Whenever I have quoted written materials from other sources, I have put them under quotation marks and given due credit to the sources by citing them and giving details in the references.

Date: Signature:

Place: Jadavpur, Kolkata (Pravin Kumar)

Registration No. - 154016 of 2020-21

Examination Roll No.- M4ELE22026B

CERTIFICATE OF APPROVAL

We recommend that the thesis entitled "***Development of Thermal Model of Three Phase Induction Motor of a given frame"*** submitted by **Pravin Kumar** bearing Examination Roll No. **M4ELE22026B** to the Department of Electrical Engineering, Faculty of Engineering and Technology, Jadavpur University, Kolkata-700 032 be accepted in partial fulfilment of the requirements for the degree of **Master of Engineering** in **Electrical Engineering** (Specialization: **Electrical Machines**) from this University after successfully defended the work by the candidate in the viva-voce examination.

Board of Examiners

1. _____ Signature with date of the examiner

Prof.

Department-

2._____ Signature with date of the supervisor

Prof. Suparna Kar Chowdhury

3._____ Signature with date of the co-supervisor (if applicable)

Prof. Arindam Kumar Sil

4._____ Signature with date of the co-supervisor (if applicable)

Prof. Dipten Maiti

ACKNOWLEDGEMENT

First and foremost, I am truly indebted and wish to express my gratitude to my supervisors Prof. Suparna Kar Chowdhury, Prof. Arindam Kimar Sil and Prof. Dipten Maiti for all of the inspiration, excellent guidance, continuing encouragement and unwavering confidence and support during every stage of this endeavour without which, it would not have been possible for me to complete this undertaking successfully. I also thank them for his insightful comments and suggestions which continually helped me to improve my understanding.

I express my deep gratitude to the Head of the Department of Electrical Engineering, Faculty of Engineering & Technology, Jadavpur University for providing all possible facilities towards this work. Thanks to all other faculty members in the department.

My whole hearted gratitude to my parents for their constant encouragement, love, wishes and support. Above all, I thank Almighty who bestowed his blessings upon us.

……..

Date: 2022 (Pravin Kumar)

Contents

List of Figures

Tables

List of Principal symbols & Abbreviation

V	Line voltage of motor
E_{ph}	Phase voltage of motor
ph	No. of phase
P_{in}	Input power of motor
f	frequency
P	No. of poles
B_{av}	Flux density or magnetic loading
ac	Ampere conductor or electrical loading
C_o	Output co-efficient
L_i	Net length of the core
D	Diameter of core
T_{ph}	Turns per phase
$T_{ph\ s}$	Turns per phase in stator
$S_{s\ ph}$	Stator slot per phase
S_s	Stator slot
K_{ws}	Stator winding factor
I_s or I_{ph}	Stator current per phase
A_s	Area of stator
w_{st}	Width of stator teeth
L_{m_T}	Length of mean turn
B_{st}	Flux density in stator teeth
A_{sc}	Area of stator core
d_{sc}	Depth of stator core
B_{sc}	Flux density in stator core
D_o	Outside diameter of stator lamination
d_{ss}	Depth of stator slot

L_g	Length of airgap
D_r	Diameter of rotor
y_{ss}	Stator slot pitch
y_{sr}	Rotor slot pitch
I_b	Rotor bar current
A_b	Area of rotor bar
R_b	Resistance of each bar
$P_{Cu\ b}$	Total Copper loss in bars
$I_{b\ e}$	End rings current
A_e	Area of end rings
$D_{o\ er}$	Outer diameter of end ring
$D_{i\ er}$	Inner diameter of end ring
R_e	Resistance of end ring
$P_{Cu\ er}$	Copper losses in end ring
$P_{Cu\ r}$	Total copper loss in rotor
$D_{i\ r}$	Inner diameter of rotor
K_{gss}	Gap concentration factor for stator slot
K_{gsr}	Gap concentration factor for rotor slot
A_g	Area of air gap
$L_{g\ effect}$	Effective length of air gap
mmf_g	Magneto motive force of air gap
A_{st}	Area of stator teeth per pole
mmf_{st}	Magneto motive force required for stator teeth
A_{sc}	Area of stator core
$L_{m\ s}$	Length of magnetic path through stator core
mmf_{sc}	Magneto motive force required for stator core
A_{rt}	Area of rotor teeth

B_{rt}	Flux density of rotor teeth
mmf_{rt}	Magneto motive force required for rotor teeth
A_{rc}	Rotor core area
$L_{m\ rc}$	Length of the flux path in rotor core
mmf_{rc}	Magneto motive force required for rotor core
I_m	Magnetising current per phase
W_{st}	Weight of stator teeth
$P_{iron\ st}$	Iron loss in stator teeth
W_{sc}	Weight of stator core
$P_{iron\ sc}$	Iron loss in stator core
$P_{iron\ total}$	Total iron loss
$P_{iron\ act}$	Total actual iron loss
F_{wl}	Frictional & windage loss
P_{nl}	No load losses
I_o	No load current
$I_{o\ ph}$	No load current per phase
pf	Power factor
η	efficiency
R_s	Resistance of stator winding
k_p	Pitch factor
k_d	Distribution factor

Abstract

Induction Motors are the most widely used motor in the industry as well as for domestic applications. To optimize energy consumption, the efficiency of the driving motor has to be maximized. The main challenges are to improve its efficiency and minimise the losses keeping the cost optimum. The maximum output obtainable from a frame size depends on the temperature rise of the motor. A large number of thermal sensors are required to measure the temperature of different parts of the motor. Inclusion of thermal sensors makes the system less rugged. So, researchers are working on development of thermal models which can estimate the temperature rise of different parts of the motor without a sensor. Thermal models can be broadly classified as:

- Lumped parameter thermal model
- Distributed parameter thermal model

Finite Element and Finite Difference methods have been used to develop distributed parameter thermal model. These models are accurate, but needs higher computation time and involve complex mathematics. On the other way the lumped parameter thermal models are simpler and easy to understand.

A lumped parameter thermal model has been developed in our laboratory to predict the temperature rises of a given Induction motor. The stator copper loss, rotor copper loss and iron loss are the input of the model and the temperature rise of different parts are the output. The detailed dimensional data are required to calculated the parameters of the thermal model. The detailed dimensional data are not available from the manufacturers. In this work we have tried to develop the parameter of the thermal model from the outer dimensions of the machine.

Chapter 1

1.1 Background

In the rotating electrical machines, electrical energy is converted to mechanical energy or vice versa due to the interaction between electrical field and magnetic field. For satisfactory performance of the machine low resistivity is necessary for electrical circuit materials and high permeability for magnetic circuit material. Electrical circuit and magnetic circuit are separated by insulation. The insulation material should have good thermal properties. Whenever the energy is transferred through air-gap, some energy is lost to supply the losses. The main losses in a rotating machine are:

- Copper loss in the conducting material
- Core loss in the magnetic material
- Windage and bearing friction loss.

These losses produce heat, which increases the temperature of the machine. The insulation performance depends on the temperature. The various undesired effects will be shown in machine due to increasing the thermal limits.

- Due to the oxidation, insulation particles accelerate which increases the dielectric loss.
- Lubrication of bearings and high viscosity reduce the oil film thickness.
- Mechanical stresses and change in geometry caused by thermal expansion of elements of machine.
- Excessive thermal heating increases thermal bending of rotor and consequently loss of eccentricity.

Estimation of temperature rise of different parts of an electrical machine is essential for estimating the performance of the machine and for condition monitoring of the machine. A large number of thermal sensors are required to measure the temperature of different parts of a machine. Inclusion of thermal sensors makes the system less rugged. So, researchers are working on development of thermal models which can estimate the temperature rise of different parts of the motor without a sensor. Thermal models can be broadly classified as:

- Lumped parameter thermal model
- Distributed parameter thermal model

Finite Element and Finite Difference methods have been used to develop distributed parameter thermal model. These models are accurate, but needs higher computation time and involve complex mathematics. On the other way the lumped parameter thermal models are simpler and easy to understand. The detailed dimensional data are required to calculated the parameters of any lumped parameter thermal model. The detailed dimensional data are not available from the manufacturers. In this work we have tried to develop the parameter of the thermal model from the outer dimensions of machine.

Classical Analytical method such as conformal mapping technique, variation, formulation, inverse method which is help to required special functions calculations. These processes are quite lengthy and require more time to solve a particular problem. The Classical Analytical methods problems are overcome by the help of numerical method. The numerical method is highly acceptable for performance calculations of large and medium rating induction machines.

The Thermal analysis of induction machine can be broadly mainly classified into two categories.

(i) Thermal Monitoring
(ii) Thermal Modelling

Thermal monitoring scheme is used for providing warning and predicting the fault at early stage. Thermal monitoring system collects information into the form of primary data then analyses the data by using the modern signal processing and analysis techniques.

Thermal model is useful for:

- designing of electrical machine,
- can be used for fault detection and
- for the correct parameter estimation.

Thermal model is mainly base on finite element method give conduction mode result in detail manner. But the convection and radiation result are quite difficult to estimate. The finite element method is applicable for solving transient or steady-state problems of particular machines parts with large temperature gradient. Problems arises from this method is applied for three dimensional and time dependent problems.

The lumped parameters model could be used for thermal failure of low and medium rated induction machine. By this method, we can easily design a machine with satisfactory life span with the slot peak or end winding temperature within the permissible thermal insulation class limit. To prevent from mechanical distortion, the temperature of the rotor must be within the limit. Therefore, it is necessary to distinguish the separate thermal model for stator and rotor components.

1.2 Literature Review

Kotnik[1] has studied the analogous thermal circuit for a non-ventilated induction motor. They have estimated temperature by lumped parameters thermal model. The thermal resistance of various motor sections has been estimated for estimating the average steady state temperature of the various motor components.

This work introduced the term "thermal generator" representing the source of watts loss

In his paper titled *"Lumped parameter thermal model for electrical machines of TEFC design"*[2], *Mellor* designed transient and steady state thermal model from design data of a three phase TEFC (Totally Enclosed Fan Cooled) induction motor. To account for the inadequate thermal contact, an additional thermal resistance is used to represent the gap between the frame and the rough stator laminations. Any radiation-related heat transfer is

ignored from the inside surfaces. In this model, symmetry is taken for the shaft and a radial plane running through the machine's centre.

A combined and distributed parameter thermal circuit has been developed by *Dr. S. Kar Cho wdhury, S. Chowdhury, S. P. Chowdhury, and S. K. Pal'*[3] using design parameters for the m achine.

For the purpose of determining the rotor resistance and losses, they use:

i)A lumped parameter Imp-Pl circuit.

ii) The estimation of the inductance parameters and core-loss was done using the finite element method.

iii) Thermal model combines distributed and lumped parameters to estimate the motor's temperature rise.

Here are the sources of heat within induction motor are following:

>Copper loss in the main and auxiliary windings,

> Tooth flux pulsation losses,

> Iron loss in the core and teeth of the stator,

>windage and bearing friction losses etc.

Each source has a heat flow channel to the atmosphere that combines conduction and convection. The number and locations of the nodes in the thermal model employed here were carefully chosen. Each node has a thermal resistance connecting it to the nodes next to it. Each node replicates its heat storage under transient conditions using a thermal capacitance.

'Namburi and Barton'[4] demonstrated the relationship between temperature rise and motor loading by fitting curves with various time constants and output power values. Steady state temperature rise under constant load has been chosen for this case as indication rather than loss.

The creations of a thermal model that would enable temperature readings over shorter time pe riods to be extrapolated to the steady state value and that could describe the steady State temp erature rise with tolerable repeatability and precision is another objective of this paper.

A lumped parameter thermal model for an electrical machine with a TEFC design is described by '*Zocholl et al*'[5]. Heat is transferred by thermal capacitance, which he assigned to each node of the model. The current sources that are injected into the equivalent circuit

node serve as a representation for heat sources, such as conductor and core losses. Since the air gap acts as a significant barrier to heat transfer, uncoupled thermal models for the stator and rotor produce accurate findings under operating conditions. The thermal model is described as follows:

- due to the relatively low heat loss compared to the heat input during a start, the heating is almost adiabatic.
- the conductor heat is dissipated while the energy is running through the insulation of the stator and finally into the ambient with the help of ventilation. Hysteresis and eddy current losses heat the iron core directly, and
- heat from the rotor conductor enters the rotor iron and exits through ventilation and shaft conduction.

A. L. Shenkman and M. Chertkov'[6] developed a lumped parameter model from experimental data, by carrying out No-Load Test, Block Rotor Test, and D.C. current Test. They also developed a thermal equivalent model based on the lumped parameter method. From the test results, they obtained a generalized thermal equivalent circuit of the induction motor and predicted its steady state temperature rise under full load.

'Dr. S. K. Choudhury and Mr. Prem Kr Bakshi'[7] have suggested a simple lumped parameter thermal model of a single phase totally enclosed fan cooled type motor.

'*Ogbonnaya Inya Okoro'*[8] proposed a thermal network model. The machine geometry is broken down into its basic components for this model, with each component identified by a node in the thermal network and its corresponding thermal capacitance and heat source. Networks for the stator iron, stator winding, and end windings are present in the machine's Stator model. It is presumed that the stator teeth are barely affected by the heat transfer from the rotor winding through the air gap to the stator winding. The machine's thermal network model is realised by linking the networks for the rotor, stator, and then collectively studies.

'Mr. Ujjwal Sinha'[9] has designed software and methodology of Induction motor and synchronous generator designs can benefit from the design methodology and software tool presented in this thesis. The system creates a set of design parameters that adhere to the performance requirements specified by the user or designer. The designer may also optimize

with respect to any performance parameter while maintaining other requirements within predetermined bounds.

'Eugene O AGBACHI, James G AMBAFI, Omokhafe J TOLA, Henry O OHIZE'[10] proposed a paper taking design consider of three phase induction motor to increase its construction, maintenance and economy. Induction machine is simple to construct and maintain. The need for an accessible method of machine design arises from the fact that the motor is used for a variety of industrial applications. Analytical equations are typically used to dimension the magnetic and electric circuits in the basic design of an electrical machine. However, computer aided design is typically used to assess the machine's accurate performance. This computer-aided design (CAD) method allows for the efficient study of the impact of a single parameter on the machine's dynamical performance while utilizing a programming language. In order to perform the design calculations, this paper demonstrates a CAD approach (using Java), which simplified the design of a three-phase induction system.

1.3 Purpose And Overview of The Research

While developing a lumped parameter thermal model it was found that it is possible to develop a satisfactory thermal model using the dimensional details of the machine. The stator copper loss, rotor copper loss and iron loss are the input of the model and the temperature rise of different parts are the output. The detailed dimensional data are required to calculated the parameters of the thermal model. It was observed that the manufacturers are unwilling to supply the detailed dimensional data. What are available for a commercially designed machine the outer dimensions of the machine. The number of stator and rotor slots and their dimensions are difficult to obtain. In this work we have tried to develop the parameter of the thermal model from the outer dimensions of the machines.

Chapter 2

Thermal Model of Three Phase Induction motor

2.1 Introduction

Now a days, the main challenge to the design engineer is to design machines having optimum cost satisfactory performance. Present market scenario always demands more output from a given frame size. That means more efficiency is always demanded. As the rating of the electrical machinery is mostly directed by its thermal behaviour, the heat generated inside the machine is the chief limitation to determine its output capability. In earlier days, when frame size was not the concerning point, the problem of temperature rise was tackled by providing more active materials machine, thereby increasing heat dissipating area or by providing more fins or by equipping the machine with bigger cooling fans. With the increase of material cost there is a tendency to reduce the frame size of these machines for a given output at the expense of poorer efficiency and a lower tolerance to thermal overload. The problems are more acute with smaller machines where the frame size is fixed for given output at given speed and use of non-standard frames are not permitted from cost consideration. Efficiency is the most importance things for the electrical machine. A large capacity motor must be designed with a high efficiency otherwise the losses are very high which the increases temperature of motor, preventing it to deliver the rated power, if the normal life expectancy is to be maintained. If sufficient cooling surface is not provided to dissipate the internal general heat the thermal equilibrium condition is attained at the considerably higher temperature. The rate of heat transfer from the outer surface of the motor to the surrounding by both convection and radiation processes increases with the rise in motor temperature. However, after a certain time, the temperature of the motor rises at a very slow rate. This occurs when the amount of heat dissipated into the surroundings ambient per unit time becomes almost equal to the heat evolved inside the motor per unit time. Such a condition of heat balance at which the motor attains a steady state temperature is reached when the motor runs continuously at constant load.

In case of three phase induction motor, determination of hotspot temperature is much more important than average winding temperature of the motor to protect the insulation from thermal damage. So, there is an increased need of determination of temperature inside a TEFC induction motor accurately for each preliminary design at the design stage. Since the development of an accurate thermal model for a 3 - phase induction motor seems to be very important. In this chapter we will discuss modelling of thermal circuit of motors used for performance analysis. The lumped parameter thermal model of induction machine and distributed parameter of thermal model will be discussed here. Where the average steady state temperature is calculated based on the thermal resistance representing the different sections of the motor. The accuracy of prediction is totally depending upon the accuracy of the modelling and not on the solution procedure.

Thermal behavior of a three-phase motor can be modeled with the help of Finite Element Method (FEM), Finite Difference Method (FDM) and lumped parameter thermal circuit method. The Circuit gives a complete physical insight of the heat flow very clearly. The field model is totally theoretical, in the sense that it lacks physical understanding. So, instead of using field model, a lumped parameter thermal model has been used. The model is based on thermal resistance and capacitance, which are calculated from the dimensional information and power loss.

2.2 STEADY STATE LUMPED PARAMETER THERMAL MODEL

In lumped parameter thermal model windings are assumed to be at the same temperature. Moreover, the proposed thermal model is axis symmetric; this is justified because of symmetrical distribution of heat sources and neglecting the influence of asymmetrical temperature distribution which exists as a result of the external fan.

The different lumped elements are chosen on the basis of thermal and physical uniformity, such as:

1. Uniformity of heat generated.
2. Uniformity of physical properties within each element.
3. Heat transfer is only in the axial and radial directions since circumferential temperature variation is negligible.
5. Heat flow in the radial and axial planes is independent of each other.
6. The mean temperature in either direction is same.
7. Radiation heat transfer is neglected.
8. Uniformity of temperatures within the element and on the surface.

The different nodes considered for the model are shown on the drawing Total twenty:

1, 10 — Ambient (non-driving end and driving end respectively)
2, 11 — Frame (non-driving end and driving end respectively)
3, 12 — Stator com (non-driving end and driving end respectively)
4, 13 — Stator slot (non-driving end and driving end respectively)
5, 14 — Stator teeth (non-driving end and driving end respectively)
6, 15 — Air (non-driving end and driving end respectively)
7, 16 — Rotor slot (non-driving end and driving end respectively)
8, 17 — Rotor teeth (non-driving end and driving end respectively)
9, 18 — Rotor core (non-driving end and driving end respectively)
19—Shaft
20, 21 — End shield (non-driving end and driving end respectively)

The proposed lumped parameter thermal model for steady state temperature analysis of an induction motor is as shown below:

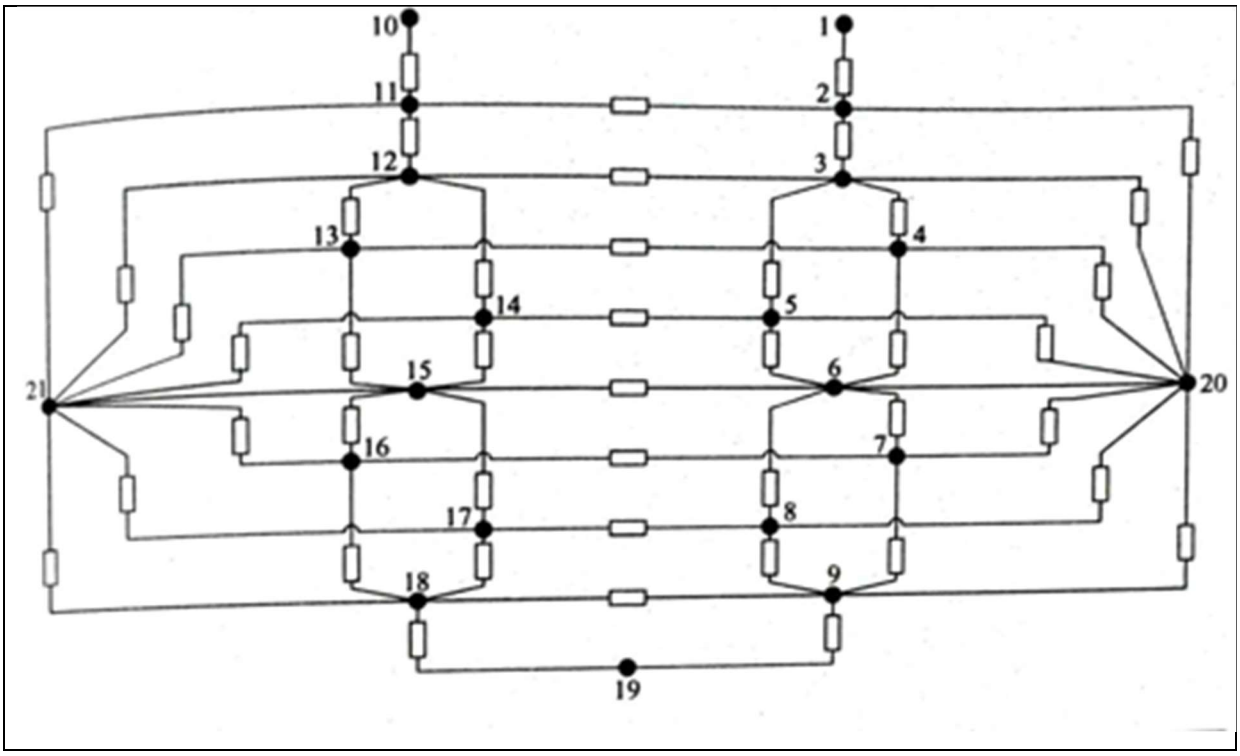

Fig. 2.1 The proposed steady state thermal model

Here in this model, there are only thermal resistances are there in between the nodes. No capacitances are considered in steady state, because according to heat balance equation steady state,

Heat generated within the body = Heat conducted away from the body

Therefore, no heat is retained within the machine. And the temperature of the machine is constant.

Under steady state condition, the thermal capacitance can be at

capacity so, $d\theta i/dt = 0$

If, $R_{i,j}$ be considered as the thermal resistance between node i and the ambient, then the steady-state nodal temperature rises are related by:

$$Q_i = \frac{\theta_i}{R_{i,i}} + \sum_{j=1}^{n} (\theta_i - \theta_j) \frac{1}{R_{ij}} \quad \text{..... (2.1)}$$

Where θ_1 and θ_n are the temperature rises of each node and Q_1 to Q_2 are the losses of each node.

Therefore, in the matrix form which can written as,

$$[G_t][\theta_t] + [Q_t] = 0 \quad \text{..... (2.2)}$$

$$[\theta_t] = -[Q_t][G_t]^{-1} \quad \text{..... (2.3)}$$

Where;

$[Q_t]$ is the internal heat generation due to losses matrix.

$[G_t]$ is the thermal conductance matrix.

$[\theta_t]$ is the temperature rise matrix.

The conductance matrix $[Q_t]$, heat generation matrix $[G_t]$ and temperature rise matrix $[\theta_t]$ can also be defined as written below.

These matrices are defined as:

$$[C_t] = \begin{bmatrix} C_1 & 0 & 0 & 0 & 0 & - & - & - & - & - & - & 0 \\ 0 & C_2 & 0 & 0 & 0 & - & - & - & - & - & - & 0 \\ 0 & 0 & C_3 & 0 & 0 & - & - & - & - & - & - & 0 \\ 0 & 0 & 0 & C_4 & 0 & - & - & - & - & - & - & 0 \\ 0 & 0 & 0 & 0 & C_5 & - & - & - & - & - & - & 0 \\ - & - & - & - & - & - & - & - & - & - & - & 0 \\ - & - & - & - & - & - & - & - & - & - & - & 0 \\ - & - & - & - & - & - & - & - & - & - & - & 0 \\ - & - & - & - & - & - & - & - & - & - & - & 0 \\ - & - & - & - & - & - & - & - & - & - & - & 0 \\ - & - & - & - & - & - & - & - & - & - & - & 0 \\ 0 & 0 & 0 & 0 & 0 & - & - & - & - & - & - & C_n \end{bmatrix} \quad \text{..... (2.4)}$$

$$[Q_t] = \begin{bmatrix} Q_1 \\ Q_2 \\ Q_3 \\ Q_4 \\ Q_5 \\ - \\ - \\ - \\ - \\ - \\ - \\ Q_n \end{bmatrix} \quad \ldots\ldots\ldots\ldots\ldots\ldots\ldots\ldots\ldots\ldots\ldots\ldots\ldots\ldots\ldots\ldots\ldots\ldots\ldots\ldots\ldots\ldots\ldots (2.5)$$

$$[G_t] = \begin{bmatrix} -\sum_{i=1}^{n} G_{1,i} & G_{1,2} & G_{1,3} & G_{1,4} & G_{1,5} & - - & G_{1,n} \\ G_{2,1} & -\sum_{i=1}^{n} G_{2,i} & G_{2,3} & G_{2,4} & G_{2,5} & - - & G_{2,n} \\ G_{3,1} & G_{3,2} & -\sum_{i=1}^{n} G_{3,i} & G_{3,4} & G_{3,5} & - - & G_{3,n} \\ G_{4,1} & G_{4,2} & G_{4,3} & -\sum_{i=1}^{n} G_{4,i} & G_{4,5} & - - & G_{4,n} \\ G_{5,1} & G_{5,2} & G_{5,3} & G_{5,4} & -\sum_{i=1}^{n} G_{5,i} & - - & G_{5,n} \\ - & - & - & - & - & - - & 0 \\ - & - & - & - & - & - - & 0 \\ G_{n,1} & G_{n,2} & G_{n,3} & G_{n,4} & G_{n,5} & - - & -\sum_{i=1}^{n} G_{n,i} \end{bmatrix} \quad \ldots\ldots\ldots\ldots\ldots\ldots (2.6)$$

$$[\theta_t] = \begin{bmatrix} \theta_1 \\ \theta_2 \\ \theta_3 \\ \theta_4 \\ \theta_5 \\ - \\ - \\ - \\ - \\ - \\ - \\ \theta_n \end{bmatrix} \quad \ldots\ldots\ldots\ldots\ldots\ldots\ldots\ldots\ldots\ldots\ldots\ldots\ldots\ldots\ldots\ldots\ldots\ldots\ldots\ldots\ldots\ldots\ldots\ldots (2.7)$$

In equation (2.3) the diagonals of the matrix can be written as,

$$G_{11} = -\{G_{12} + G_{13} + G_{14} + \cdots + G_{1n}\} \quad \text{..... (2.8)}$$

$$G_{22} = -\{G_{21} + G_{23} + G_{24} + \cdots + G_{2n}\} \quad \text{..... (2.9)}$$

.....

$$G_{nn} = -\{G_{n1} + G_{n2} + G_{n3} + \cdots + G_{n(n-1)}\} \quad \text{..... (2.10)}$$

Here, $G_{li} = 1/R_{1i}$, etc. Also due to symmetry $G_{12}=G_{21}$, $G_{13}= G_{31}$ & so on.

Therefore, the steady state temperature rise can easily determine by solving the equation (2.3). However, some of the parameters in G and especially in Q are temperature-dependent, so Gauss-Sidel iterative process, as discussed earlier, should be used where the temperature-dependent parameters are updated until the error is sufficiently small.

2.3 TRANSIENT STATE LUMPED PARAMETER THERMAL MODEL

With the help of simple thermal network model we can solve both transient and steady state solutions for the temperature analysis between the element and the ambient air temperature. Heating & cooling of electrical machine are always transient in nature. However, steady State condition is said to have been occurred when the temperature reaches about 98% of the final value starting from the initial condition. In the steady state model the temperature are calculated at all the nodes placed at discrete intervals apart in space but in the transient thermal analysis the temperature of all the nodes vary with time. So, the nodal temperatures in this case are calculated at discrete interval of time.

A simple lumped parameter thermal equivalent circuit representation is shown in fig 2.2 for transient state condition.

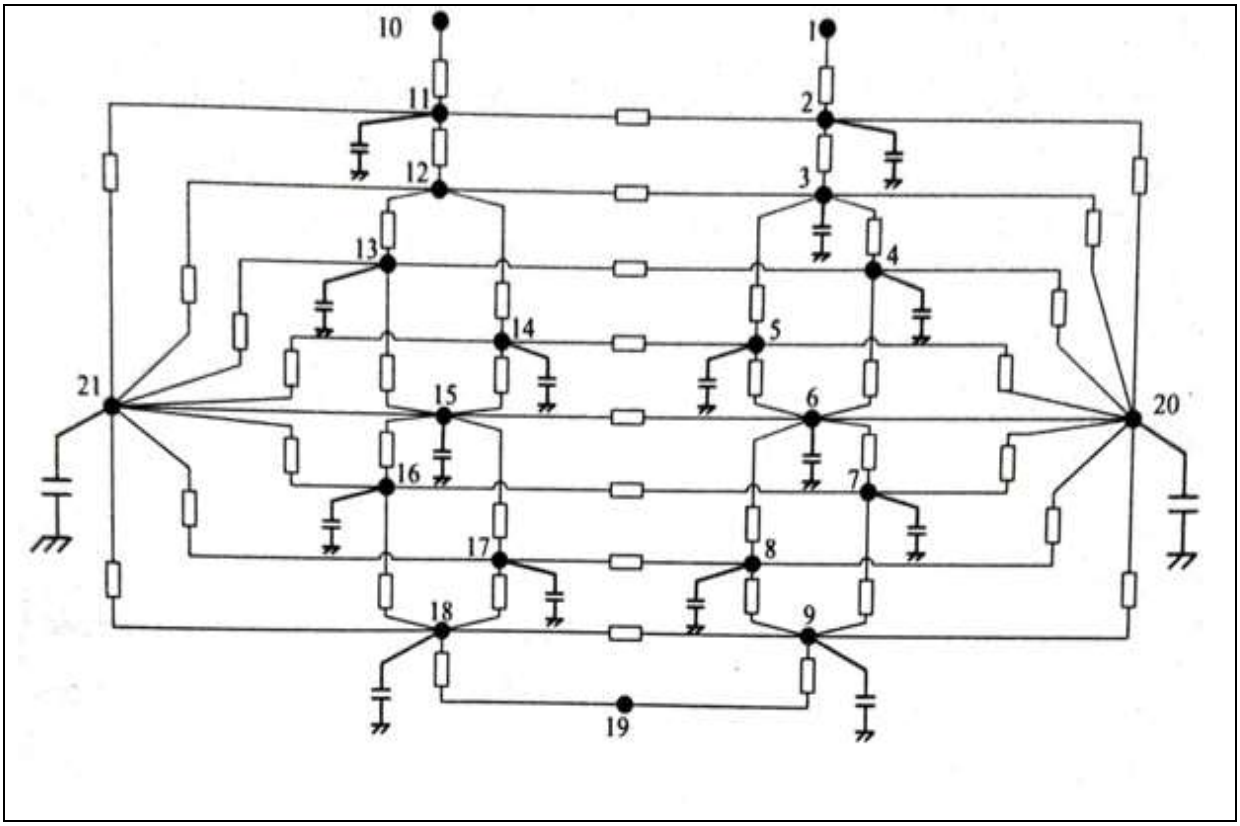

Fig. 2.2 The proposed Transient state thermal model

Unlike the previous steady State model, here both thermal resistances and capacitances are considered at the nodes. Heat balance equation under steady State,

Heat generated within body = Heat conducted away from body + Heat retained in body

As case of transient state, temperature of each node varies with time,
Therefore, the general transient equation for a thermal network at any node 'i' can be given by Eq. 2.3

In the matrix form the equation (2.3) can be written as,

$$\frac{d\theta t}{dt} = [C_t]^{-1}[Q_t] + [C_t]^{-1}[G_t][\theta_t] \quad \ldots\ldots (2.11)$$

Where,

$[C_{t]}$ is thermal capacitance matrix.

$[Q_t]$ is the internal heat generation due to losses matrix.

$[G_t]$ is the thermal conductance matrix.

$[\theta_t]$is the temperature rise matrix.

This equation can be solved by using Gauss-Sidel iterative method as in case of steady state model or simply by implementing the thermal network model in a simulation package defining all the as we have done in our thesis work.

2.4 SOFTWARE PACKAGE

An interactive software package has been developed in SIMULINK in windows environment for determination of the steady state and the transient state thermal characteristics of a 3-phase induction motor. In this software, the user needs to input only dimensional details of a motor and percentage loading. The program calculates the temperature at each node for each time instant, and then average value is computed for surface and slot corresponding to each time instant. Steady State temperature is plotted against loading and transient temperature is plotted against time.

2.5 STABILITY OF THE SOLUTION

The numerical method presented here represents the approximate solution of the equation, since the derivatives are replaced by finite differences. The error introduced by this approximation, are termed as truncation errors. Numerical errors are also introduced into a solution by virtue of the inability or impracticality, of performing the numerical computation with a significant number of digits of significant figures.

The other problem, which is faced to obtain satisfactory results, is the upper limit of the allowable time increment. In practice it is to use a time increment much smaller than the permissible maximum. This is done to improve of the results by reducing the truncation error in time and to avoid instabilities caused by higher value of $\delta\tau$.For each node $\Sigma(1/R_{ij}C_i))$ is calculated and the time step is so that $<\Sigma[1/(1/R_{ij}C_i))]_{min.}$

2.6 CONCLUSION

Development of a package for determination of the transient state thermal model of an induction motor has been described in this chapter. It gives a good knowledge of the temperature distribution inside the motor and is very helpful to estimate the temperature of the motor at the design stage. This package has been used to estimate temperature of the motor used for experiments. Though for the calculation of so many thermal resistance and capacitance, a digital computer is essential, but now-a-days, the use of computers for machine design and analysis is very common.

The software developed here is on the dimensional information, physical constants and the heat transfer characteristics of the different mediums are involved. The software is thus readily adaptable to a wide range of machine sizes and ratings. The maximum error in estimated final temperature from the measured one is 2-5 ^{0}C for the whole cross-sectional analysis.

The simulation method using the thermal model can be applied for all the ranges of motors and for different voltage ratings. However, the heat transfer co-efficient should be properly chosen to derive the parameters with sufficient accuracy.

The transient condition during starting, have not been studied, due to a very small value of the starting time of the order of 0.1 sec, due to considerable amount of starting torque and low inertia of the system.

Chapter 3

Data Analysis of given Three Phase Induction Motor

3.1 Introduction

In this part we briefly study and measure all essential parameters (which are generally seen when the frame is open) of a given Three phase Induction Motor. By the help of digital venire calliper we measured

- Dimension of stator: the length and diameter of stator core,
- Dimension of frame,
- Dimension of rotor: length and diameter of rotor core, number of rotor bar, end rings dimensions.

From this information we have to calculate

- flux density in different parts of motor,
- slot pitch in stator and rotor,
- total no. of conductors,
- length of rotor bar,
- rotor bar current,
- resistance of winding,
- ohmic loss in stator and rotor windings.
- area of different portions of motor.
- Core loss in stator core,
- length of air gap between stator and rotor.
- friction and windage losses,
- Total loss,
- efficiency.

The above information is necessary to develop the thermal equivalent circuit of the motor. The thermal circuit of the motor is required in order to estimate the performance of the motor. As

discussed in the previous chapter, the thermal circuit parameters must be calculated from the motor's dimensions and material characteristics for design purposes.

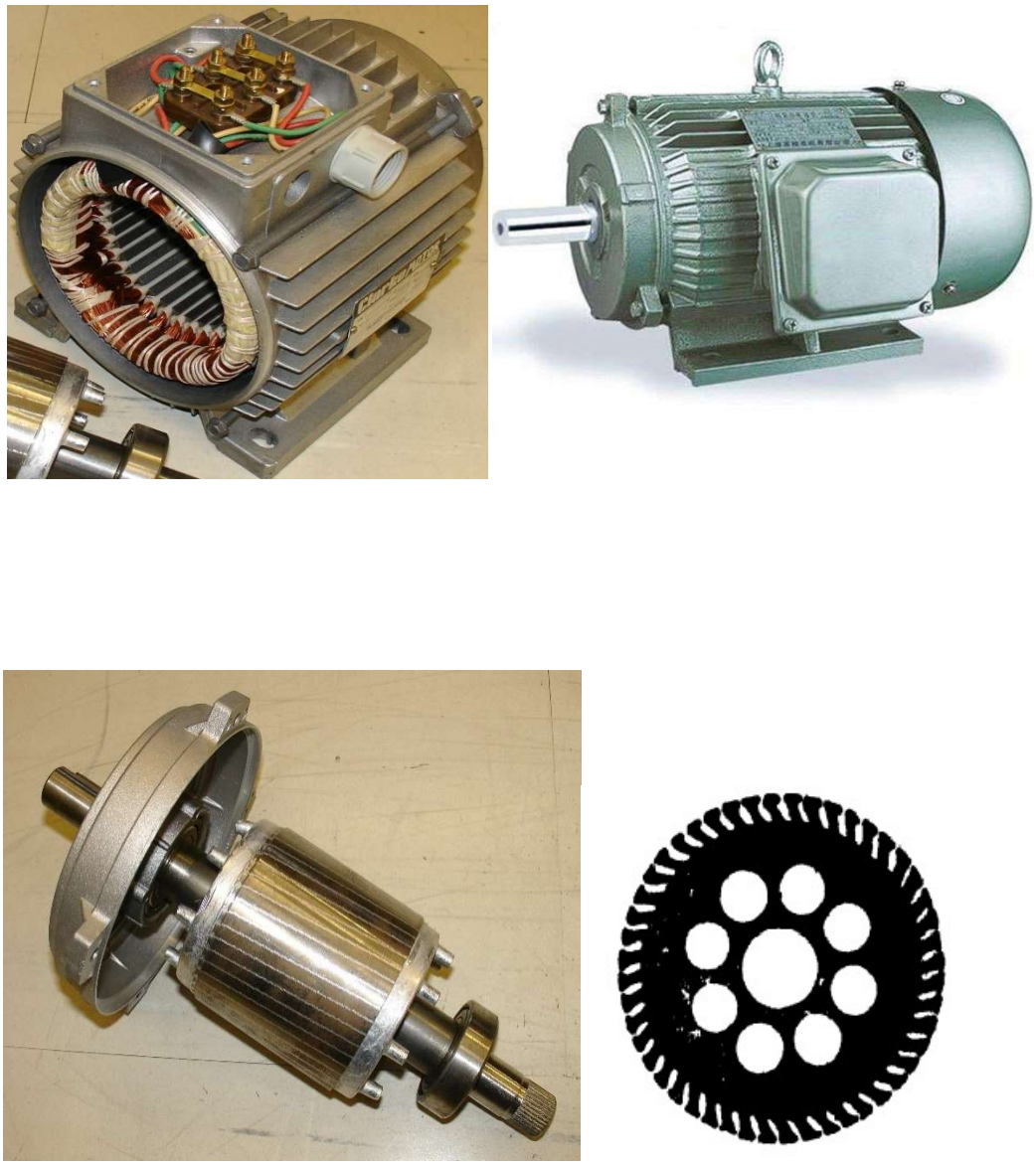

Fig 3.1 Different Parts of an Induction Motor

3.2 Calculation of different Internal dimensions of motor

3.2.1 Number of Stator Slots

Following factors are considered while selecting the number of stator slots:

I. **Tooth pulsation loss:** In motors with open type slots, slot opening effects on air gap reluctance. The slots should be so proportioned that minimum variations in the air gap reluctance are produced which results in tooth pulsation losses and noise. This effect can be minimized by using large no. of narrow slots.

II. **Leakage Reactance:** If No. of slots (↑), Leakage reactance (↓). If no. of slots is more, then large no. of slots is required to insulate and therefore width of the insulation becomes more. This means that, leakage reactance has longer path through air and due to this leakage flux reduces. Due to the reduction of leakage flux, leakage reactance also reduces.

III. **Overload capacity:** If no. of slots (↑), overload capacity (↑). If no. of slots is more, then leakage reactance reduces. With small values of leakage reactance the diameter of circle diagram is large and hence the overload capacity increases.

IV. **Ventilation:** If no. of slots is larger for a given diameter, the smaller will be the slot pitch. If the slot pitch is small, the tooth width is also small. Due to this thickness of teeth becomes smaller and the teeth may become mechanically weak and they may have to be supported by radial ventilating ducts.

V. **Magnetizing current and iron loss:** If no. of slots (↑), magnetizing current and iron loss (↑). If no. of slots is larger than teeth section is reduced. Therefore, the use of larger no. of slots may result in excessive flux density in teeth giving rise to higher magnetizing current and higher iron loss.

VI. **Cost:** (↑). With larger no. of slots there are larger no. of coils to wind, insulate and install involving higher costs. It is good to use as many slots as economically possible.

In general, no. of slots per pole per phase q, should not be less than 2 otherwise the leakage reactance becomes high.

3.2.2 Selection of Number of Rotor Slots

In the paper titled "*Slot Combinations of Induction Motors*", GABRIEL KRON concluded that

A Vibration and noise are liable to be present under the following conditions.

1. When the slots differ by one or by the number of poles plus or minus one, the fundamental m.m.f. and the oscillating permeance produce a flux differing by two poles from the fundamental flux. When the speed of the resulting unbalanced pull is the same as the critical speed of the rotor, circular vibrations and noise occur.

2. When the slots differ by half the number of poles, the fundamental m.m.f. and the oscillating permeance produce a fundamental single-phase flux. When the frequency of torsional vibrations is the same as the critical frequency of the rotor, torsional vibrations and noise occur.

3. When the slots differ by the number of poles the fundamental m.m.f. and the oscillating permeance produce a parasitic fundamental flux revolving with a different speed than the fundamental flux. These two fluxes set up torsional vibrations and noise, and also rumbling noises unaccompanied by critical vibrations. The chances that the noise occurs in the working range are greater with smaller number of poles, higher speed and with smaller critical speeds. When these noises do occur, the motor is practically useless.

B. Crawling may be present under the following conditions.

1. When the slots differ by the number of poles and the rotor has more slots than the stator, the fundamental m.m.f. and the oscillating permeance produce a parasitic fundamental flux. At a rotor speed S ($2 / G_2$) the speed of the parasitic flux is the same as the speed of the fundamental flux, the two fluxes lock and the motor crawls as if it were a synchronous motor (reaction machine effect). When the rotor has less slots, the synchronous crawling occurs at a negative speed.

2. When the rotor slots are greater than ($G_1 + p$) by, say 80 percent, the fundamental m.m.f. and the stator slot-opening produce a flux having less pole s than the number of rotor bars. At a rotor speed $S/ (G_1 + p)$ the motor crawls due to induction motor effect.

3. When the rotor slots are greater than ($G_1 - p$) by, say 80 percent, crawling occurs at $S/ (G_1 - p)$ if, driven backward, due to the same reason as in point ‘2’.

4. When the rotor slots in a two-phase motor are divisible by the number of poles, the fifth harmonic flux due to the distribution of winding may cause crawling at one-fifth synchronous speed.

5. Any two-phase motor may crawl at one-third synchronous speed if driven backward, due to the backward revolving third harmonic flux caused by the distribution of windings.

6. When $G_2 / 2$ p is an integer equal to or close to unity, crawling may occur at S/G_2 due to the "Gorges " effect.

7. When the vibrations under A occur at low speeds, the motor crawls.

8. When the harmonic flux, due to the distribution of winding, is large, say larger than 10 percent of the fundamental, the motor may crawl.

C. Smaller irregularities and hooks in the speed torque curve may appear under the following conditions.

1. When the rotor slots are greater than (G_1 + p) a hook occurs at S (G_1 + p) r.p.m.

2. When the rotor slots are greater than (G_1 - p) a hook occurs at S/ (G_1 - p) r.p.m. if the motor is driven backward. G_1 = no. of stator slots

3. When the rotor slots are divisible by the number of poles, a hook occurs at S /G_2 rpm. G_2= no. of slots in rotor

4. When the rotor slots are divisible by the number of poles, a hook occurs at one-seventh synchronous speed in a three-phase motor and at one-fifth synchronous speed in a two-phase motor. In both cases, the hook is accompanied by another hook at S/G_2 r.p.m,

5. When G_2 = 2p (1 + k ψ) 2p, where ψ = number of phases, a small synchronous locking (synchronous motor; effect occurs at, 5 (2 / k_2 G_2) r.p.m.

6. A two-phase motor has a hook at one-third synchronous speed if it is driven backward.

7. When a winding introduces a harmonic flux larger than, say 8 percent of the fundamental, it always produces a hook.

Depending on the above criteria some standard slot combinations are used for induction machine design as given in the following table.

Number of Poles	Number of Stator Slots	Number of Rotor Slots	Number of Poles Number	Number of Stator Slots	Number of Rotor Slots
2	24	28, 16, 22	6	36	42, 48, 54, 30
	36	24, 28, 48, 16		54	72, 88, 48
	48	40, 52		72	90, 88, 84, 50
4	36	24, 40, 42, 60	8	36	48
	48	60, 84, 56, 44		48	72, 60
	60	72, 48, 84, 44		72	96

Table 3.1 : Slot combination of stator and rotor for different values of poles.

Since machine is small so, slot per phase per pole 'q' as 2. Thus S_s=24 and S_r= 22.

3.3 Output Equation

The permitted KVA output from a frame size is given by

$$KVA = C_o D^2 L n_s \quad \therefore \; D^2 L = KVA/C_o n_s$$

This equation shows that for a machine of given rating the size or volume of the active parts as given by $\mathbf{D^2\ L}$ depends upon two factors:

- The output coefficient $\mathbf{C_0}$
- The speed $\mathbf{n_s}$.

The higher the values of $\mathbf{C_0}$ and $\mathbf{n_s}$, lower is the volume $\mathbf{D^2\ L}$ and therefore the size of the machine decreases. As the speed is given in the specification, to obtain smallest dimensions of the machine the output coefficient $\mathbf{C_0}$ must have highest possible value. Since C_0 is proportional to specific magnetic loading $\mathbf{B_{av}}$ and specific electric loading '**ac**'. Thus, we conclude that the size and hence the cost of the machine depends on $\mathbf{B_{av}}$ and '**ac**'.

3.3.1 Choice of Specific Electrical and Magnetic loadings

3.3.1.1 Choice of Average Flux Density (B_{av}) in Air gap

I. **Power factor:** The value of flux density in air gap should be small as otherwise the machine will draw a large magnetizing current giving a poor power factor. In induction motors, flux density in air gap should be such that there is no saturation in any part of the magnetic circuit.

II. **Iron loss:** A high value of flux density in the air gap leads to higher value of flux in the iron parts of the machine which results in increased iron losses If gap density (↑), iron losses (↑) and efficiency (↓).

III. **Transient short circuit current:** A high value of gap density results in decrease in leakage reactance and hence increased value of armature current under short circuit conditions.

IV. **Overload capacity:** If flux density (↑), overload capacity (↑). A high value of flux density means flux per pole is large. Thus, for the same voltage, the winding requires less turns per phase. If the number of turns is less, the leakage reactance becomes small. With small leakage reactance the circle diagram of machine has a large diameter which means that the maximum output which

means the machine has large overload capacity. Thus, with the assumption of a higher value of B_{av}, we get higher value of overload capacity.

- For 50Hz machine of small design, $\mathbf{B_{av}}$ = 0.3 to 0.6 Wb/m2
- For machines where a large overload capacity is required, $\mathbf{B_{av}}$ = 0.65 Wb/m2

3.3.1.2 Choice of Ampere Conductors (ac) per Meter

I. **Copper loss and temperature rise:** If ac (↑), copper loss (↑) and Temperature (↑). A large value of ac means a greater amount of copper is employed in the machine. This results in higher copper losses and large temperature rise of embedded conductors.

II. **Voltage:** A higher value of '**ac**' can be used for low voltage machines since the space required for the insulation will be smaller. A small value of 'ac' should be taken for high voltage machines as in their case the space required for insulation is large.

III. **Overload capacity:** If ac (↑), overload capacity (↓). A large value of ampere conductors would result in large number of turns per phase. This would mean that the leakage reactance of the machine becomes high. Due to this, diameter of circle diagram reduces resulting in reduced value of overload capacity. Therefore, the higher value of ac, the lower would be the overload capacity.

The value of '**ac**' varies between 5000 to 45000 ampere conductors per meter depending upon the factors listed above

3.4 Determination of Number of Conductor per Slot

For any average flux density in air gap $\mathbf{B_{av}}$; the flux per pole of a machine with length of armature **L** and pole pitch $\boldsymbol{\tau = \pi D/p}$ is given by $\boldsymbol{\emptyset_m = B_{av} \times L \times \tau \times SF}$ Wb

If, $\mathbf{E_{ph}}$ is the voltage per turn then turn per phase $\boldsymbol{T_s = E_{ph}/(4.44 \times f \times \emptyset_m \times k_{ws})}$

∴ Total no. of conductors = $\boldsymbol{C_{total} = 3 \times 2 \times T_s}$

$$\therefore no.of\ conductor\ per\ slot = \boldsymbol{C_{total}/S_s}$$

3.5 Determination of Stator Slot Dimensions

For the machine under study the frame size is fixed. But the size and shape of the stator slots are unknown. The dimension of the stator slot was determined based on the assumption that the output from the frame size is maximum, i.e. the efficiency of the machine is maximum. As the diameter is fixed the ratio of depth of stator core to depth of stator slot only can be varied within an allowable limit. Let

D_f= stator frame outer diameter in m

t_f = thickness of frame in m

D_o= stator stamping outer diameter in m

D=stator stamping inner diameter or air gap diameter in m

D_r=rotor stamping outer diameter in m

D_{sh}=shaft diameter in m

L=length of armature in m

L_f=length of frame in m

k_{ws}= winding facor

d_{sc}=depth of stator core in mm

d_{st}=depth of stator teeth in mm

w_{st}=width of stator teeth in mm

w_{ssb}=width of stator slot base in mm

w_{sst}=width of stator slot top in mm

B_{av} = average flux density in Wb/m^2

3.5.1 Determination of Stator Slot Depth [d_{st}]

Now $\boldsymbol{d_{sc} + d_{st} = .5 \times (D_o - D) \times 1000\ mm}$

Now let $\boldsymbol{d_{st}/d_{sc} = n}$

$$\boldsymbol{d_{st} + d_{sc} = (1 + n)d_{sc};}$$

$\therefore\ \boldsymbol{d_{sc} = (d_{st} + d_{sc})/(1 + n) = 0.5 \times (D_o - D)/(1 + n)}$ and $\boldsymbol{d_{st} = n \times d_{sc}}$

We may change the ratio '**n**' [d_{sc}/d_{st}] within a specified range mainly in the range of 1.0 to 1.5 for small rating 3-phase Induction motor and estimate the losses.

3.5.2 Determination of Stator Slot Width [w_{sst} and w_{ssb}]

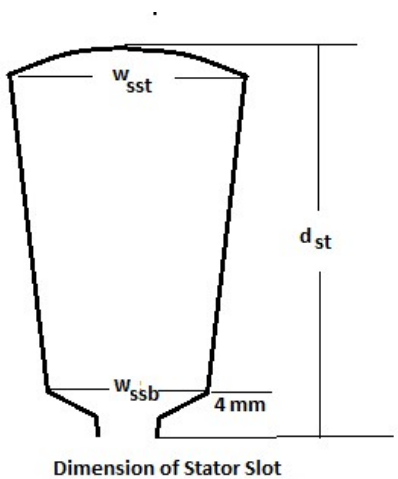

Dimension of Stator Slot

As the motor rating is small, a semi-enclosed slot is considered.

For maximum allowable flux density 1.7 Wb/m^2, minimum allowable teeth ($w_{st(min)}$) width is given by

$$\boldsymbol{w_{st(min)} = 1000 \times \emptyset_m/(1.7 \times (S_s/pole) \times L \times SF}$$

Let w_{st} $(>\ w_{st(min)})$

$$\therefore\ w_{sst} = \pi(D \times 1000 + 2 \times d_{st})/s_s - w_{st}$$ and

$$w_{ssb} = \pi \times (D \times 1000 + 2 \times 4)/s_s - w_{st}$$

3.5.3 Determination of Current Density in Stator Winding

The available area in slot is given by

$$A_{slot} = .5 \times (d_{st} - 4)(w_{ssb} + w_{sst})$$

Considering slot space factor = 0.4;

Total area of conductor is: $A_{total} = .4 \times A_{slot}$;

$$\therefore area\ of\ each\ conductor = a_c = A_{total}/C_{total}$$

$$\therefore diameter\ of\ conductor\ d_c = \sqrt{(4 \times a_c)/\pi}$$

$$stator\ current\ per\ phase\ I_s = kW/3 \times (E_{ph} \times efficiency \times pf)$$

$$\therefore current\ density\ in\ stator\ \delta_s = I_s/a_c$$

If we change the ratio 'd_{st}/d_{sc}'; the stator slot dimension will change. So, to accommodate the stator number of turn we must change the conductor dimension, thus changing the stator current density. This will change the stator copper loss.

3.5.4 Determination Stator Copper Loss

Length of mean turn of stator winding is given by

$L_{mt} = 2L + 2.3\tau + 0.24$ (where L and τ are expressed in meter)

$$\therefore per\ phase\ resistance\ of\ stator\ winding\ r_{ph} = (.021 \times L_{mt} \times T_s)/a_c$$

$$\therefore total\ copper\ loss\ of\ stator\ winding\ P_{cu-stator} = 3 \times I_s^2 r_{ph}$$

3.6 Determination of Rotor Slot Dimension:

3.6.1 Rotor Bar Current:

If, rotor mmf = 0.8 stator mmf,

Number of rotor bars N_b = no. of rotor slot S_r,

Rotor mmf = $I_b \times N_b / 2$

Stator mmf = $3 \times I_s \times T_s \times k_{ws}$

, $\therefore I_b \times N_b/2 = 0.8 \times 3 \times I_s \times T_s \times k_{ws}$

∴ Rotor bar current 'I_b' = [2 × 0.8 [3 × I_s × T_s×k_{ws}]] / N_b

3.6.2 Copper Losses in the Rotor Bars:

The rotor bar area is given by: $\mathbf{A_b = I_b / \delta_b}$

Where: $\mathbf{\delta_b}$= Current density, its value ranges between 4 to 7A/mm$^{2.}$.

Length of rotor bar '$\mathbf{L_b}$' = **L + Allowance for skewing**.

Taking allowance for skewing = 10 mm.

Therefore, Resistance per bar, $b_r = 0.035 x L_b$ in m^2 /A_b in mm^2

Hence, **total copper losses in the rotor bars,**

'$\mathbf{P_{Cu-b}}$'= $\mathbf{(I_b)^2 \times r_b \times}$ **number of rotor bar (**$\mathbf{N_b}$**)**

3.6.3 End ring current:

Considering a group of rotor bar less than one pole pitch, one half would send current to an end ring in one direction and the other half in the other direction. If the maximum value of current in each bar is $I_{b(max)}$ and if the current is maximum in all the bars at same time, the maximum value of the current in the end ring:

$$\boldsymbol{I_e = bars\ per\ pole/2 \times current\ per\ bar}$$

However, the current is not maximum in all the bars under one pole at the same time but varies sinusoidally; hence, the maximum value of the current in the end ring is the average of the current of half the bars under one pole.

$$\therefore \boldsymbol{maximum\ value\ of\ endring\ current}\ \boldsymbol{I_{e(max)} = \frac{2}{\pi} \times \frac{S_r}{2P} \times I_{b(max)}}$$

The bar current varies sinusoidally $\therefore\ \boldsymbol{I_{b(max)} = \sqrt{2}\, I_b}$

$$\therefore\ \boldsymbol{I_{e(max)} = \frac{2}{\pi} \times \frac{S_r}{2P} \times \sqrt{2} I_b}$$

Rms value of end ring current

$$\boldsymbol{I_e = I_{e(max)}/\sqrt{2} = \frac{1}{\sqrt{2}} \times \frac{2}{\pi} \times \frac{S_r}{2P} \times \sqrt{2} I_b = S_r I_b / \pi P}$$

3.6.4 Area of End Rings:

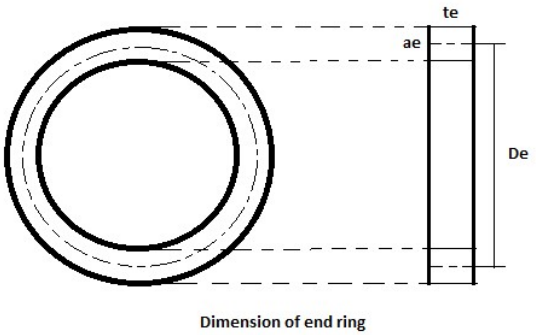

Dimension of end ring

As ventilation is generally better for end rings and therefore a slightly higher value of current density is allowable. Area of each end ring is given by $a_e = I_e / \delta_e$; where end rings current density δ_e is between 5 to 8 A/mm^2.

$$\boldsymbol{area\ of\ ring\ a_e} = \boldsymbol{depth\ of\ end\ ring} \times \boldsymbol{thickness\ of\ end\ ring} = \boldsymbol{d_e \times t_e}$$

3.6.5 Copper Losses in End Rings:

Mean length of the current path $\mathbf{L_{me} = \pi D_e}$

Where $\mathbf{D_e}$ =mean diameter of end ring.

Resistance of end Ring:

$\mathbf{R_e = [\rho \times L_{me}] / a_e}$

= where $\mathbf{L_{me}}$ is in 'm' and $\mathbf{a_e}$ in 'mm^2'.

Therefore, Total copper losses in the end rings is $\mathbf{P_{cu\text{-}er} = 2 \times I_e^2 \times R_e}$

3.6.6 Rotor Losses

Rotor losses consist of copper and iron losses. During normal operation of induction motors, since the slip is very small, the magnetic reversals in the rotor core are only in the order of one or two per second. The iron losses caused by this are very small hence can be neglected.

Resistance of each bar $\mathbf{r_b = \rho\ L_b / a_b}$

$\therefore$ Total copper losses in all the bars = $\mathbf{I_b^2 . r_b . S_r}$

$\therefore$ Total copper loss in both the end rings = $\mathbf{2\ I_e^2 . R_e}$

∴ Total copper loss in Rotor = $\mathbf{I_b^2.r_b .S_r + 2 I_e^2. R_e}$

3.7 Determination of Magnetic circuit losses

A classical model is the Bertotti's three-term loss separation model [13], where the total losses P are divided into three components: the hysteresis loss P_h, the classical eddy current loss P_{ec}, and the excess loss P_e.

$P = P_h + P_{ec} + P_e$

If the term of the excess loss is ignored, then (41) can be reduced to

$P = P_h + P_{ec}$

The ignored term of the excess loss is actually included in the other two terms: the hysteresis loss and the classical eddy current loss[14]. The iron loss ($P_h + P_{ec}$) in stator teeth and core is found out by calculating their respective weights. At 50 Hz the specific iron loss (iron loss per kg) corresponding to the flux densities can be taken as:

$\boldsymbol{p_i = a\, B_m^{\,2}\ W/kg}$, where $\boldsymbol{a = 4.7}$ for core**.** For the same flux density the specific iron loss is greater in teeth, so $\boldsymbol{a = 6.5}$ for teeth.

The frequency of flux reversals in rotor is at slip frequency '***sf '***. As the value of slip is very small, the iron loss in the rotor is neglected.

3.7.1 Iron Loss in Stator Core

Volume of stator core can be calculated as

$$\boldsymbol{V_{core} = cross\ sectional\ area\ of\ core \times length\ of\ armature}$$

$$\boldsymbol{outer\ diameter\ of\ stator\ core = D_{so}}$$

$$\boldsymbol{depth\ of\ stator\ core = d_{sc}}$$

$$\boldsymbol{inner\ diameter\ of\ stator\ core = D_{so} - 2 \times d_{sc}}$$

$$\boldsymbol{mean\ diameter\ of\ stator\ core = .5 \times (D_{so} + D_{so} - 2 \times d_{sc}) = D_{so} - d_{sc}}$$

$$\boldsymbol{cross\ sectional\ area\ of\ stator\ core} = \boldsymbol{\pi \times (D_{so} - d_{sc}) \times d_{sc}}$$

$$\therefore \boldsymbol{V_{core} = \pi \times (D_{so} - d_{sc}) \times d_{sc} \times L}$$

$$\therefore \boldsymbol{weight\ of\ stator\ core\ W_{core} = V_{core} \times density\ of\ iron}$$

Flux density in stator core is given by:

$$\boldsymbol{B_{sc} = \emptyset_m / (2 \times area\ of\ stator\ core) = \emptyset_m / (2 \times d_{sc} \times L \times SF)}$$

Iron loss in stator core = $\boldsymbol{P_{core} = W_{core} \times 4.7 \times B_{sc}^{\ 2}}$

3.7.2 Iron Loss in Stator Teeth

Volume of stator teeth can be calculated as

$$\boldsymbol{V_{teeth} = cross\ sectional\ area\ of\ each\ teeth \times length\ of\ armature \times no.of\ teeth}$$

$$\boldsymbol{V_{teeth} = d_{st} \times w_{st} \times L \times S_s}$$

$$\therefore \boldsymbol{weight\ of\ stator\ teeth\ W_{teeth} = V_{teeth} \times density\ of\ iron}$$

Flux density in stator teeth is given by:

$$\boldsymbol{B_{st} = \emptyset_m / (S_s \times area\ of\ one\ stator\ teeth) = \emptyset_m / (S_s \times w_{st} \times L \times SF)}$$

Iron loss in stator core = $\boldsymbol{P_{teeth} = W_{teeth} \times 6.5 \times B_{st}^{\ 2}}$

Total iron loss is taken as $\boldsymbol{2 \times (P_{core} + P_{teeth})}$

3.8 Analysis of the Results

The internal dimensions of a 1.1kW 415V 3 phase induction motor were calculated using the equations described above. Flux density in different parts of the machine; current density in the stator and rotor winding for different values of $\mathbf{B_{av}}$ [0.45 Wb/m^2 ; 0.5 Wb/m^2 **;** 0.55 Wb/m^2 **;** 0.6 Wb/m^2 **;** 0.65 Wb/m^2 **]** and the ratio $\boldsymbol{d_{st}/d_{sc}}$ [1.1; 1.2; 1.3; 1.4; 1.5; 1.6; 1.7;1.8; 1.9,2.0] are tabulated in **Tabe 3.2A; Tabe 3.2B; Tabe 3.2C; Tabe 3.2D; Tabe 3.2E.** For any value of $\mathbf{B_{av}}$ as we increase $\boldsymbol{d_{st}/d_{sc}}$ ratio, the stator slot depth increases and stator core depth decreases. As the diameters are fixed, the stator slot area increases, decreasing the stator current density and stator copper loss. On the other hand, the stator core flux density increases increasing the stator core loss. This results in change in efficiency of the machine. If $\mathbf{B_{av}}$ is increased, it is found that for more than certain value of $\boldsymbol{d_{st}/d_{sc}}$, the stator core flux density become too high, rendering the design

unacceptable [marked in red in the Table]. The efficiency of the machine is maximum for $\mathbf{B_{av}=0.55\ Wb/m^2}$ and $\boldsymbol{d_{st}/d_{sc} = 1.6}$.[marked in yellow in the Table]. The results are plotted and analysed in Chapter 4.

Table 3.2A

		dst/dsc ---------->									
	parameters	1.1	1.2	1.3	1.4	1.5	1.6	1.7	1.8	1.9	2
Bav = 0.45 Wb/m^2	Bsc	1.164	1.219	1.275	1.330	1.38	1.441	1.496	1.552	1.607	1.663
	Bst	1.133	1.133	1.133	1.133	1.133	1.133	1.133	1.133	1.133	1.133
	stator current density	6.488	6.075	5.737	5.456	5.218	5.014	4.837	4.682	4.545	4.424
	Brc	0.854	0.870	0.884	0.898	0.91	0.922	0.933	0.944	0.954	0.963
	Brt	1.236	1.236	1.236	1.236	1.2364	1.236	1.236	1.236	1.236	1.236
	rotor current density	6.488	6.075	5.737	5.456	5.218	5.014	4.837	4.6822	4.55	4.424
	P_copper loss stator	212.575	199.059	187.993	178.769	170.962	164.2712	158.4748	153.4038	148.931	144.957
	P_copper loss bar	110.454	103.431	97.681	92.888	88.832	85.356	82.344	79.7088	77.385	75.319
	P_copper loss End ring	36.261	33.790	31.771	30.0911	28.672	27.4578	26.4072	25.4895	24.6811	23.9636
	P_copper loss total	359.291	336.281	317.446	301.748	288.467	277.085	267.225	258.602	250.997	244.240
	P_core loss st	7.764	8.085	8.377	8.646	8.893	9.121	9.332	9.529	9.71	9.881
	P_core loss sc	20.152	21.210	22.268	23.326	24.383	25.441	26.499	27.556	28.6142	29.672
	P_core loss(st + sc)	55.833	58.590	61.292	63.9444	66.5539	69.1253	71.663	74.1705	76.651	79.1071
	P_loss fw	11	11	11	11	11	11	11	11	11	11
	P_iron loss total	66.833	69.590	72.292	74.944	77.554	80.125	82.663	85.170	87.651	90.107
	input power (kW)	1.526	1.505	1.489	1.47	1.466	1.4572	1.449	1.444	1.438	1.434
	efficiency	0.720	0.730	0.738	0.745	0.750	0.755	0.759	0.762	0.765	0.767

Table 3.2B

		dst/dsc ---------->									
parameters		1.1	1.2	1.3	1.4	1.5	1.6	1.7	1.8	1.9	2.0
Bav = 0.50 Wb/m^2	Bsc	1.2936	1.3552	1.4168	1.4784	1.54	1.6016	1.6632	1.7248	1.7864	1.848
	Bst	1.1333	1.1333	1.1333	1.1333	1.1333	1.1333	1.1333	1.1333	1.1333	1.1333
	stator current density	6.165	5.770	5.447	5.178	4.950	4.755	4.585	4.437	4.307	4.191
	Brc	0.989	1.01	1.029	1.047	1.063	1.079	1.094	1.108	1.122	1.134
	Brt	1.236	1.236	1.236	1.236	1.236	1.236	1.236	1.236	1.236	1.236
	rotor current density	6.1652	5.7704	5.4473	5.178	4.9502	4.755	4.5858	4.4379	4.307	4.191
	P_copper loss stator	181.607	169.979	160.461	152.529	145.817	140.066	135.084	130.726	126.884	123.47
	P_copper loss bar	94.363	88.321	83.376	79.254	75.767	72.778	70.19	67.925	65.929	64.155
	P_copper loss End ring	31.523	29.379	27.621	26.170	24.939	23.886	22.974	22.178	21.477	20.855
	P_copper loss total	307.493	287.681	271.466	257.954	246.524	236.732	228.249	220.831	214.290	208.48
	P_core loss st	8.626	8.983	9.308	9.607	9.881	10.135	10.369	10.5875	10.790	10.979
	P_core loss sc	24.879	26.185	27.491	28.797	30.103	31.408	32.714	34.020	35.326	36.632
	P_core loss(st + sc)	67.013	70.337	73.600	76.80	79.969	83.087	86.168	89.215	92.233	95.223
	P_loss fw	11	11	11	11	11	11	11	11	11	11
	P_iron loss total	78.013	81.337	84.600	87.8088	90.969	94.087	97.168	100.215	103.233	106.223
	input power(kW)	1.485	1.469	1.456	1.445	1.437	1.430	1.425	1.421	1.417	1.414
	efficiency	0.740	0.748	0.755	0.760	0.765	0.768	0.771	0.7741	0.776	0.777

Table 3.2C

		dst/dsc ---------->									
parameters		1.1	1.2	1.3	1.4	1.5	1.6	1.7	1.8	1.9	2
Bav = 0.55 Wb/m^2	Bsc	1.423	1.490	1.558	1.626	1.694	1.761	1.829	1.897	1.965	2.033
	Bst	1.133	1.133	1.133	1.133	1.133	1.133	1.133	1.133	1.133	1.133
	stator current density	5.953	5.569	5.255	4.993	4.771	4.581	4.417	4.273	4.147	4.034
	Brc	1.09	1.121	1.143	1.163	1.183	1.201	1.219	1.235	1.250	1.265
	Brt	1.236	1.236	1.236	1.236	1.236	1.236	1.236	1.236	1.236	1.236
	rotor current density	5.953	5.569	5.255	4.993	4.771	4.581	4.417	4.273	4.147	4.034
	P_copper loss stator	159.707	149.402	140.969	133.943	127.999	122.907	118.497	114.640	111.240	108.219
	P_copper loss bar	82.984	77.629	73.248	69.597	66.508	63.862	61.571	59.567	57.800	56.230
	P_copper loss End ring	27.968	26.060	24.501	23.205	22.109	21.173	20.3621	19.654	19.03	18.477
	P_copper loss total	270.659	253.093	238.719	226.745	216.618	207.942	200.430	193.861	188.070	182.927
	P_core loss st	9.489	9.881	10.239	10.568	10.869	11.148	11.407	11.646	11.869	12.077
	P_core loss sc	30.104	31.685	33.265	34.845	36.457	38.005	39.585	41.165	42.745	44.325
	P_core loss(st + sc)	79.188	83.133	87.009	90.825	94.589	98.306	101.982	105.622	109.228	112.806
	P_loss fw	11	11	11	11	11	11	11	11	11	11
	P_iron loss total	90.188	94.133	98.009	101.825	105.589	109.306	112.982	116.622	120.228	123.804
	input power(kW)	1.461	1.447	1.437	1.429	1.422	1.417	1.413	1.410	1.408	1.407
	efficiency	0.753	0.760	0.766	0.77	0.773	0.776	0.778	0.779	0.781	0.782

Table 3.2D

		dst/dsc ---------->									
parameters		1.1	1.2	1.3	1.4	1.5	1.6	1.7	1.8	1.9	2
Bav = 0.60 Wb/m^2	Bsc	1.5523	1.6262	1.7002	1.7741	1.848	1.9219	1.9958	2.0698	2.1437	2.2176
	Bst	1.1333	1.1333	1.1333	1.1333	1.1333	1.1333	1.1333	1.1333	1.1333	1.1333
	stator current density	5.8029	5.4252	5.1162	4.8589	4.6412	4.4548	4.2934	4.1523	4.0279	3.9174
	Brc	1.1756	1.1997	1.2221	1.2432	1.263	1.2817	1.2993	1.316	1.3319	1.3469
	Brt	1.2364	1.2364	1.2364	1.2364	1.2364	1.2364	1.2364	1.2364	1.2364	1.2364
	rotor current density	5.8029	5.4252	5.1162	4.8589	4.6412	4.4548	4.2934	4.1523	4.0279	3.9174
	P_copper loss stator	142.5914	133.3111	125.719	119.3947	114.0467	109.466	105.4993	102.0315	98.9743	96.2593
	P_copper loss bar	74.0906	69.2686	65.3237	62.0376	59.2588	56.8787	54.8176	53.0157	51.4272	50.0164
	P_copper loss End ring	25.0602	23.3389	21.9332	20.764	19.7767	18.9322	18.2018	17.5639	17.0021	16.5037
	P_copper loss total	241.7422	225.9187	212.9758	202.1964	193.0822	185.2769	178.5187	172.611	167.4036	162.7795
	P_core loss st	10.3522	10.78	11.1705	11.5286	11.858	12.162	12.4435	12.705	12.9483	13.1755
	P_core loss sc	35.827	37.7074	39.5877	41.468	43.3484	45.2287	47.1091	48.9894	50.8698	52.7501
	P_core loss(st + sc)	92.3584	96.9746	101.5165	105.9932	110.4127	114.7815	119.1052	123.3888	127.6362	131.8512
	P_loss fw	11	11	11	11	11	11	11	11	11	11
	P_iron loss total	103.3584	107.9746	112.5165	116.9932	121.4127	125.7815	130.1052	134.3888	138.6362	142.8512
	input power(kW)	1.4451	1.4339	1.4255	1.4192	1.4145	1.4111	1.4086	1.407	1.406	1.4056
	efficiency	0.7612	0.7671	0.7717	0.7751	0.7777	0.7796	0.7809	0.7818	0.7823	0.7826

Table 3.2E

		dst/dsc ---------->									
parameters		1.1	1.2	1.3	1.4	1.5	1.6	1.7	1.8	1.9	2
Bav = 0.65 Wb/m^2	Bsc	1.682	1.762	1.842	1.922	2.002	2.082	2.162	2.242	2.322	2.402
	Bst	1.133	1.133	1.133	1.133	1.133	1.133	1.133	1.133	1.133	1.133
	stator current density	5.727	5.350	5.043	4.78	4.569	4.384	4.223	4.083	3.959	3.849
	Brc	1.247	1.274	1.297	1.318	1.339	1.358	1.375	1.392	1.408	1.424
	Brt	1.236	1.236	1.236	1.236	1.236	1.236	1.236	1.236	1.236	1.236
	rotor current density	5.727	5.350	5.042	4.786	4.566	4.384	4.223	4.083	3.959	3.849
	P_copper loss stator	129.961	121.42	114.435	108.619	103.702	99.492	95.847	92.661	89.854	87.360
	P_copper loss bar	67.528	63.09	59.460	56.439	53.884	51.696	49.803	48.147	46.688	45.393
	P_copper loss End ring	22.924	21.337	20.042	18.965	18.055	17.277	16.605	16.018	15.501	15.042
	P_copper loss total	220.413	205.8474	193.937	184.022	175.641	168.465	162.254	156.826	152.043	147.796
	P_core loss st	11.2149	11.6783	12.1014	12.4893	12.8461	13.1755	13.4805	13.763	14.027	14.273
	P_core loss sc	42.047	44.2538	46.4606	48.6674	50.874	53.080	55.287	57.494	59.701	61.908
	P_core loss(st + sc)	106.5237	111.8641	117.124	122.313	127.440	132.512	137.536	142.516	147.457	152.363
	P_loss fw	11	11	11	11	11	11	11	11	11	11
	P_iron loss total	117.524	122.864	128.12	133.313	138.440	143.512	148.536	153.516	158.457	163.363
	input power(kW)	1.438	1.428	1.422	1.417	1.414	1.412	1.410	1.410	1.410	1.411
	efficiency	0.765	0.770	0.773	0.776	0.778	0.779	0.779	0.78	0.779	0.779

Chapter 4

OBSERVATION, GRAPHS AND RESULT

The internal dimensions of a 1.1kW 415V 3 phase induction motor were calculated using the equations described in Chapter 3. Flux density in different parts of the machine; current density in the stator and rotor winding for different values of $\mathbf{B_{av}}$ and the ratio $\boldsymbol{d_{st}/d_{sc}}$ tabulated in **Tabe 3.2** are plotted below.

4.1 GRAPHS FOR B_{av} = 0.45 Wb/m^2

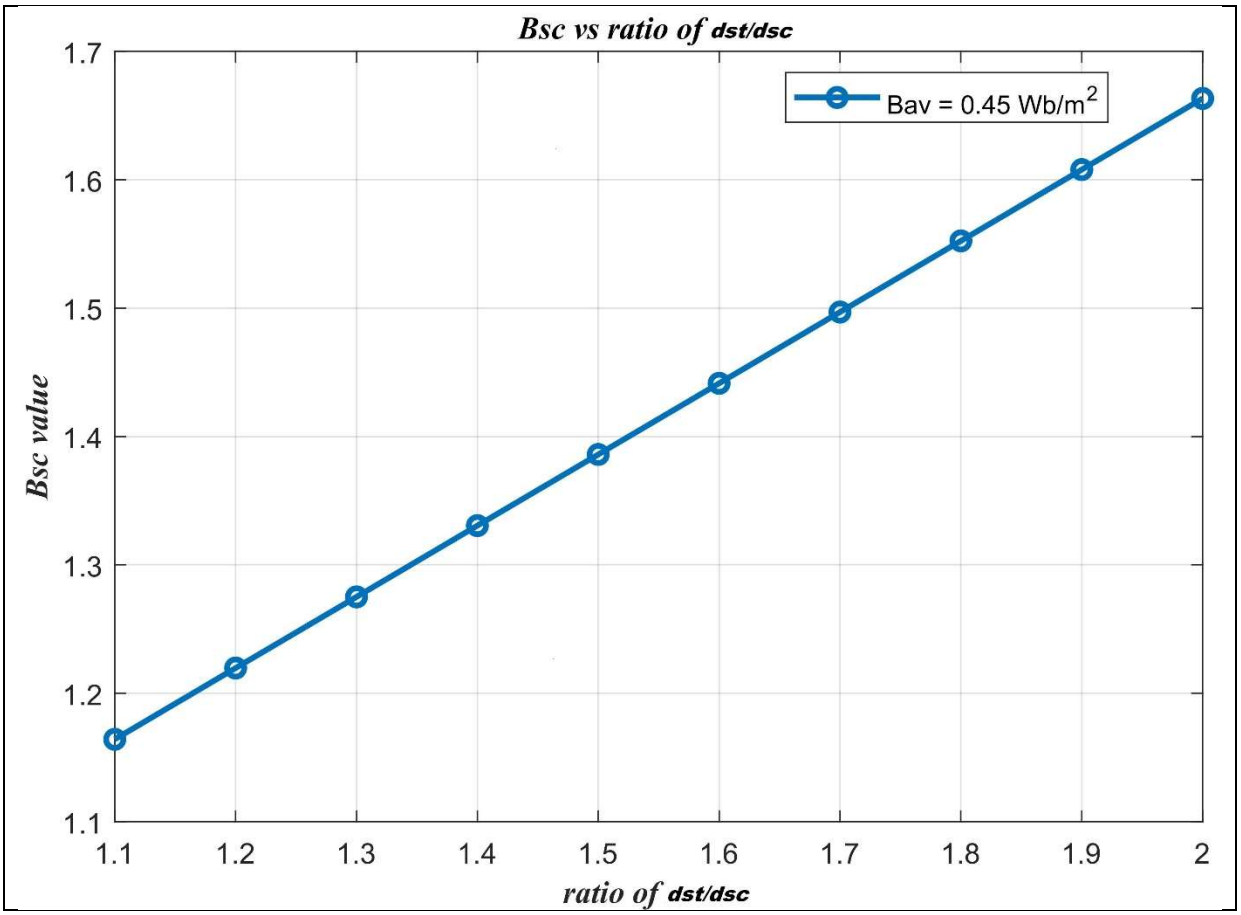

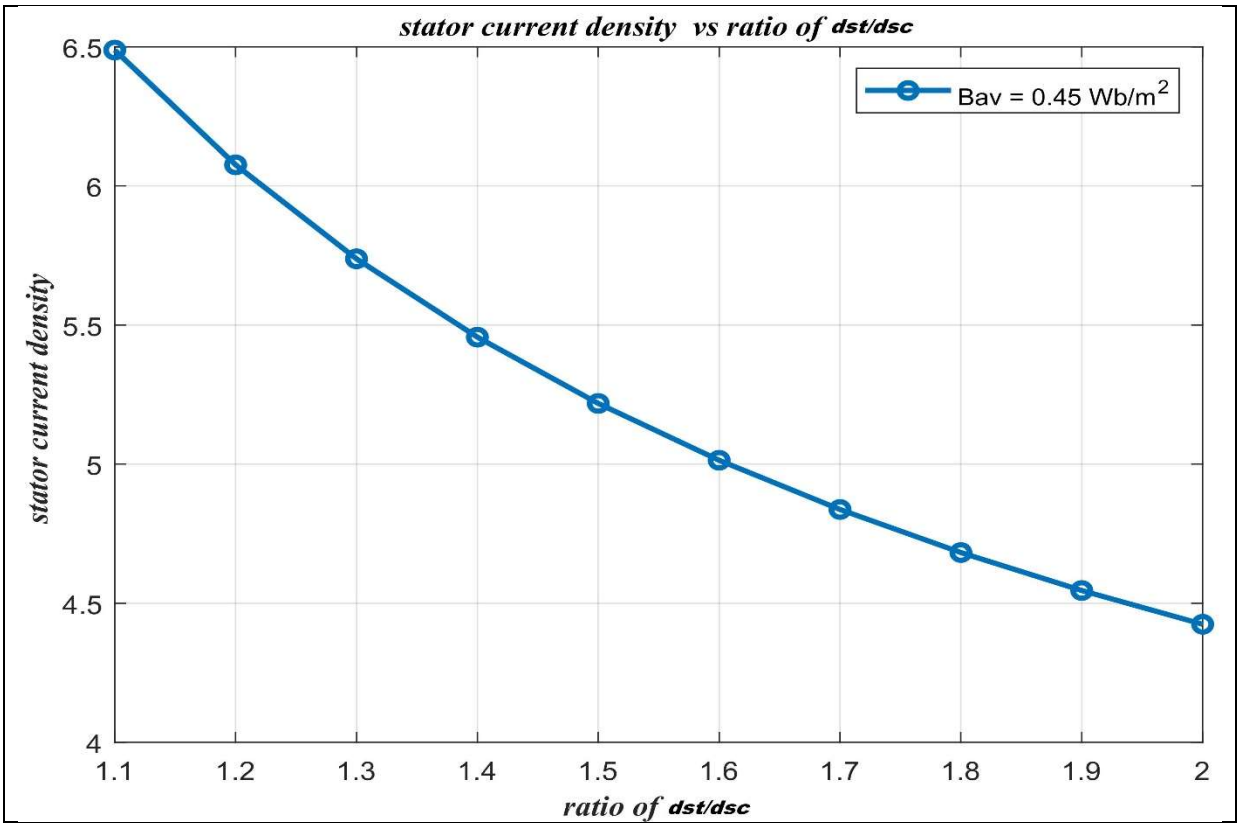
stator current density vs ratio of dst/dsc
Bav = 0.45 Wb/m2
stator current density
ratio of dst/dsc
6.5
6
5.5
5
4.5
4
1.1
1.2
1.3
1.4
1.5
1.6
1.7
1.8
1.9
2

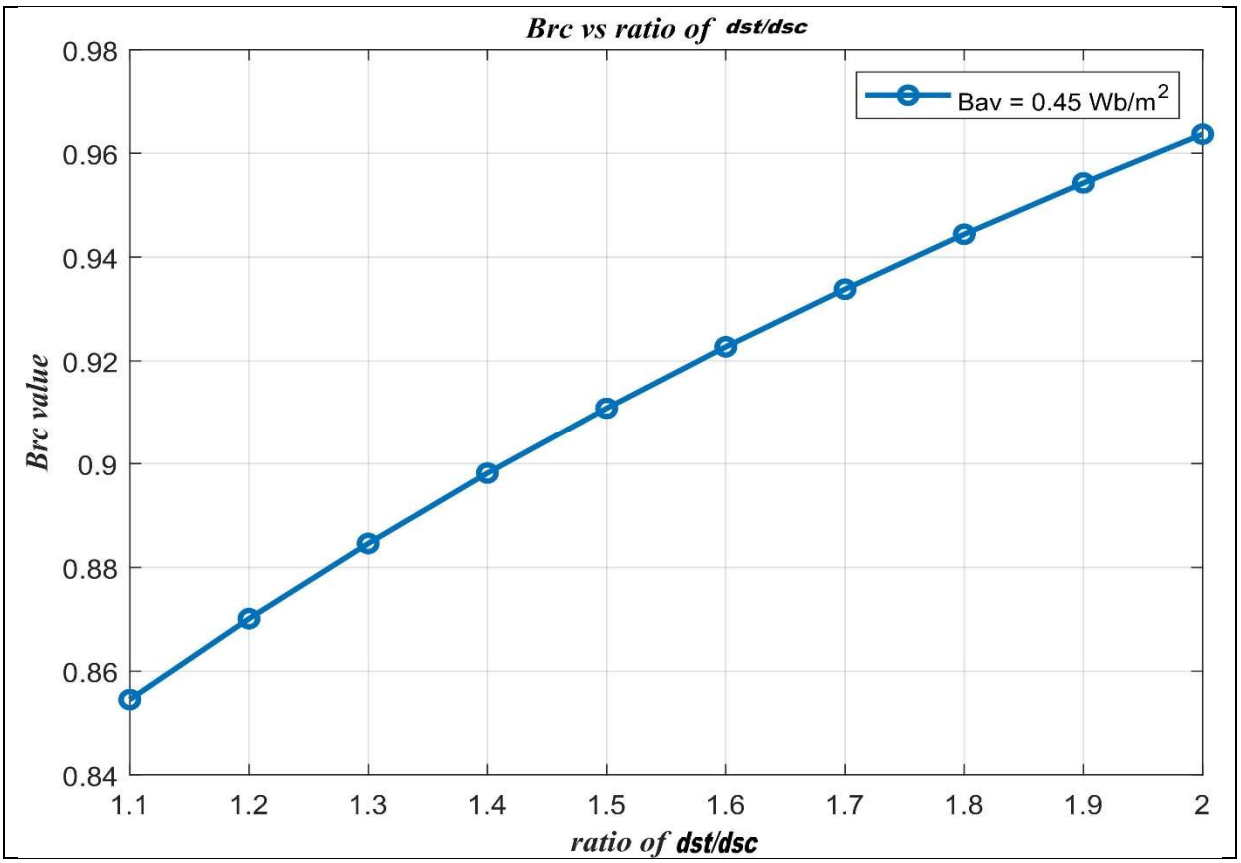
Brc vs ratio of dst/dsc
Bav = 0.45 Wb/m2
Brc value
ratio of dst/dsc
0.98
0.96
0.94
0.92
0.9
0.88
0.86
0.84
1.1
1.2
1.3
1.4
1.5
1.6
1.7
1.8
1.9
2

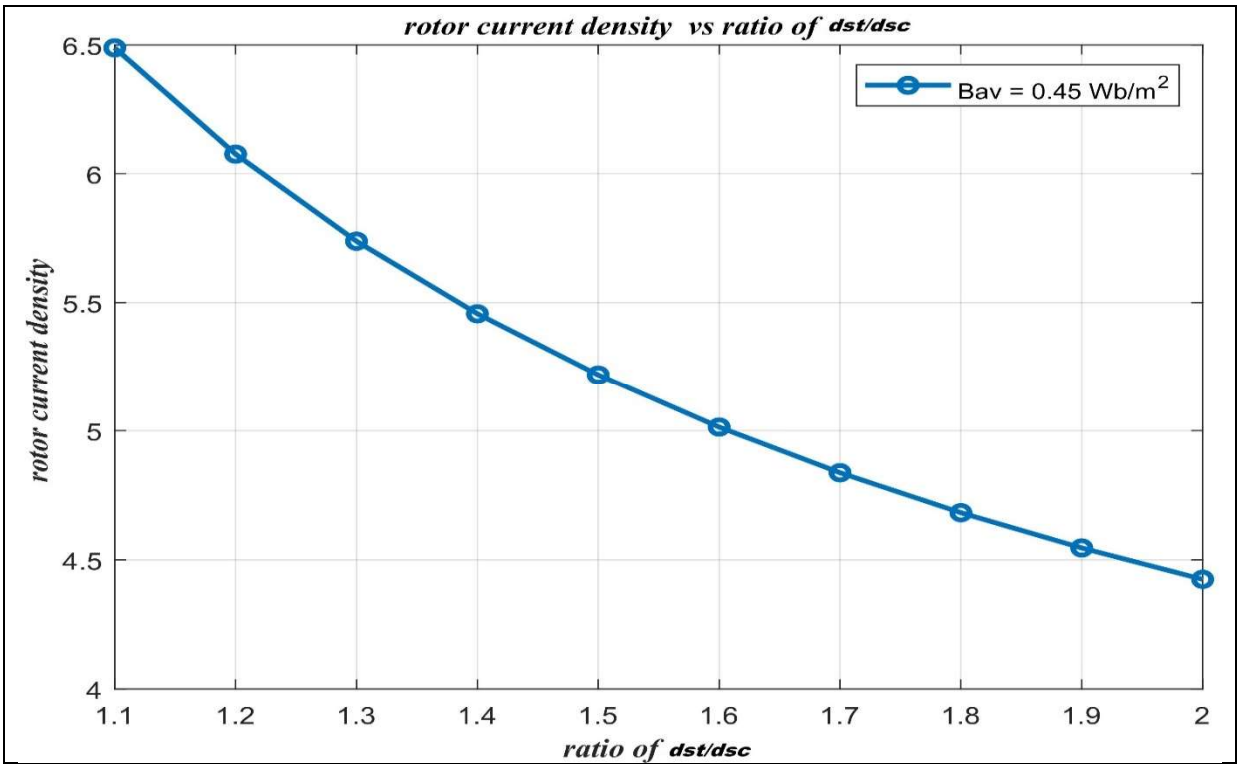
rotor current density vs ratio of dst/dsc
Bav = 0.45 Wb/m2
rotor current density
ratio of dst/dsc
6.5
6
5.5
5
4.5
4
1.1
1.2
1.3
1.4
1.5
1.6
1.7
1.8
1.9
2

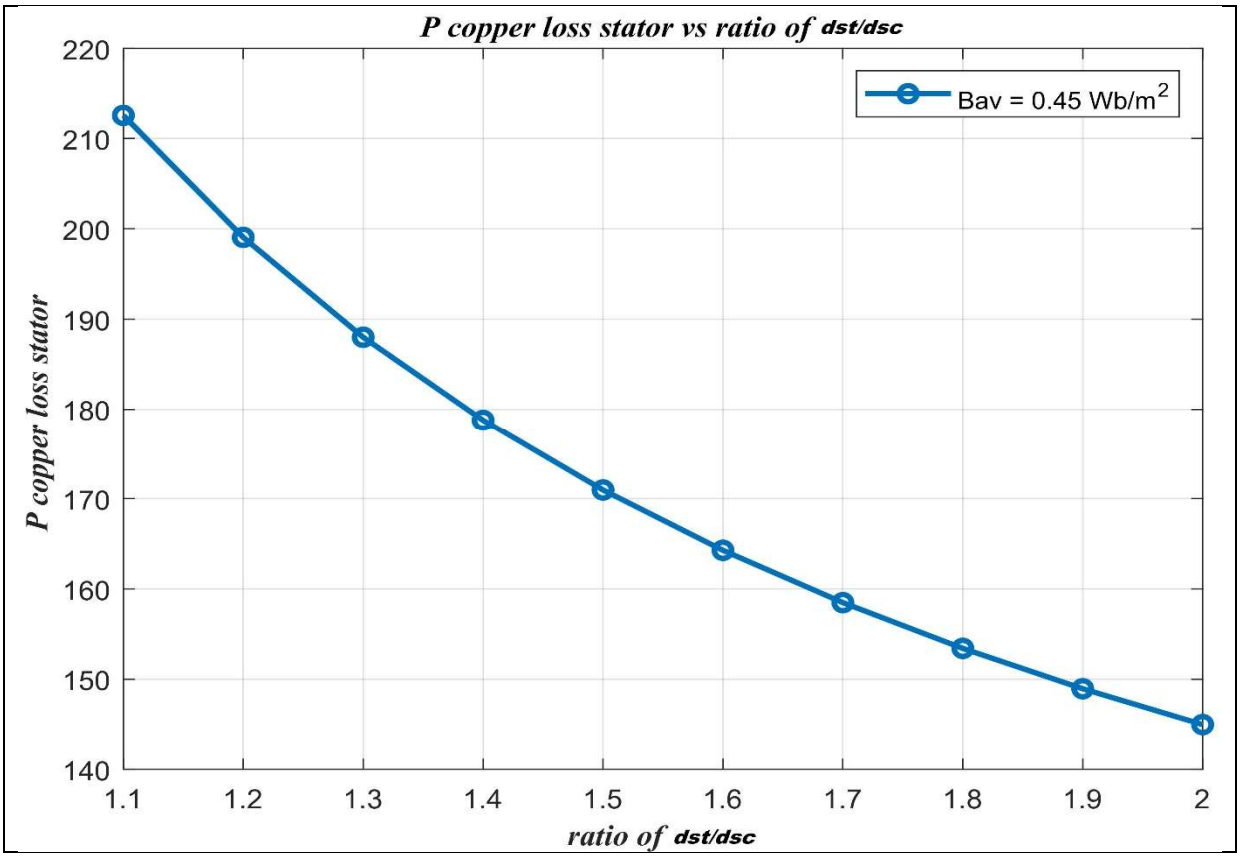
P copper loss stator vs ratio of dst/dsc
Bav = 0.45 Wb/m2
P copper loss stator
ratio of dst/dsc
220
210
200
190
180
170
160
150
140
1.1
1.2
1.3
1.4
1.5
1.6
1.7
1.8
1.9
2

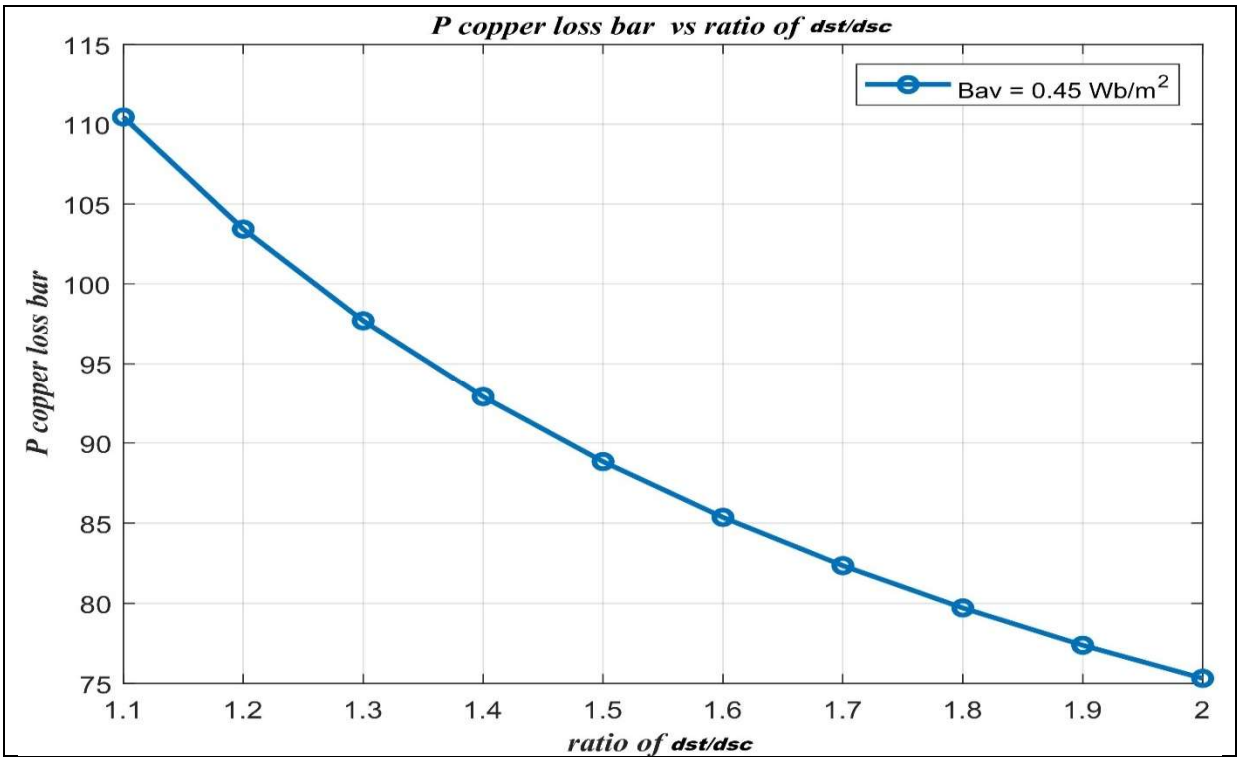
P copper loss bar vs ratio of dst/dsc
Bav = 0.45 Wb/m2
P copper loss bar
ratio of dst/dsc
115
110
105
100
95
90
85
80
75
1.1
1.2
1.3
1.4
1.5
1.6
1.7
1.8
1.9
2

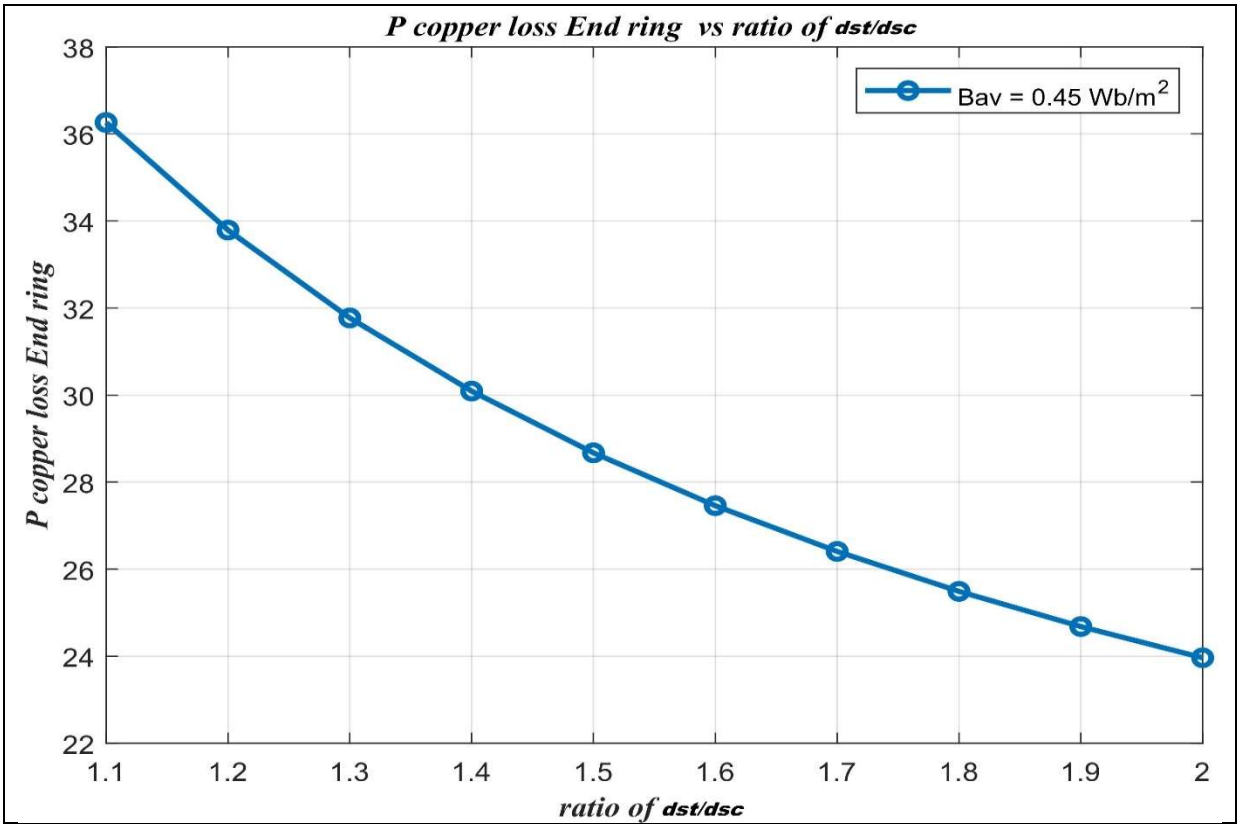
P copper loss End ring vs ratio of dst/dsc
Bav = 0.45 Wb/m2
P copper loss End ring
ratio of dst/dsc
38
36
34
32
30
28
26
24
22
1.1
1.2
1.3
1.4
1.5
1.6
1.7
1.8
1.9
2

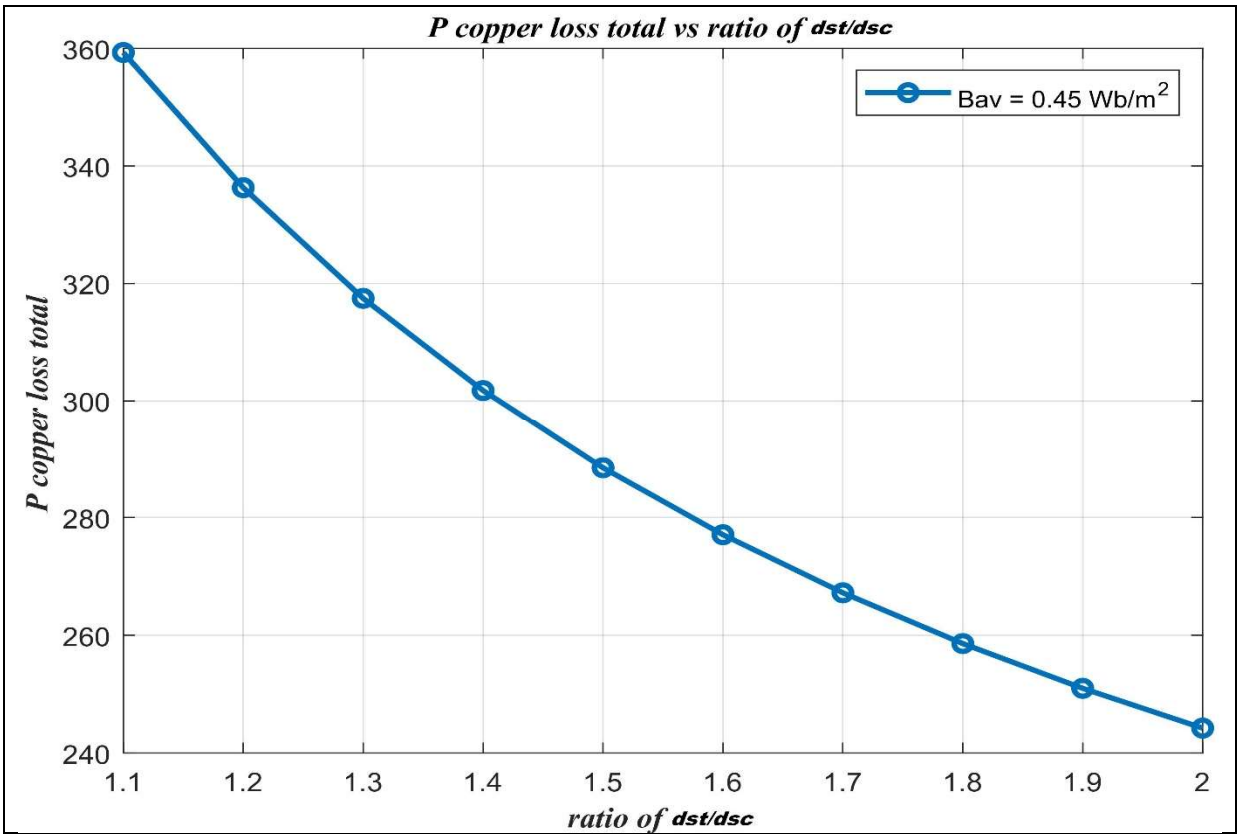
P copper loss total vs ratio of dst/dsc
Bav = 0.45 Wb/m2
P copper loss total
ratio of dst/dsc
360
340
320
300
280
260
240
1.1
1.2
1.3
1.4
1.5
1.6
1.7
1.8
1.9
2

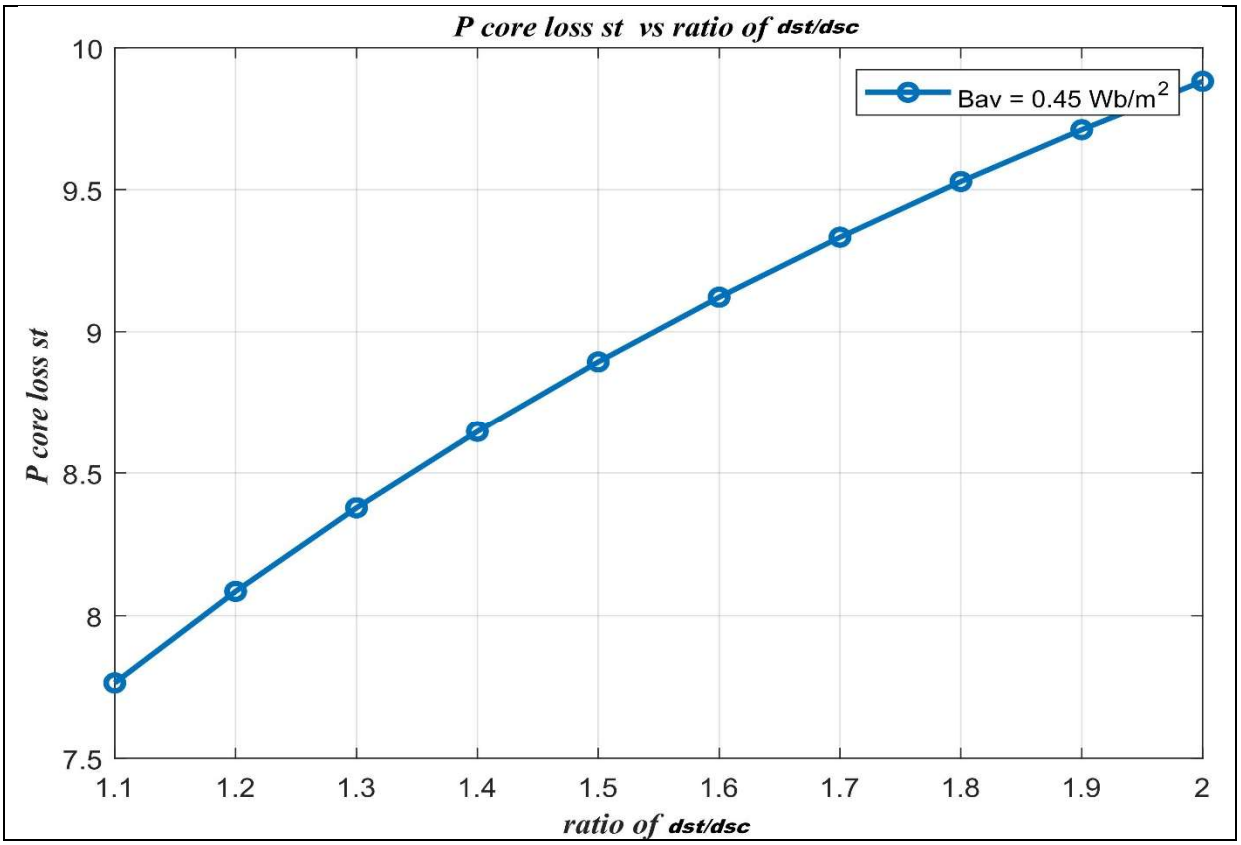
P core loss st vs ratio of dst/dsc
Bav = 0.45 Wb/m2
P core loss st
ratio of dst/dsc
10
9.5
9
8.5
8
7.5
1.1
1.2
1.3
1.4
1.5
1.6
1.7
1.8
1.9
2

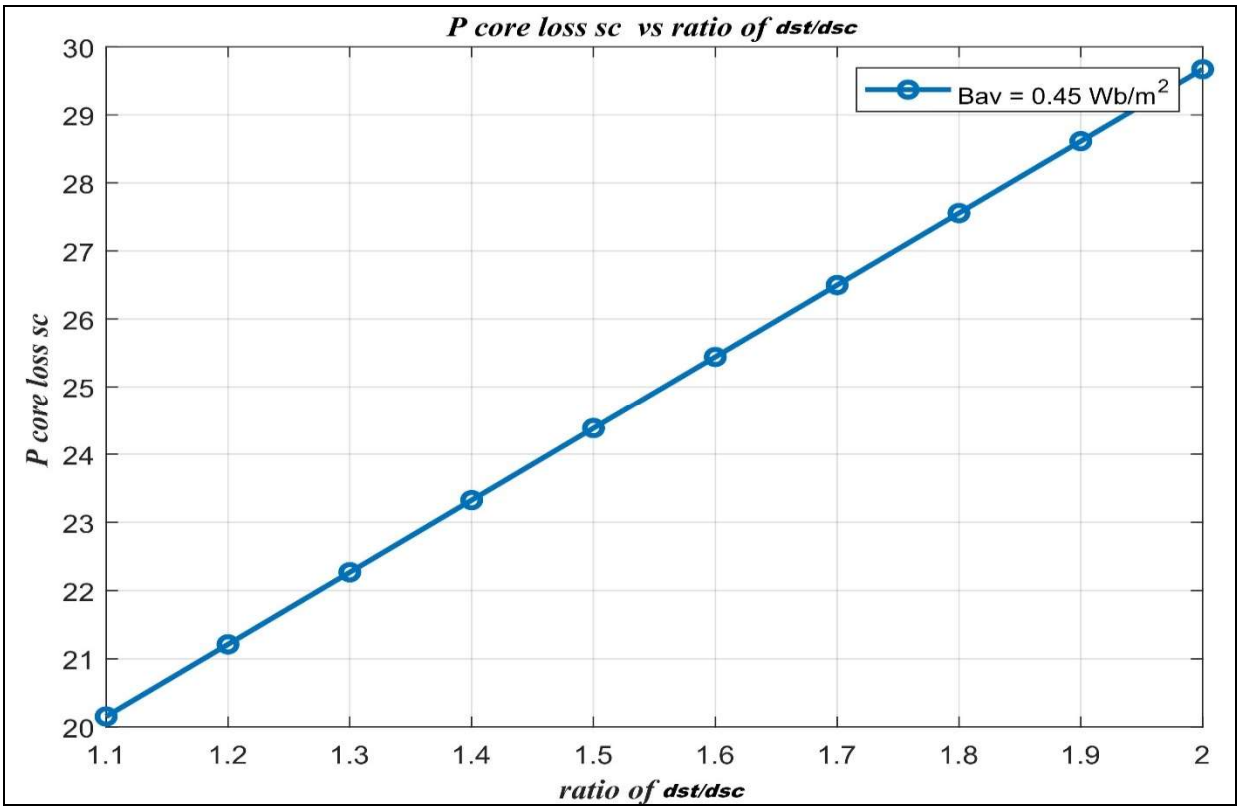
P core loss sc vs ratio of dst/dsc
Bav = 0.45 Wb/m2
P core loss sc
ratio of dst/dsc
30
29
28
27
26
25
24
23
22
21
20
1.1
1.2
1.3
1.4
1.5
1.6
1.7
1.8
1.9
2

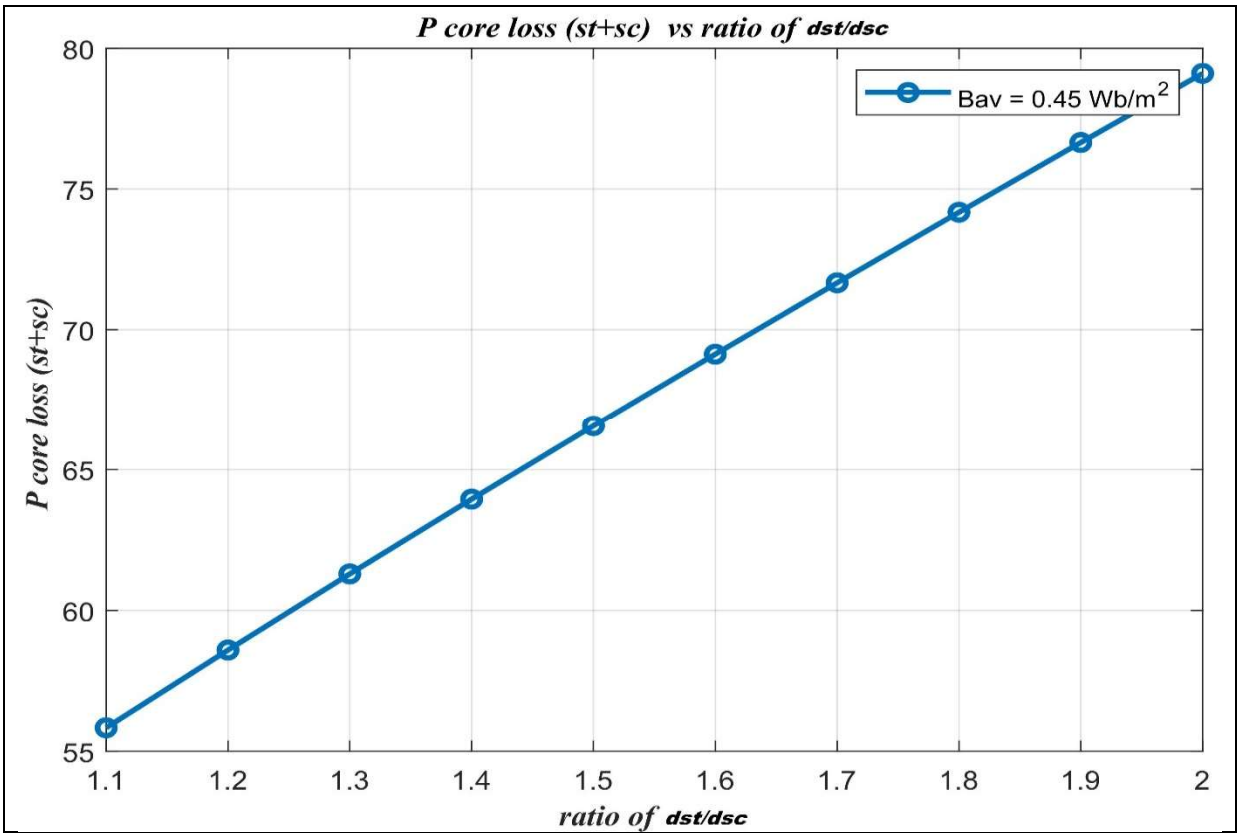
P core loss (st+sc) vs ratio of dst/dsc
Bav = 0.45 Wb/m2
P core loss (st+sc)
ratio of dst/dsc
80
75
70
65
60
55
1.1
1.2
1.3
1.4
1.5
1.6
1.7
1.8
1.9
2

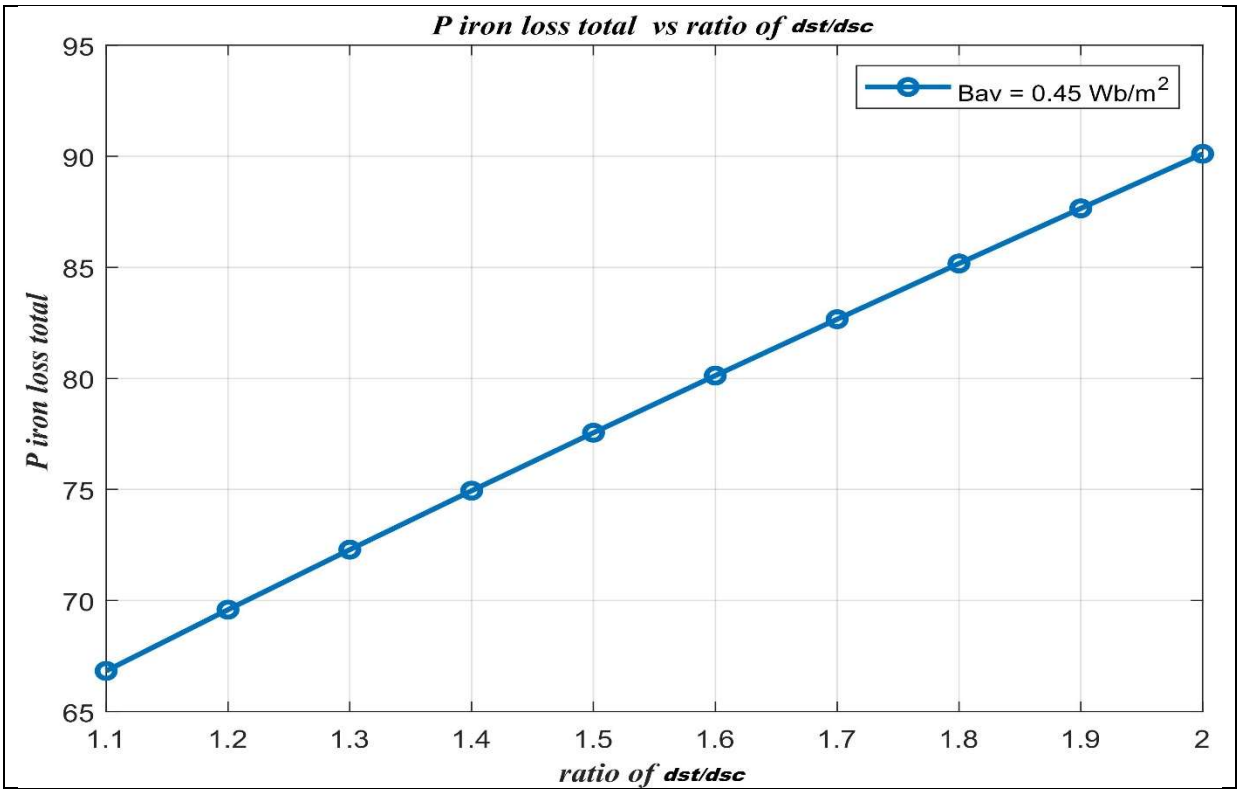
P iron loss total vs ratio of dst/dsc
Bav = 0.45 Wb/m2
P iron loss total
ratio of dst/dsc
95
90
85
80
75
70
65
1.1
1.2
1.3
1.4
1.5
1.6
1.7
1.8
1.9
2

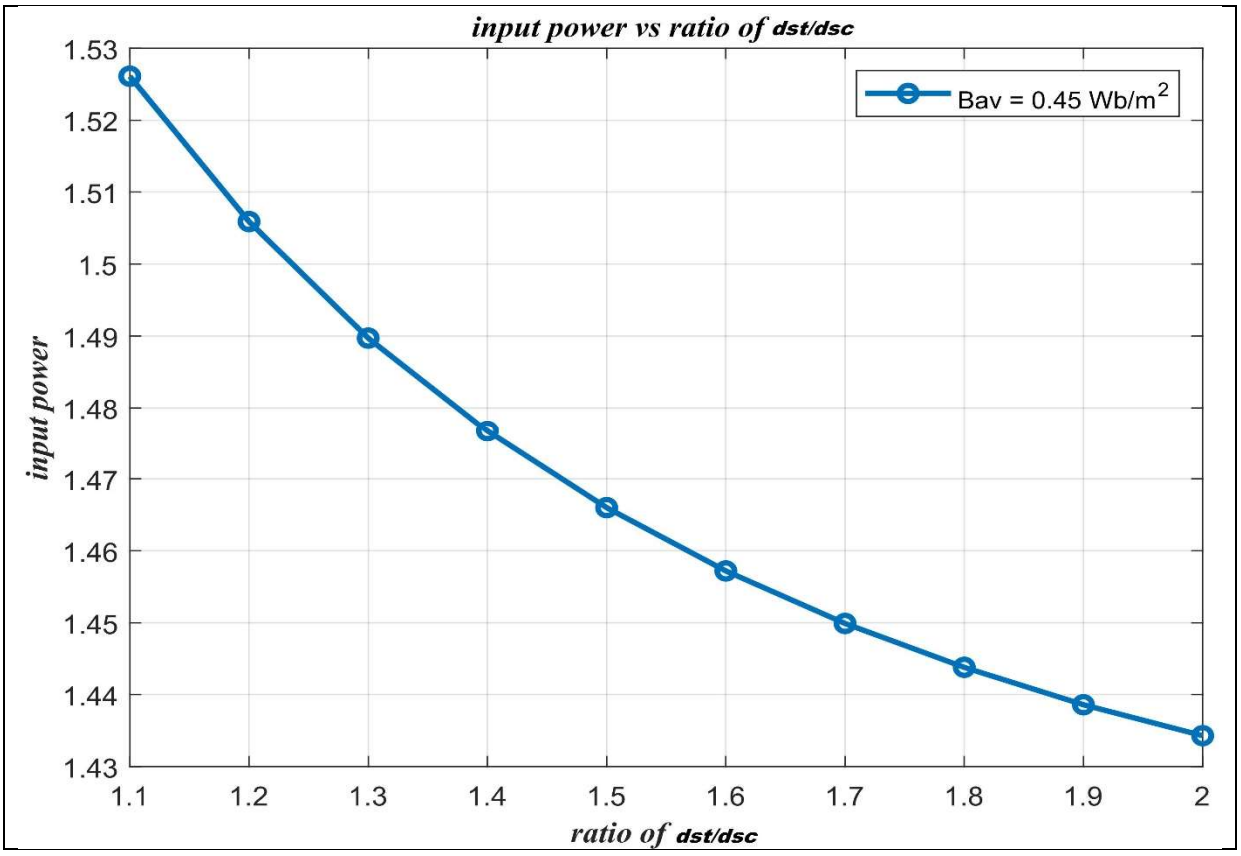
input power vs ratio of dst/dsc
Bav = 0.45 Wb/m2
input power
ratio of dst/dsc
1.53
1.52
1.51
1.5
1.49
1.48
1.47
1.46
1.45
1.44
1.43
1.1
1.2
1.3
1.4
1.5
1.6
1.7
1.8
1.9
2

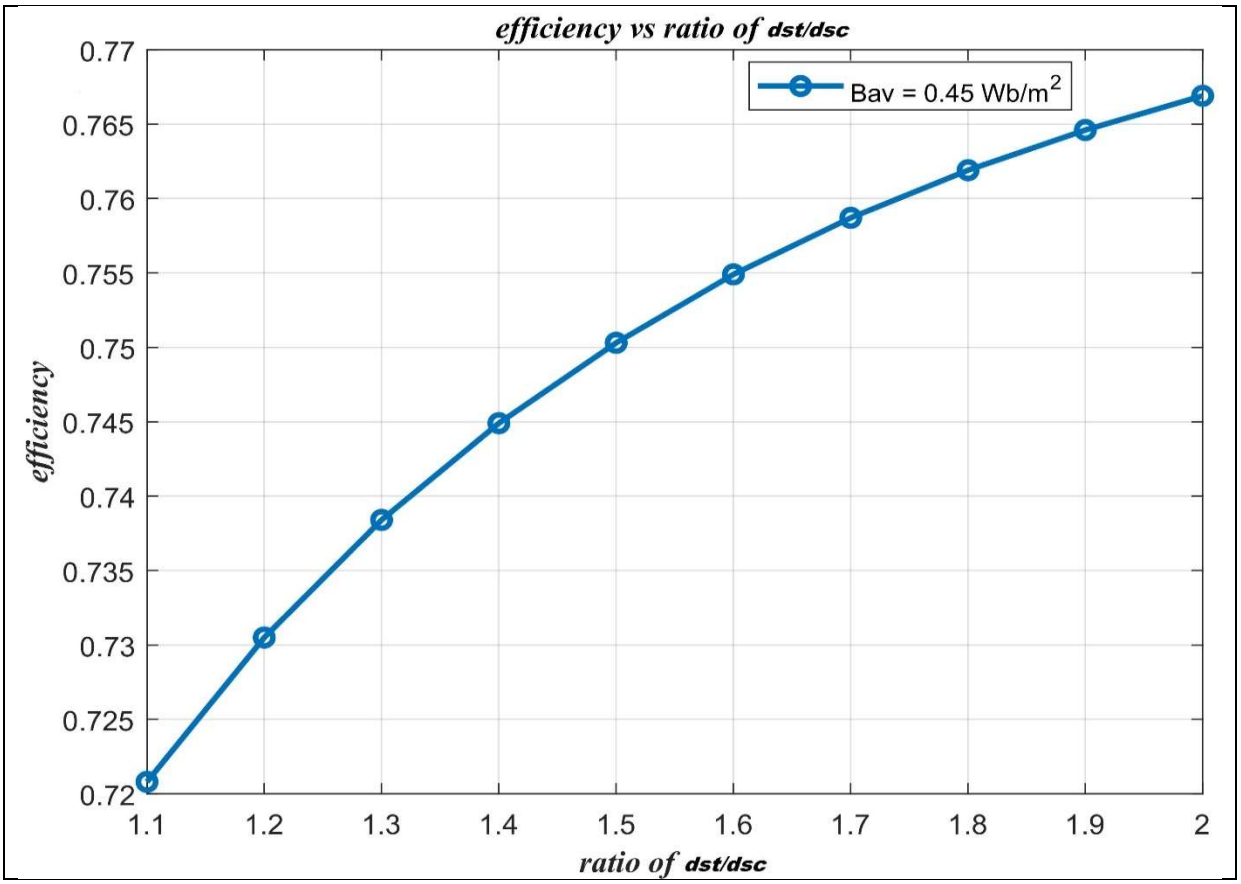

4.2 COMPARISION BETWEEN DIFFERENT B_{av} VALUES

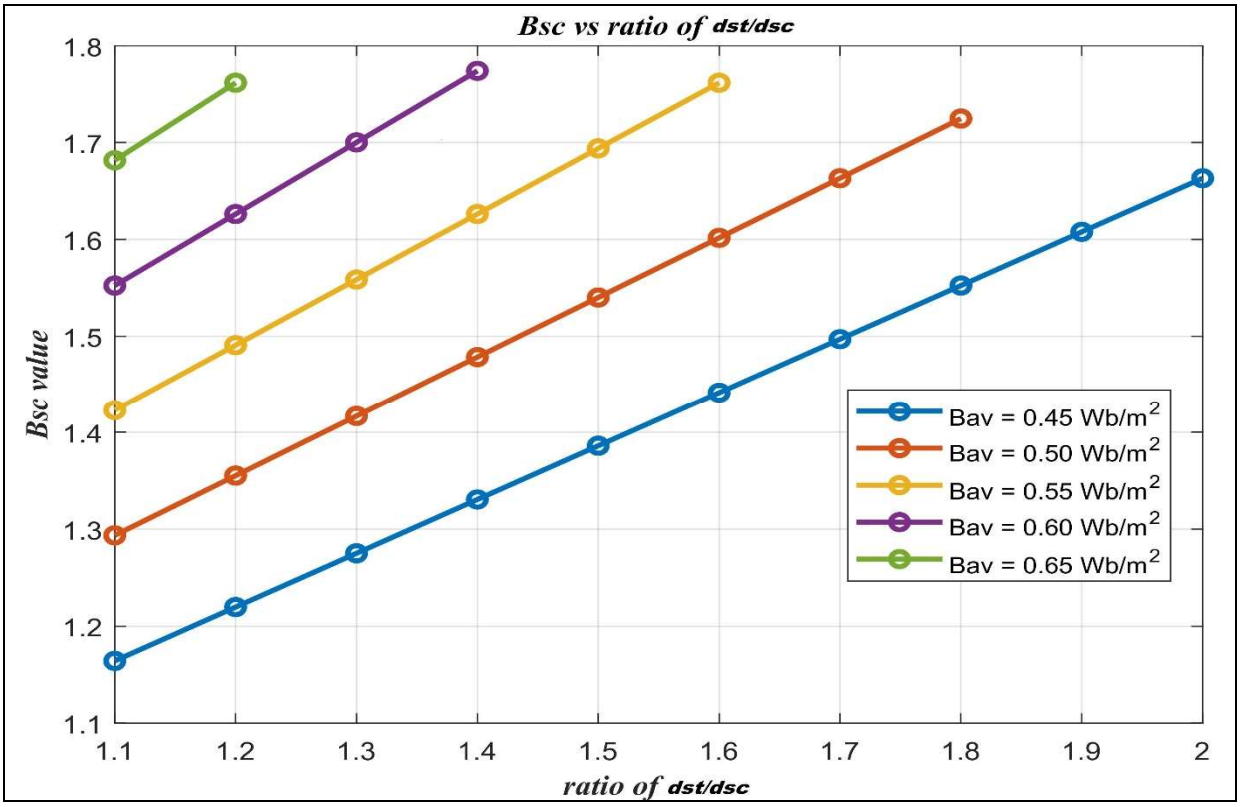

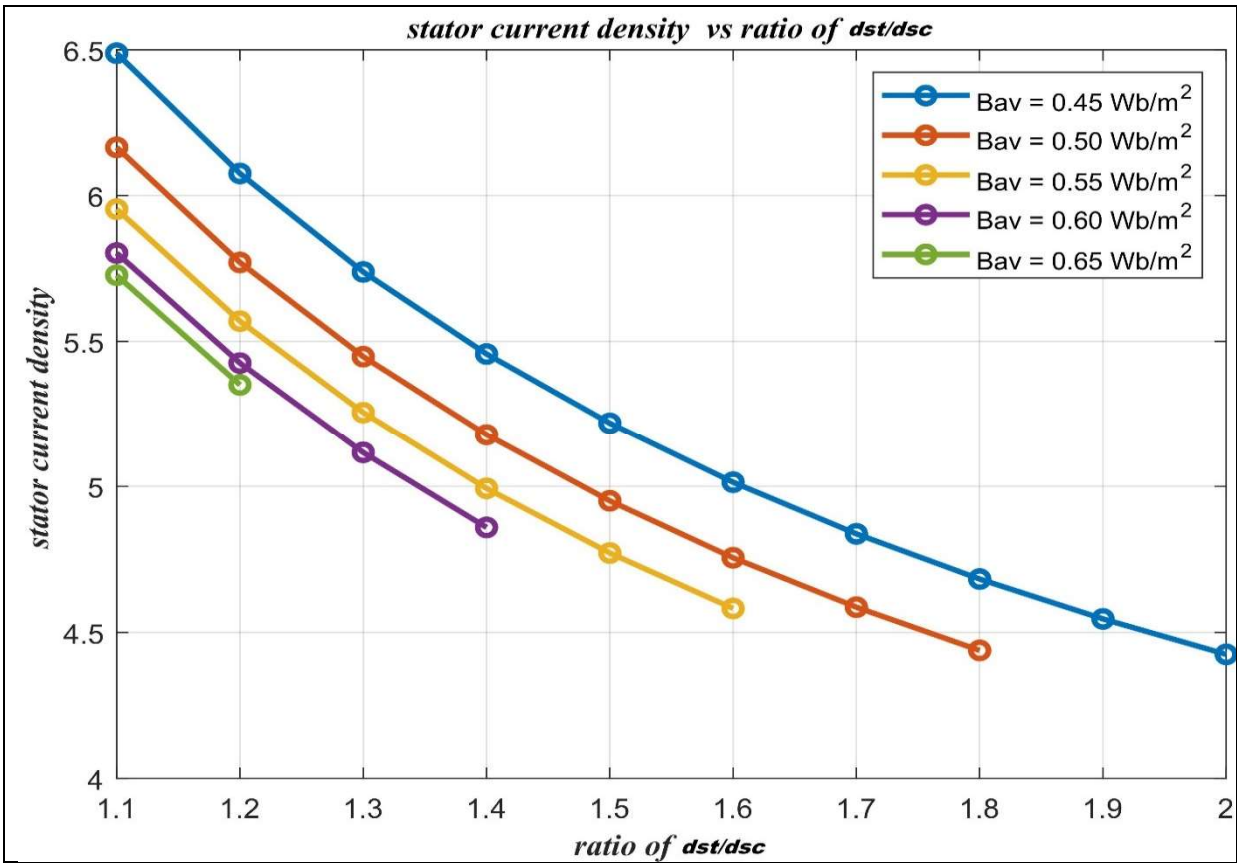
stator current density vs ratio of dst/dsc
stator current density
ratio of dst/dsc
Bav = 0.45 Wb/m2
Bav = 0.50 Wb/m2
Bav = 0.55 Wb/m2
Bav = 0.60 Wb/m2
Bav = 0.65 Wb/m2
6.5
6
5.5
5
4.5
4
1.1
1.2
1.3
1.4
1.5
1.6
1.7
1.8
1.9
2

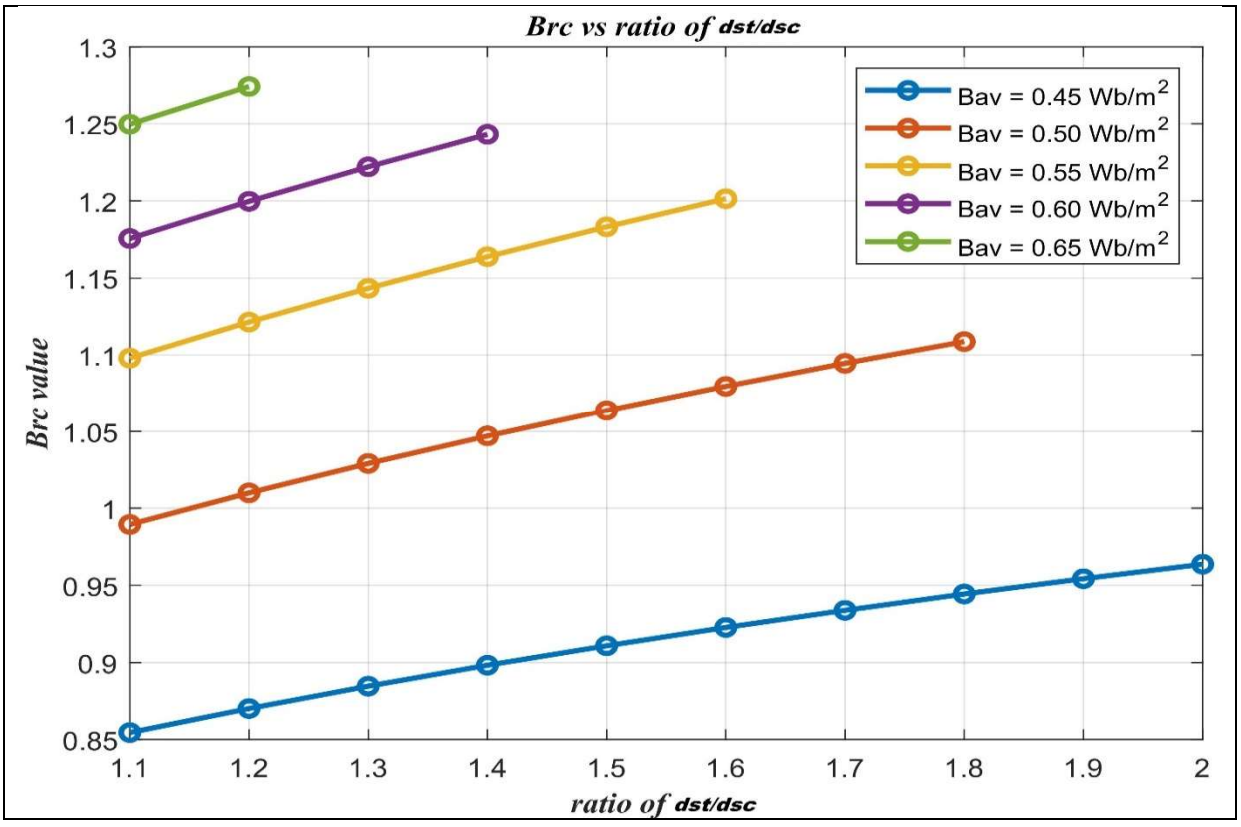
Brc vs ratio of dst/dsc
Brc value
ratio of dst/dsc
Bav = 0.45 Wb/m2
Bav = 0.50 Wb/m2
Bav = 0.55 Wb/m2
Bav = 0.60 Wb/m2
Bav = 0.65 Wb/m2
1.3
1.25
1.2
1.15
1.1
1.05
1
0.95
0.9
0.85
1.1
1.2
1.3
1.4
1.5
1.6
1.7
1.8
1.9
2

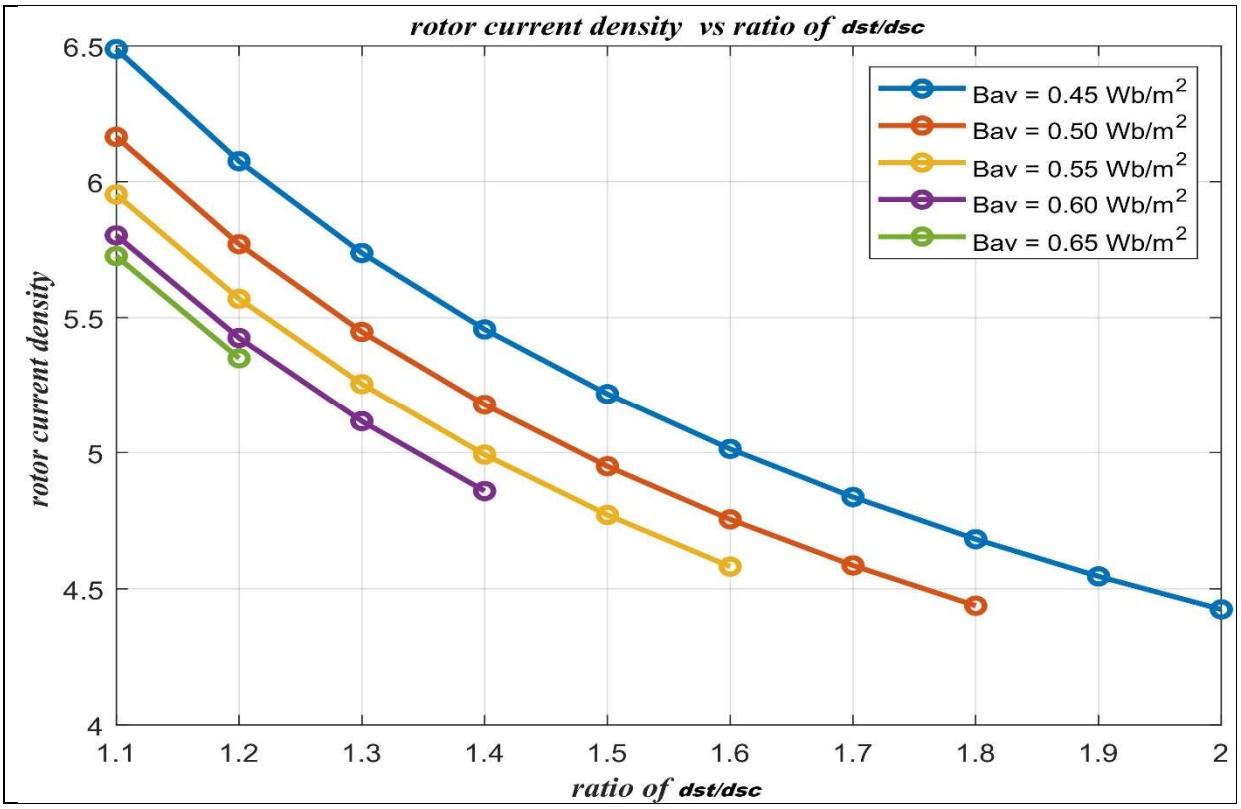
rotor current density vs ratio of dst/dsc
rotor current density
ratio of dst/dsc
Bav = 0.45 Wb/m2
Bav = 0.50 Wb/m2
Bav = 0.55 Wb/m2
Bav = 0.60 Wb/m2
Bav = 0.65 Wb/m2
6.5
6
5.5
5
4.5
4
1.1
1.2
1.3
1.4
1.5
1.6
1.7
1.8
1.9
2

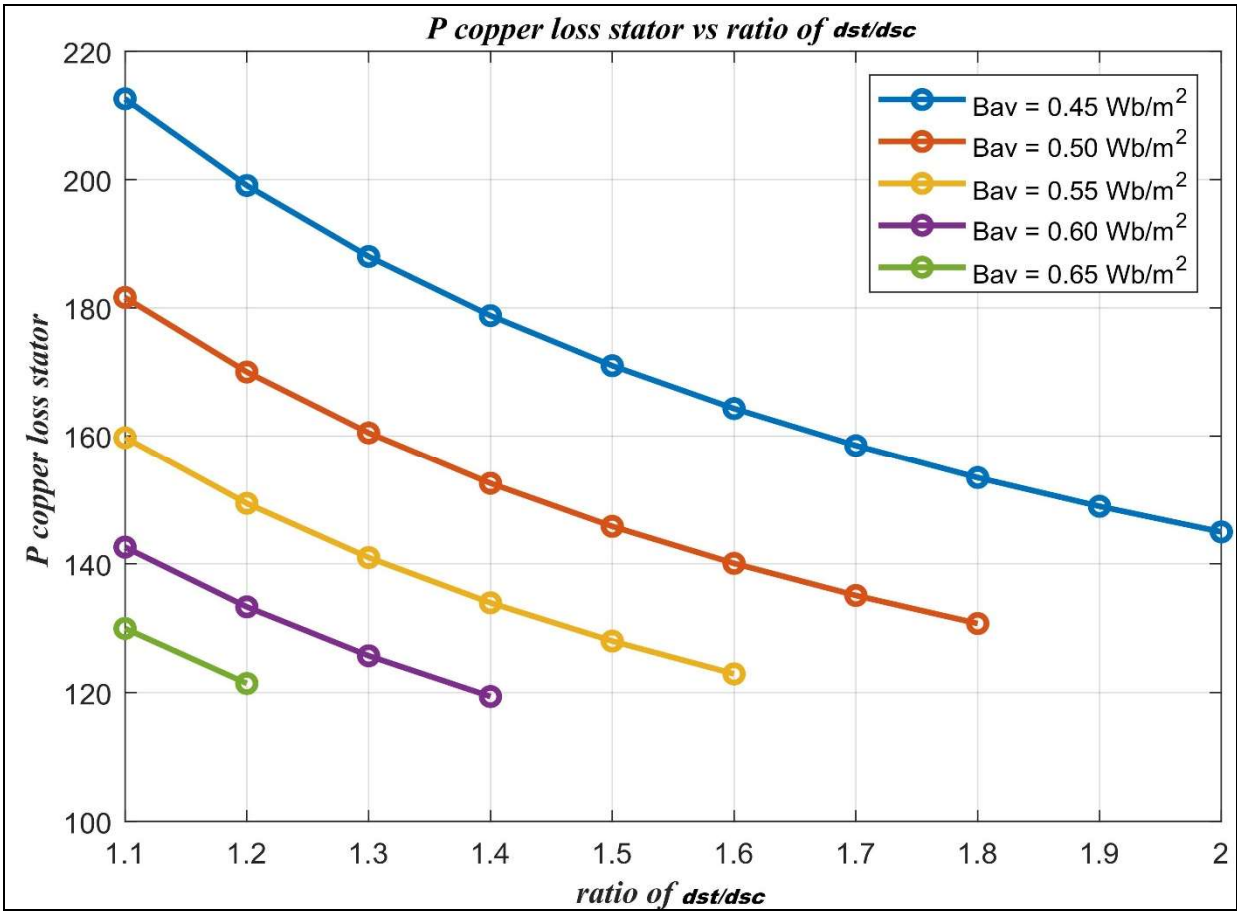
P copper loss stator vs ratio of dst/dsc
P copper loss stator
ratio of dst/dsc
Bav = 0.45 Wb/m2
Bav = 0.50 Wb/m2
Bav = 0.55 Wb/m2
Bav = 0.60 Wb/m2
Bav = 0.65 Wb/m2
220
200
180
160
140
120
100
1.1
1.2
1.3
1.4
1.5
1.6
1.7
1.8
1.9
2

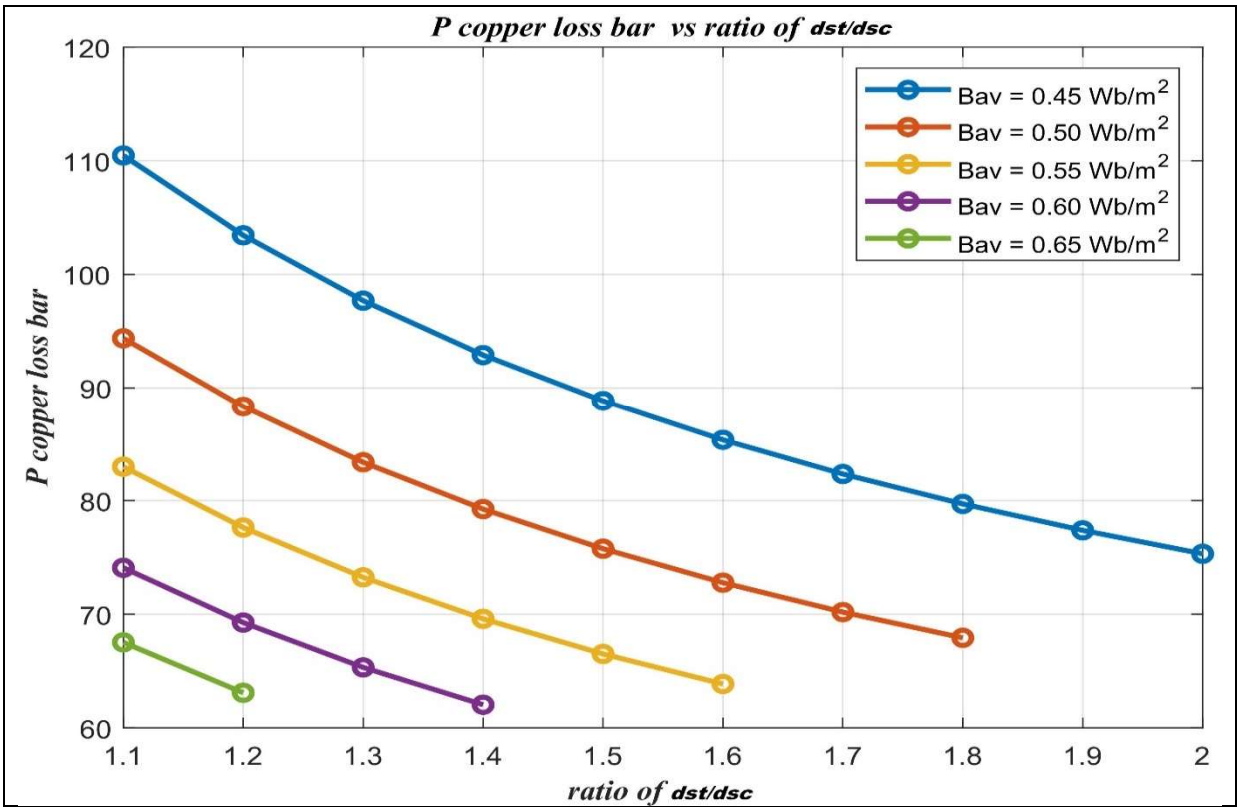
P copper loss bar vs ratio of dst/dsc
P copper loss bar
ratio of dst/dsc
Bav = 0.45 Wb/m2
Bav = 0.50 Wb/m2
Bav = 0.55 Wb/m2
Bav = 0.60 Wb/m2
Bav = 0.65 Wb/m2
120
110
100
90
80
70
60
1.1
1.2
1.3
1.4
1.5
1.6
1.7
1.8
1.9
2

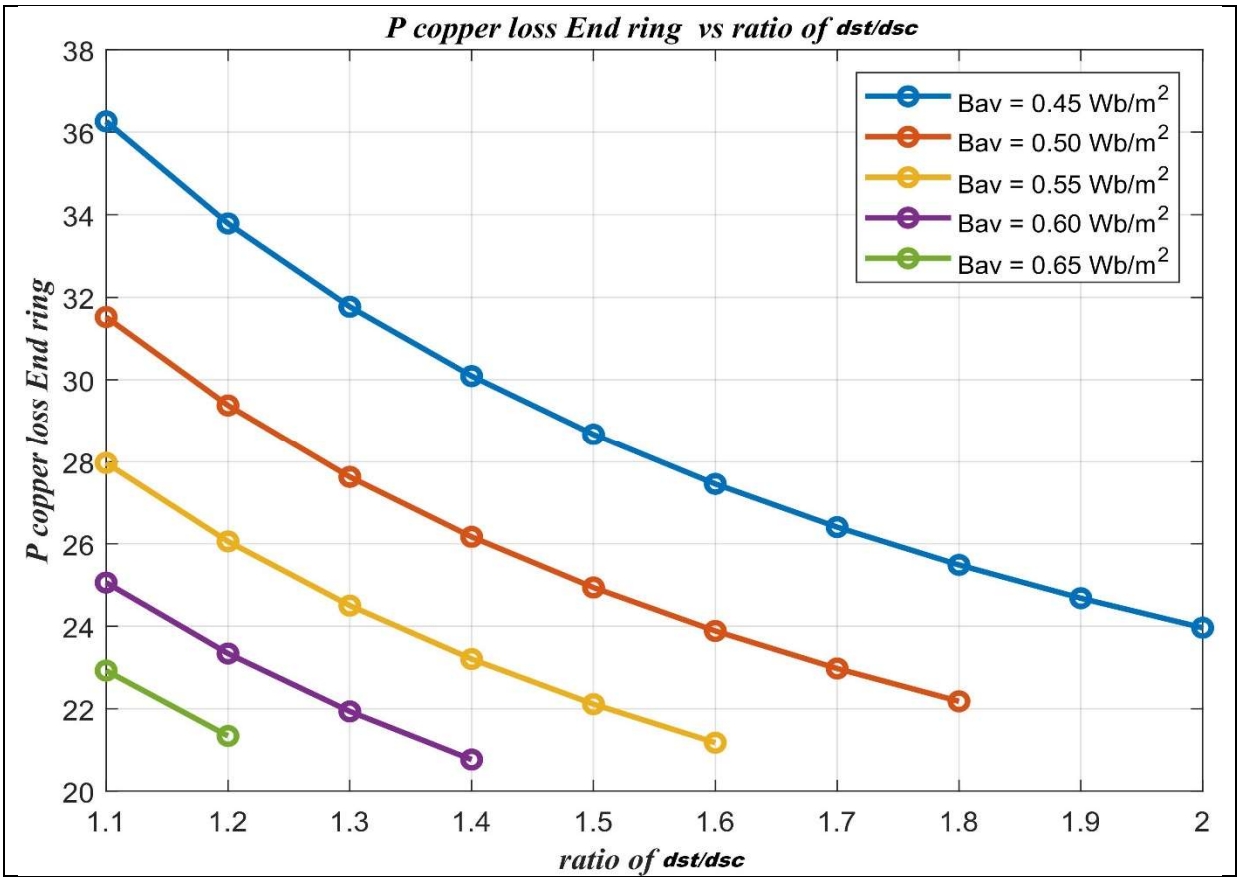
P copper loss End ring vs ratio of dst/dsc
P copper loss End ring
ratio of dst/dsc
Bav = 0.45 Wb/m2
Bav = 0.50 Wb/m2
Bav = 0.55 Wb/m2
Bav = 0.60 Wb/m2
Bav = 0.65 Wb/m2
38
36
34
32
30
28
26
24
22
20
1.1
1.2
1.3
1.4
1.5
1.6
1.7
1.8
1.9
2

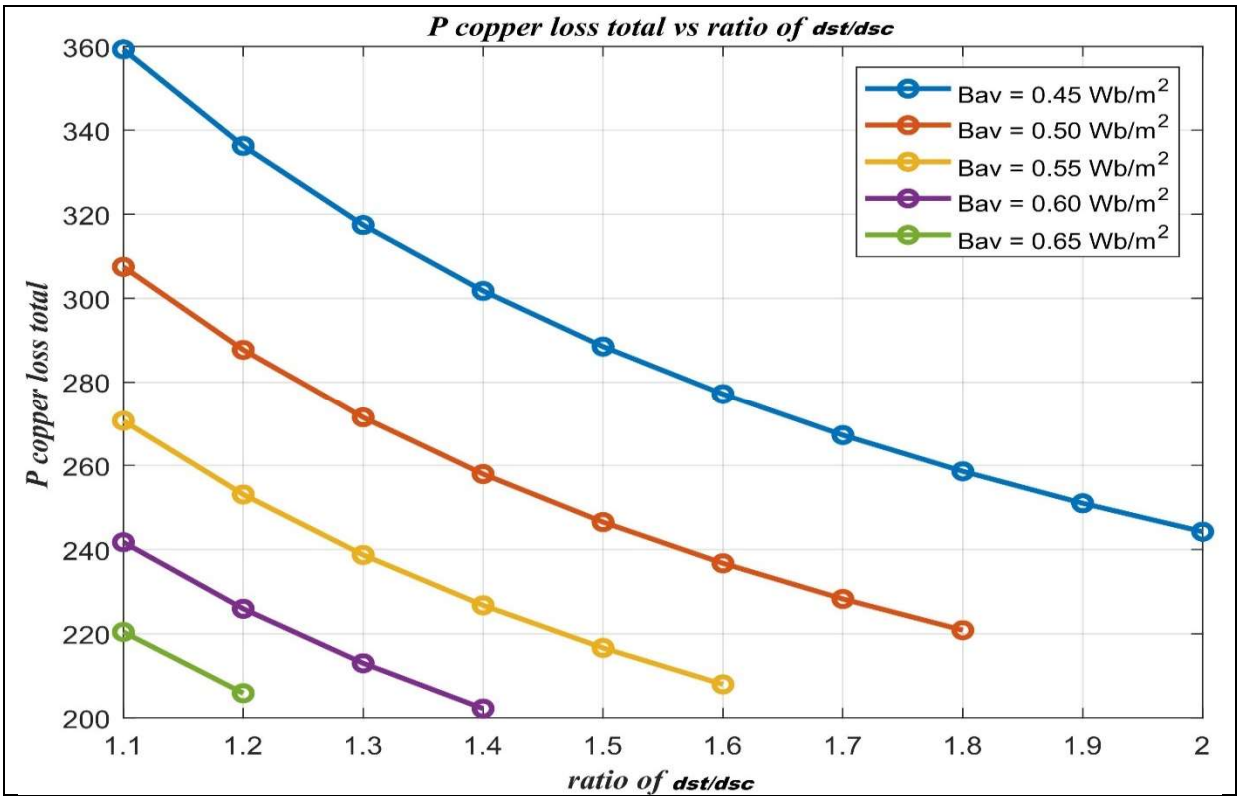
P copper loss total vs ratio of dst/dsc
P copper loss total
ratio of dst/dsc
Bav = 0.45 Wb/m2
Bav = 0.50 Wb/m2
Bav = 0.55 Wb/m2
Bav = 0.60 Wb/m2
Bav = 0.65 Wb/m2
360
340
320
300
280
260
240
220
200
1.1
1.2
1.3
1.4
1.5
1.6
1.7
1.8
1.9
2

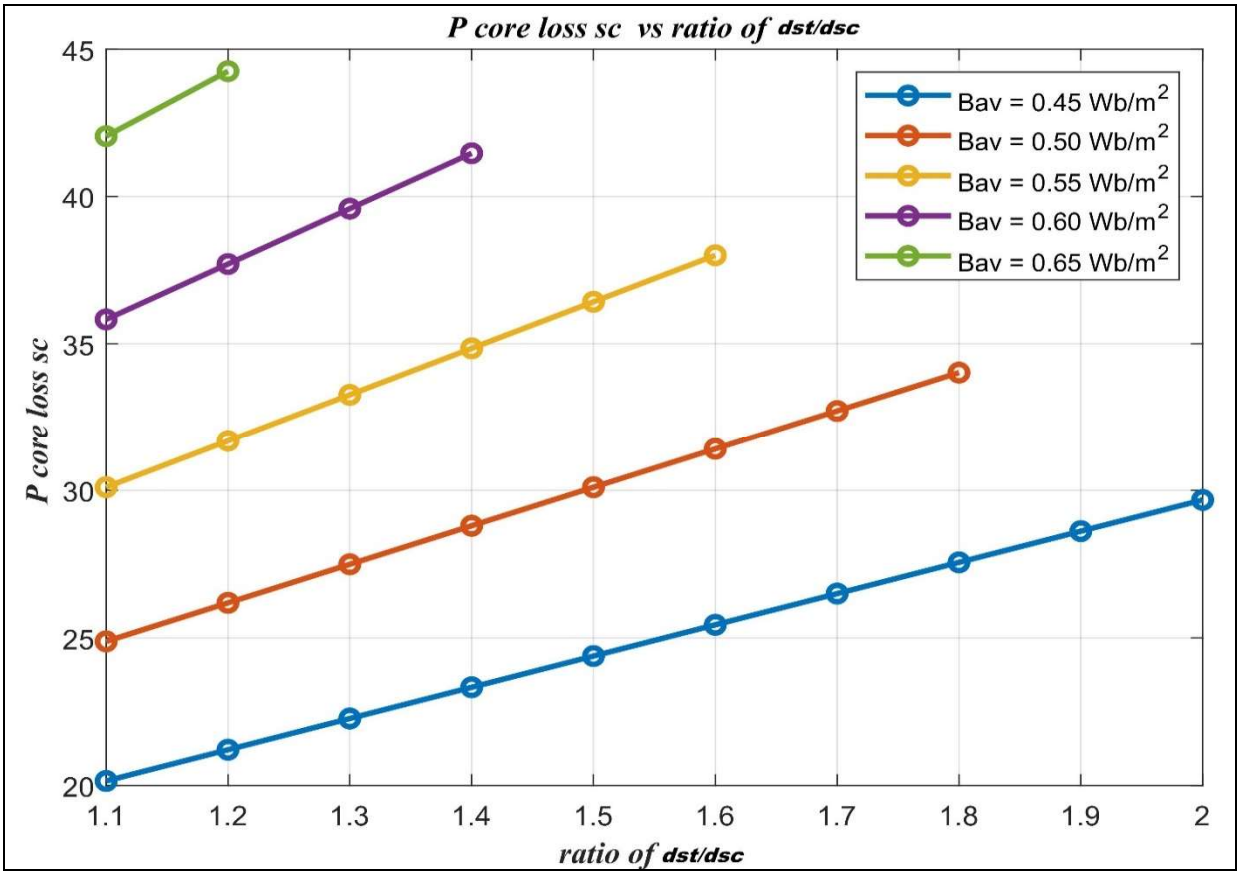
P core loss sc vs ratio of dst/dsc
P core loss sc
ratio of dst/dsc
Bav = 0.45 Wb/m2
Bav = 0.50 Wb/m2
Bav = 0.55 Wb/m2
Bav = 0.60 Wb/m2
Bav = 0.65 Wb/m2
45
40
35
30
25
20
1.1
1.2
1.3
1.4
1.5
1.6
1.7
1.8
1.9
2

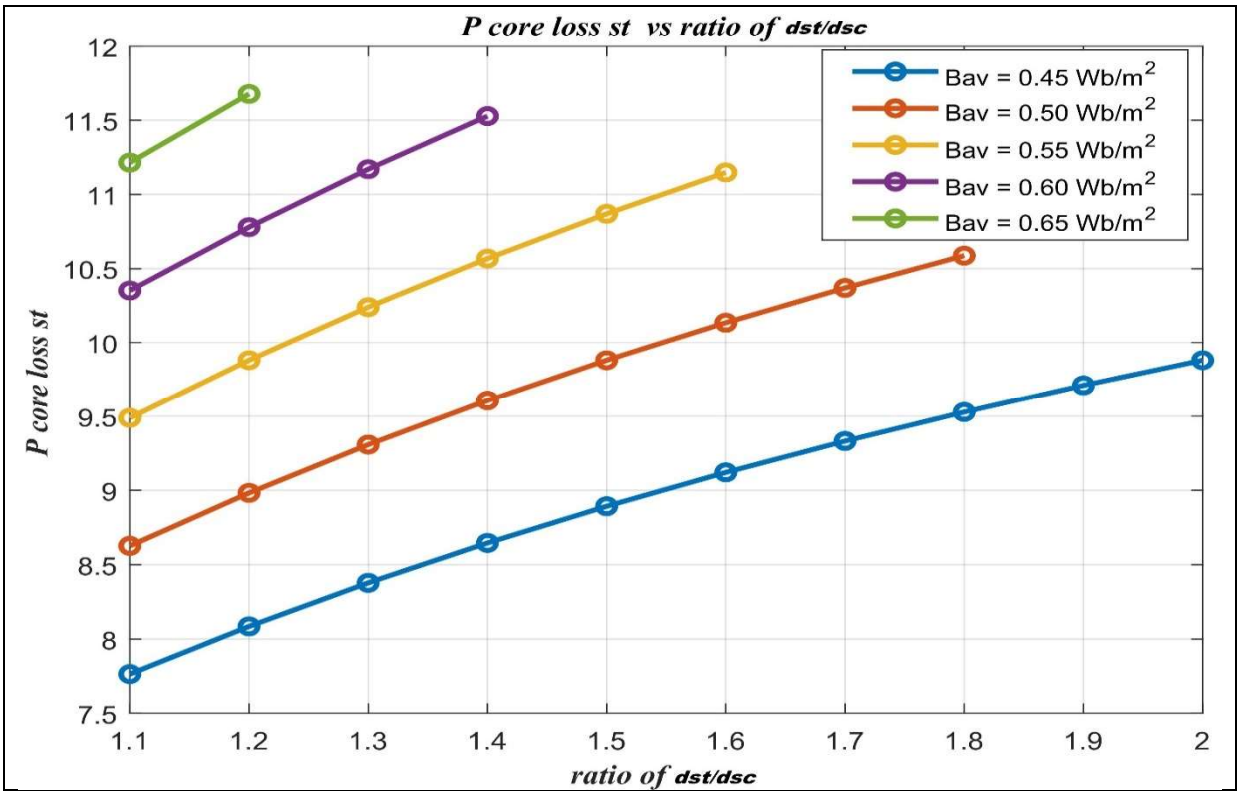
P core loss st vs ratio of dst/dsc
P core loss st
ratio of dst/dsc
Bav = 0.45 Wb/m2
Bav = 0.50 Wb/m2
Bav = 0.55 Wb/m2
Bav = 0.60 Wb/m2
Bav = 0.65 Wb/m2
12
11.5
11
10.5
10
9.5
9
8.5
8
7.5
1.1
1.2
1.3
1.4
1.5
1.6
1.7
1.8
1.9
2

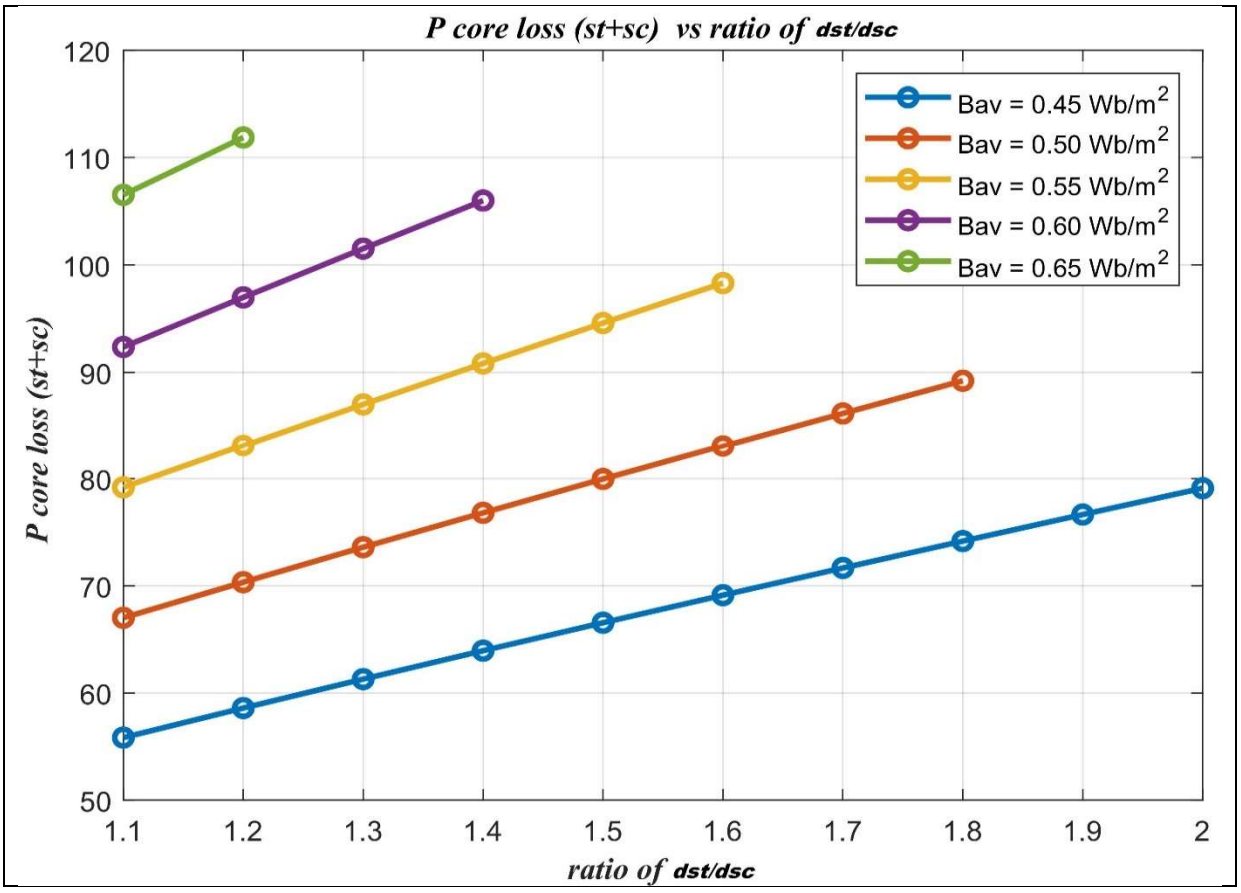
P core loss (st+sc) vs ratio of dst/dsc
P core loss (st+sc)
ratio of dst/dsc
Bav = 0.45 Wb/m2
Bav = 0.50 Wb/m2
Bav = 0.55 Wb/m2
Bav = 0.60 Wb/m2
Bav = 0.65 Wb/m2
120
110
100
90
80
70
60
50
1.1
1.2
1.3
1.4
1.5
1.6
1.7
1.8
1.9
2

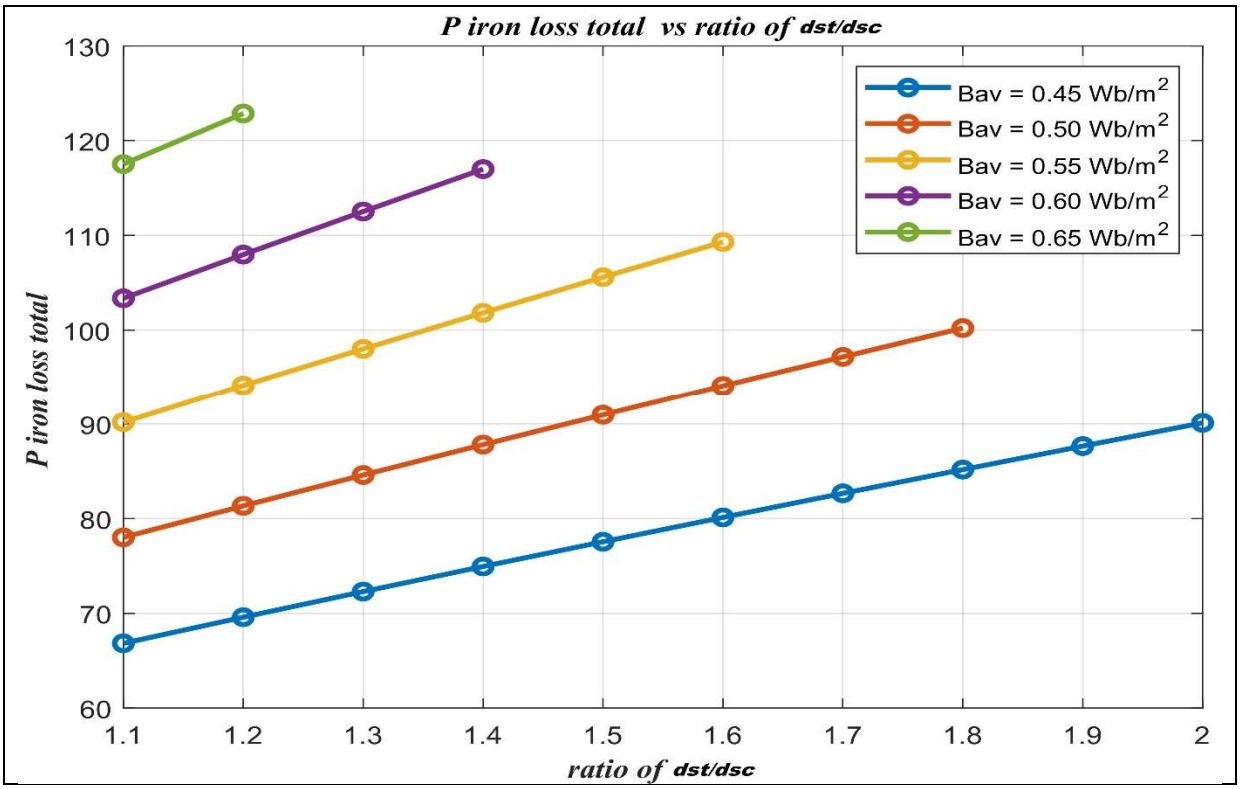
P iron loss total vs ratio of dst/dsc
P iron loss total
ratio of dst/dsc
Bav = 0.45 Wb/m2
Bav = 0.50 Wb/m2
Bav = 0.55 Wb/m2
Bav = 0.60 Wb/m2
Bav = 0.65 Wb/m2
130
120
110
100
90
80
70
60
1.1
1.2
1.3
1.4
1.5
1.6
1.7
1.8
1.9
2

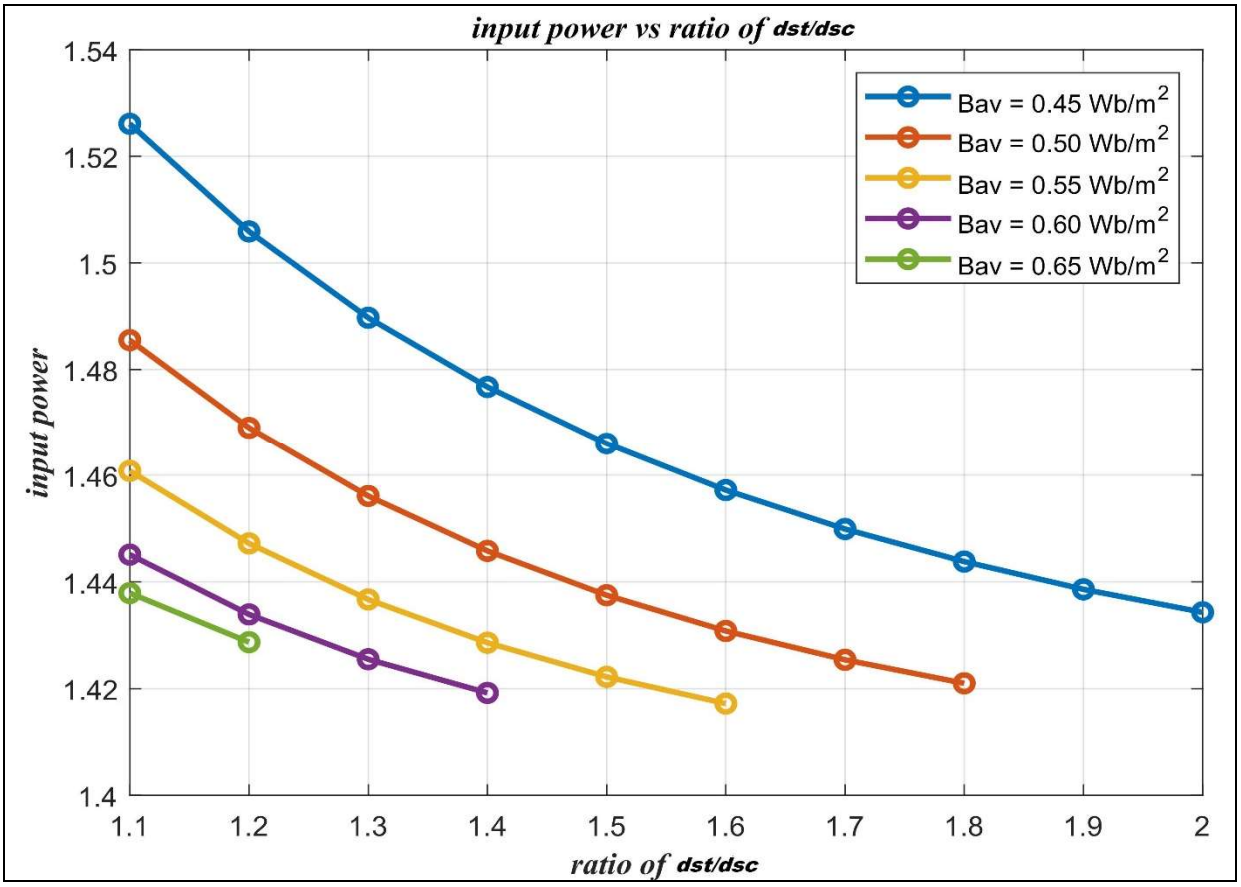
input power vs ratio of dst/dsc
input power
ratio of dst/dsc
Bav = 0.45 Wb/m2
Bav = 0.50 Wb/m2
Bav = 0.55 Wb/m2
Bav = 0.60 Wb/m2
Bav = 0.65 Wb/m2
1.54
1.52
1.5
1.48
1.46
1.44
1.42
1.4
1.1
1.2
1.3
1.4
1.5
1.6
1.7
1.8
1.9
2

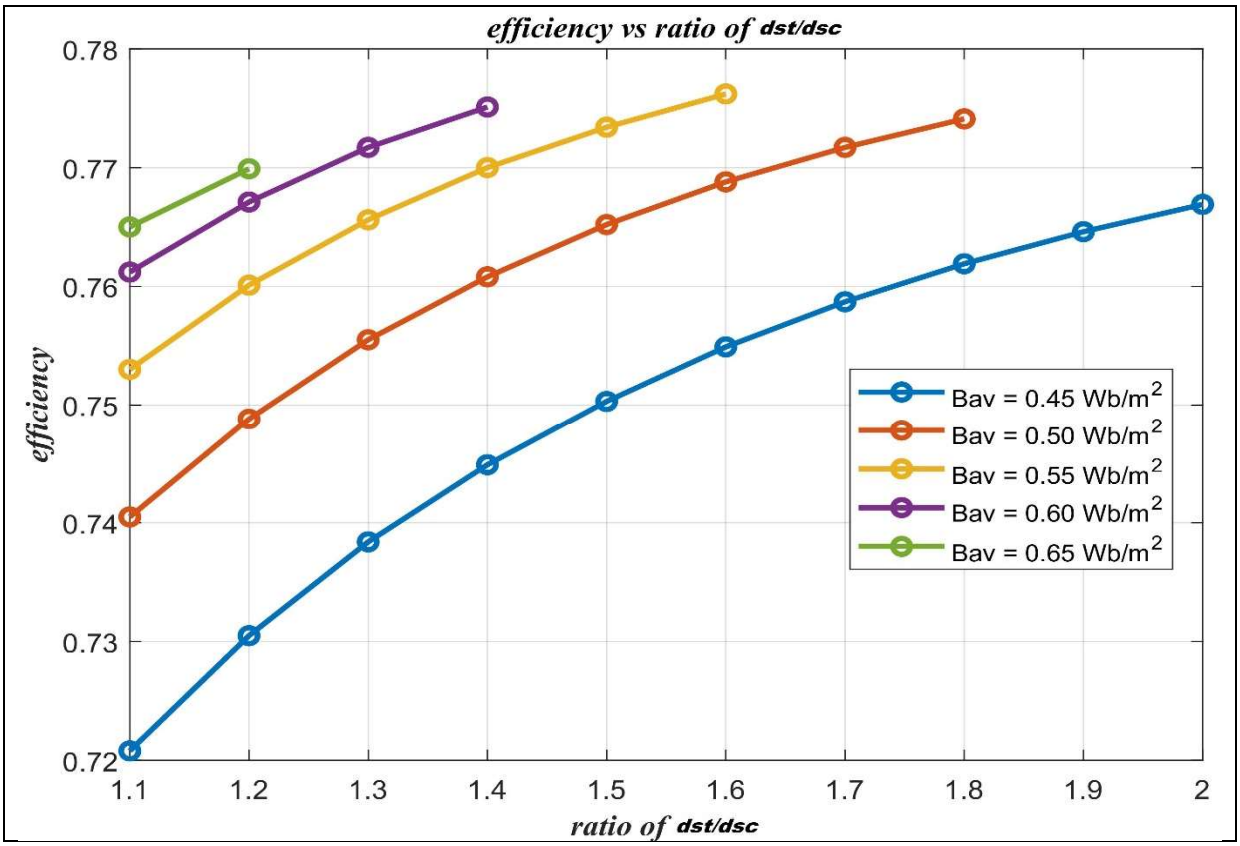

4.3 PLOTTING FOR MAXIMUM EFFICIENCY

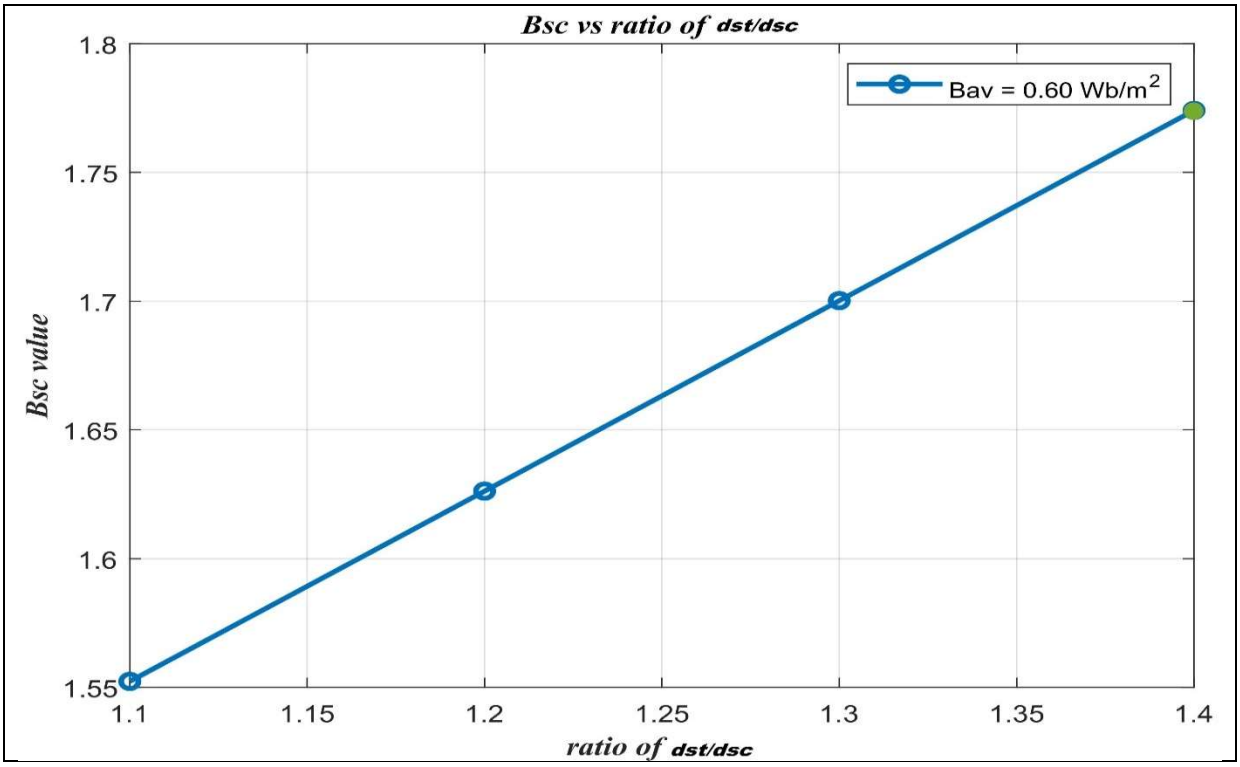

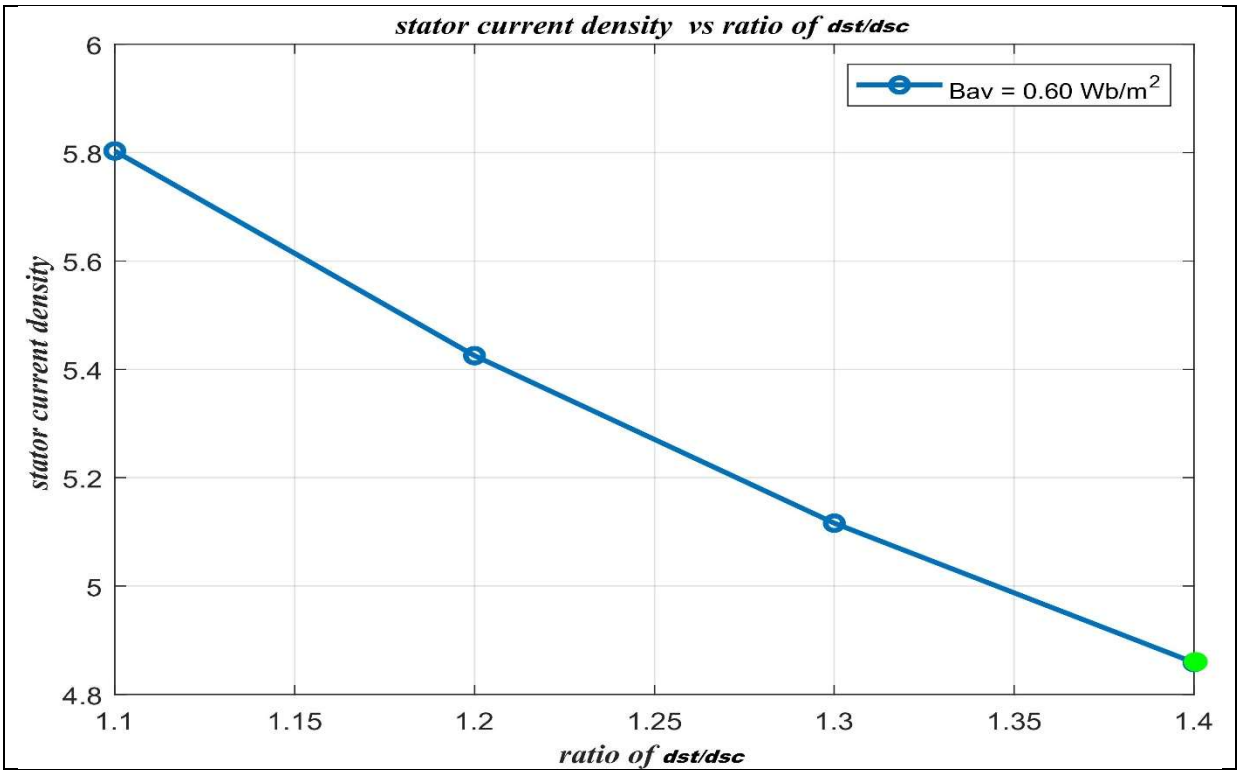
stator current density vs ratio of dst/dsc
Bav = 0.60 Wb/m2
stator current density
ratio of dst/dsc
6
5.8
5.6
5.4
5.2
5
4.8
1.1
1.15
1.2
1.25
1.3
1.35
1.4

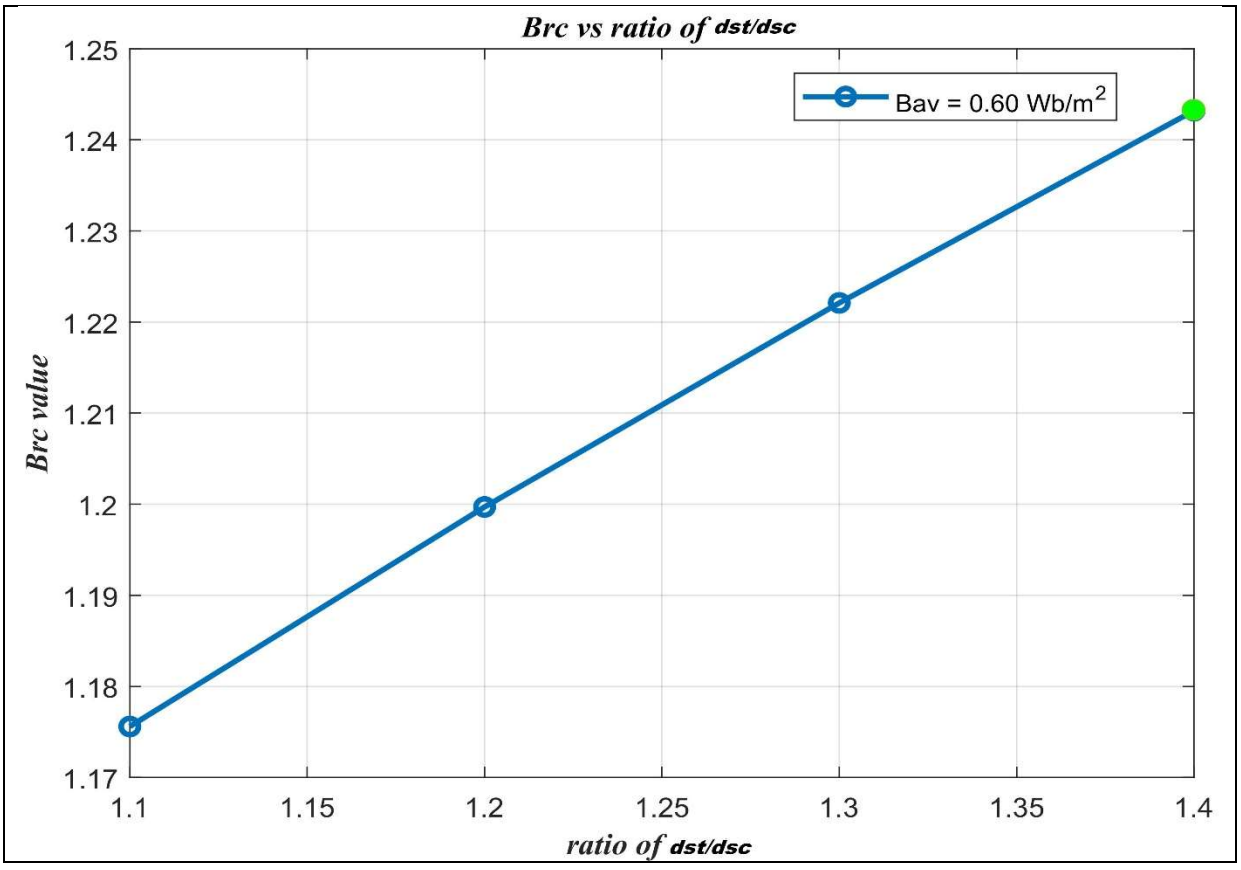
Brc vs ratio of dst/dsc
Bav = 0.60 Wb/m2
Brc value
ratio of dst/dsc
1.25
1.24
1.23
1.22
1.21
1.2
1.19
1.18
1.17
1.1
1.15
1.2
1.25
1.3
1.35
1.4

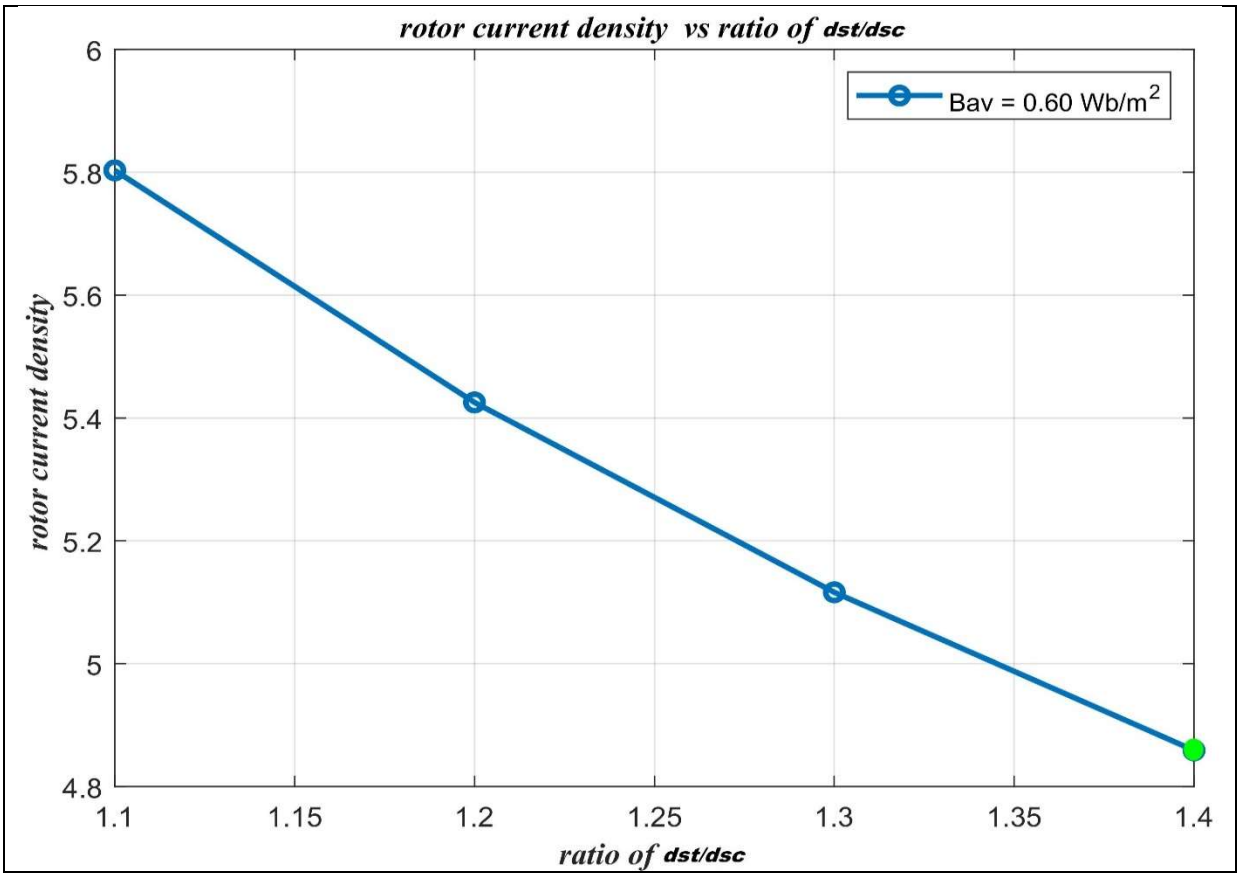
rotor current density vs ratio of dst/dsc
Bav = 0.60 Wb/m2
rotor current density
ratio of dst/dsc
6
5.8
5.6
5.4
5.2
5
4.8
1.1
1.15
1.2
1.25
1.3
1.35
1.4

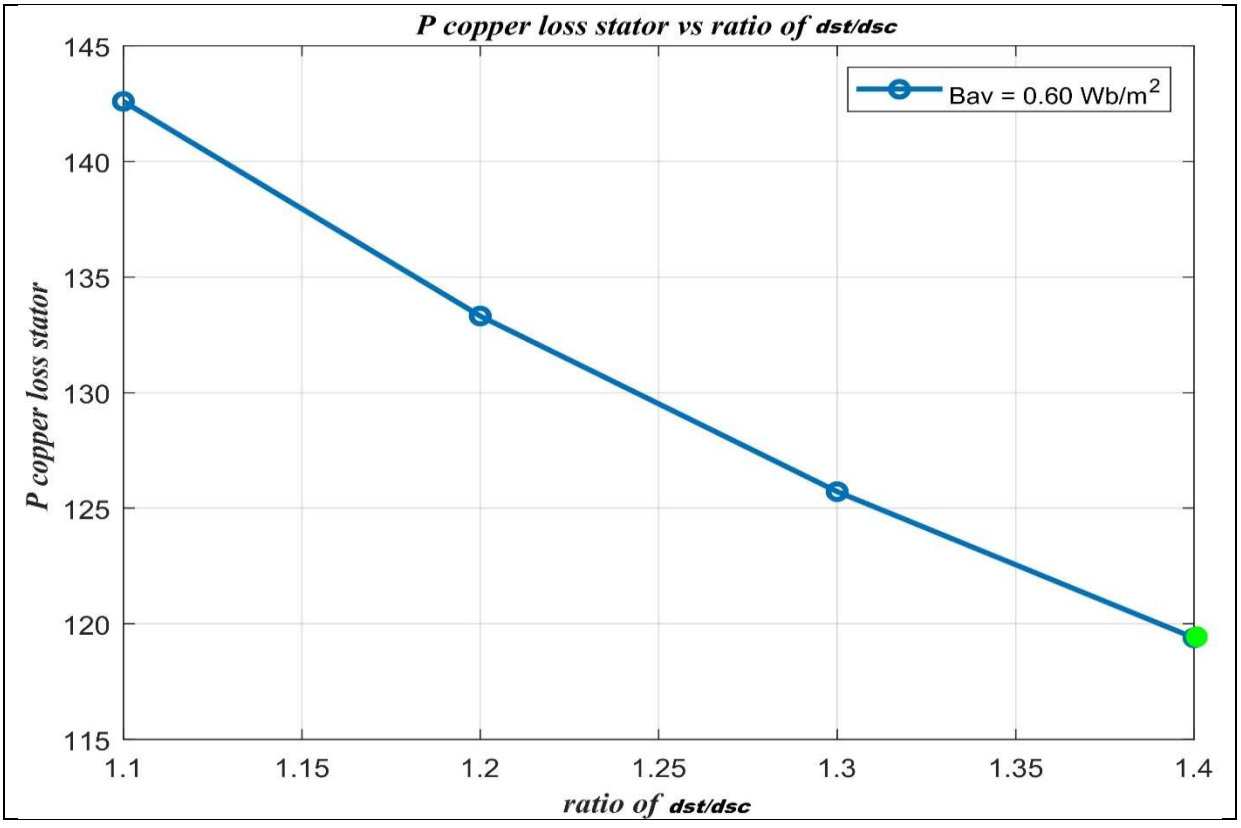
P copper loss stator vs ratio of dst/dsc
Bav = 0.60 Wb/m2
P copper loss stator
ratio of dst/dsc
145
140
135
130
125
120
115
1.1
1.15
1.2
1.25
1.3
1.35
1.4

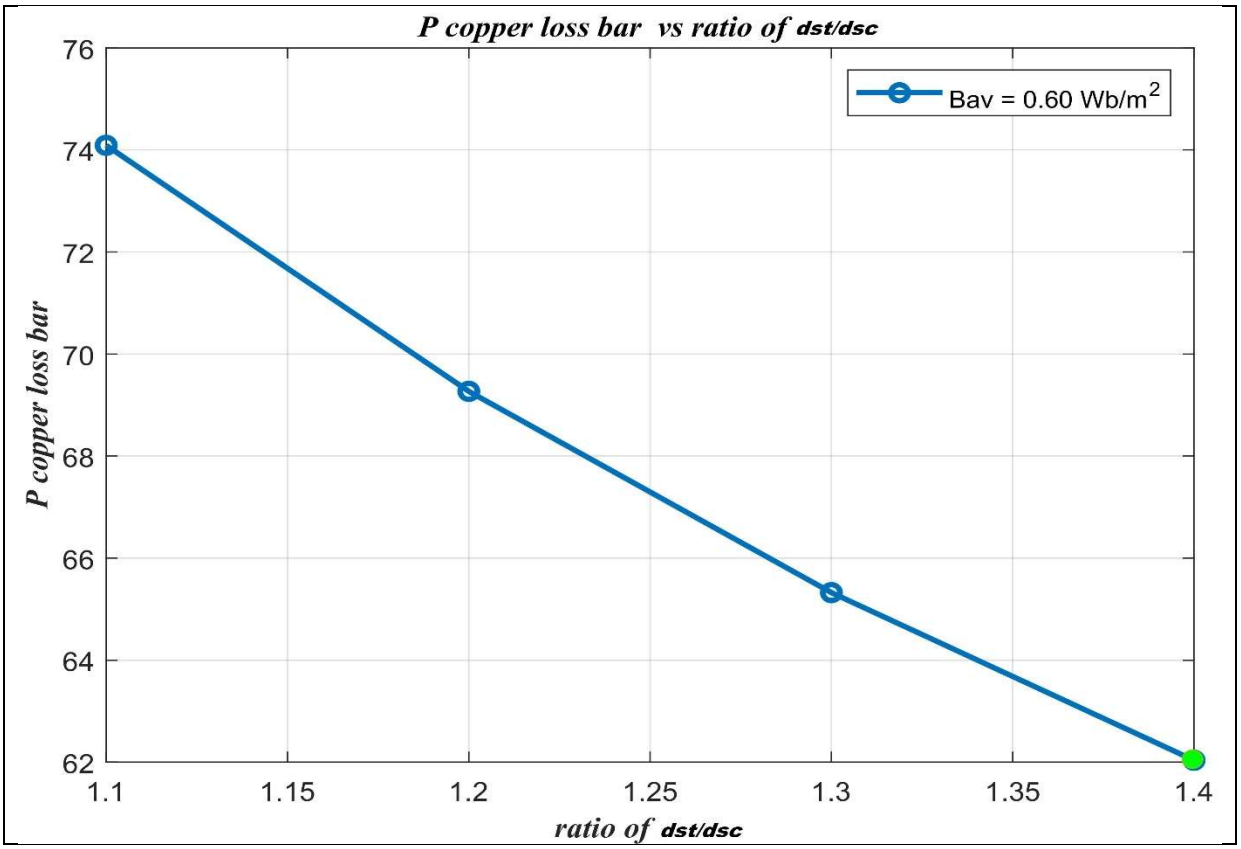
P copper loss bar vs ratio of dst/dsc
Bav = 0.60 Wb/m2
P copper loss bar
ratio of dst/dsc
76
74
72
70
68
66
64
62
1.1
1.15
1.2
1.25
1.3
1.35
1.4

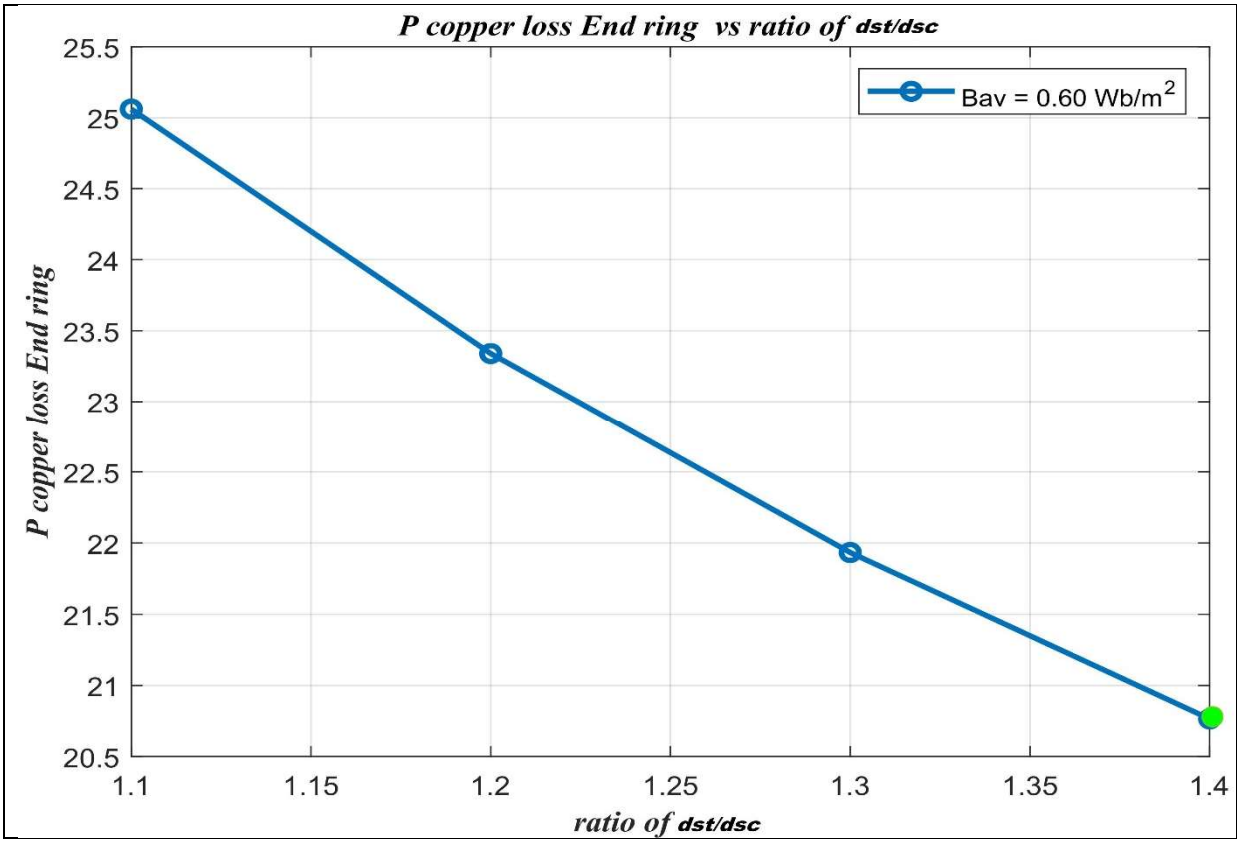
P copper loss End ring vs ratio of dst/dsc
Bav = 0.60 Wb/m2
P copper loss End ring
ratio of dst/dsc
25.5
25
24.5
24
23.5
23
22.5
22
21.5
21
20.5
1.1
1.15
1.2
1.25
1.3
1.35
1.4

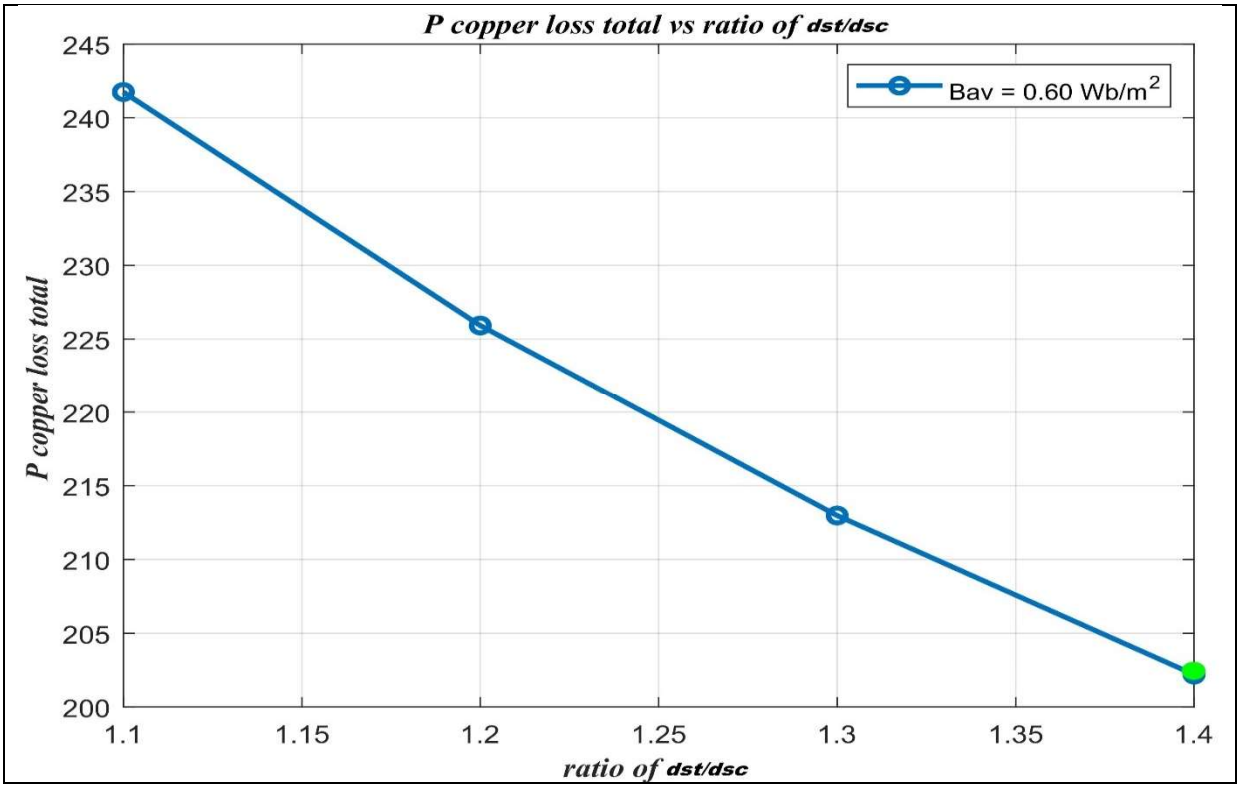
P copper loss total vs ratio of dst/dsc
Bav = 0.60 Wb/m2
P copper loss total
245
240
235
230
225
220
215
210
205
200
1.1
1.15
1.2
1.25
1.3
1.35
1.4
ratio of dst/dsc

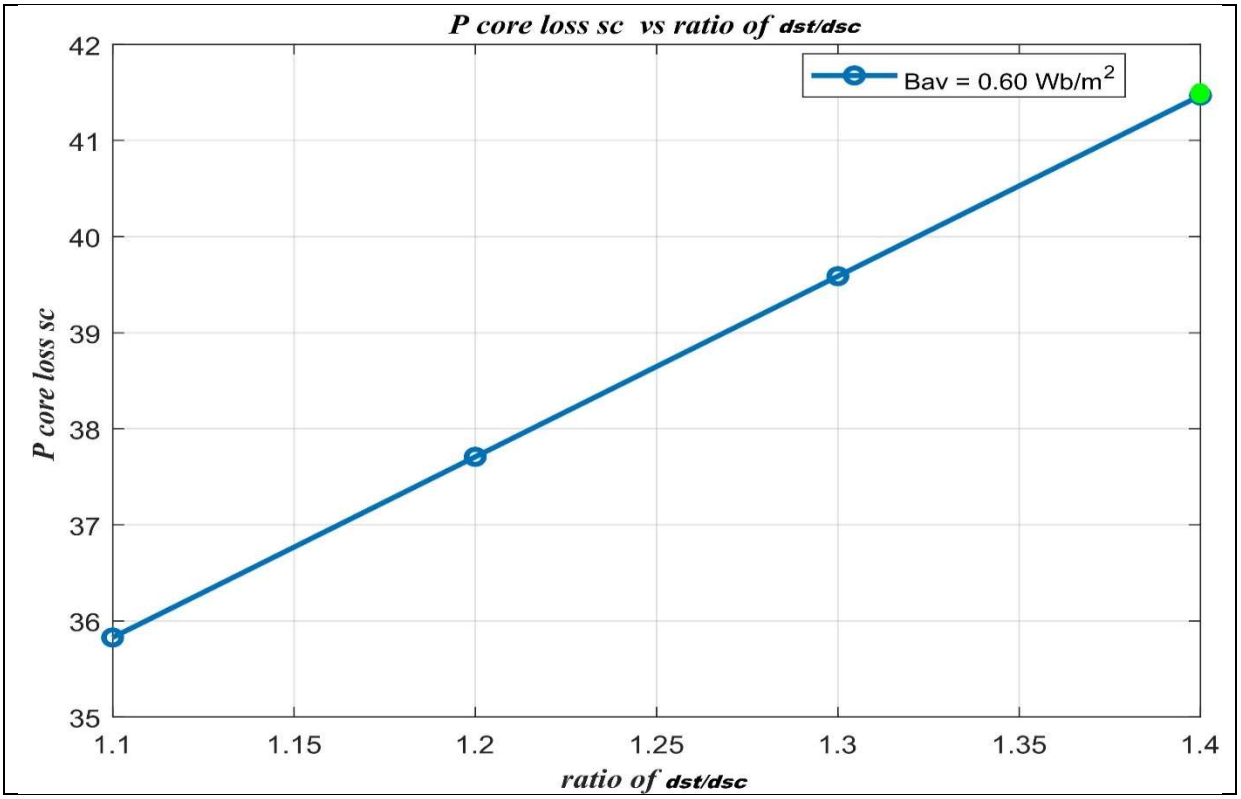
P core loss sc vs ratio of dst/dsc
Bav = 0.60 Wb/m2
P core loss sc
42
41
40
39
38
37
36
35
1.1
1.15
1.2
1.25
1.3
1.35
1.4
ratio of dst/dsc

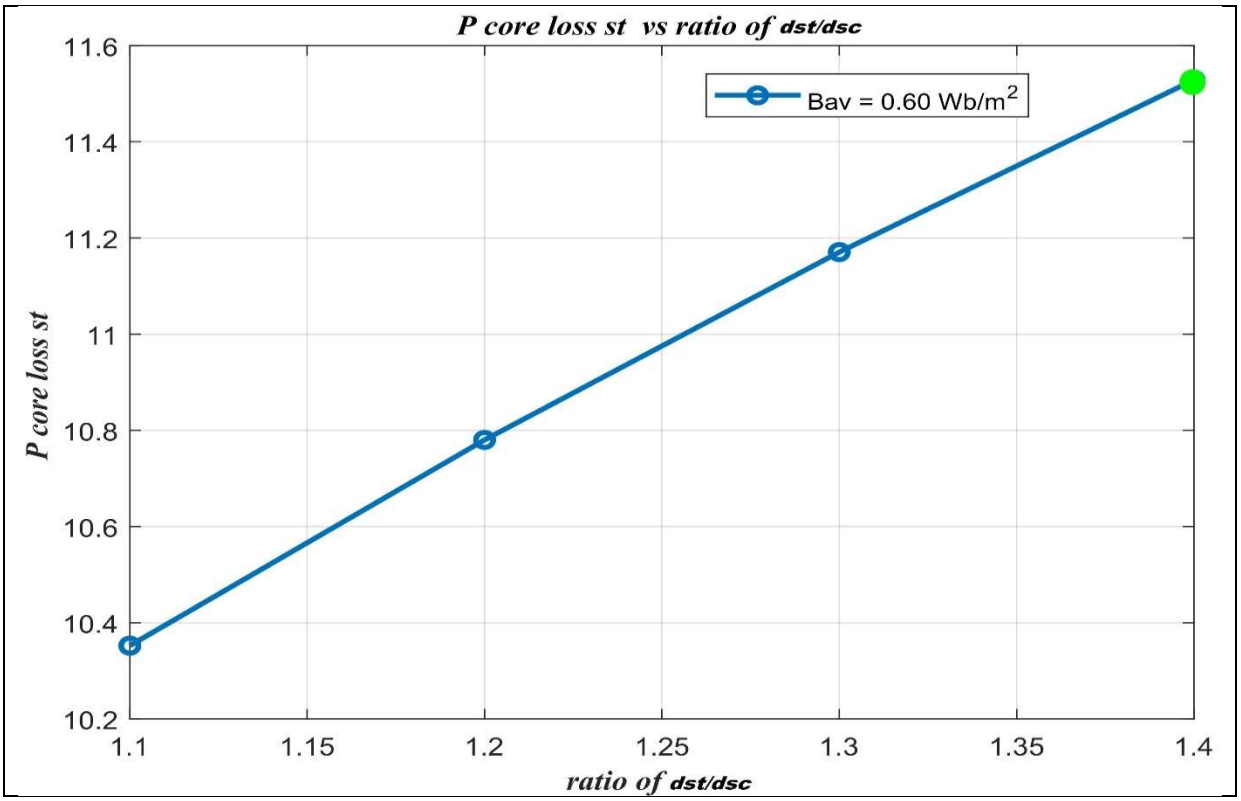
P core loss st vs ratio of dst/dsc
Bav = 0.60 Wb/m2
P core loss st
ratio of dst/dsc
11.6
11.4
11.2
11
10.8
10.6
10.4
10.2
1.1
1.15
1.2
1.25
1.3
1.35
1.4

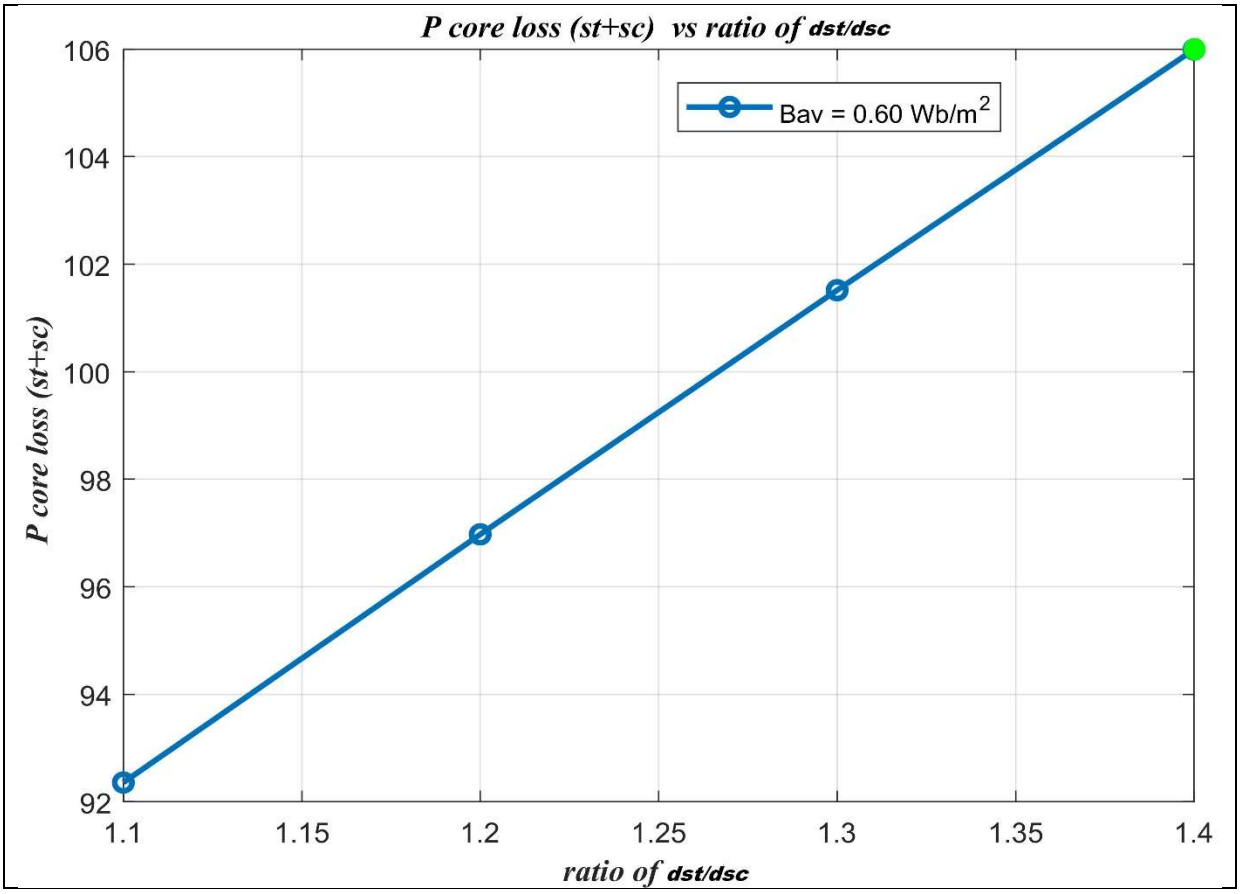
P core loss (st+sc) vs ratio of dst/dsc
Bav = 0.60 Wb/m2
P core loss (st+sc)
ratio of dst/dsc
106
104
102
100
98
96
94
92
1.1
1.15
1.2
1.25
1.3
1.35
1.4

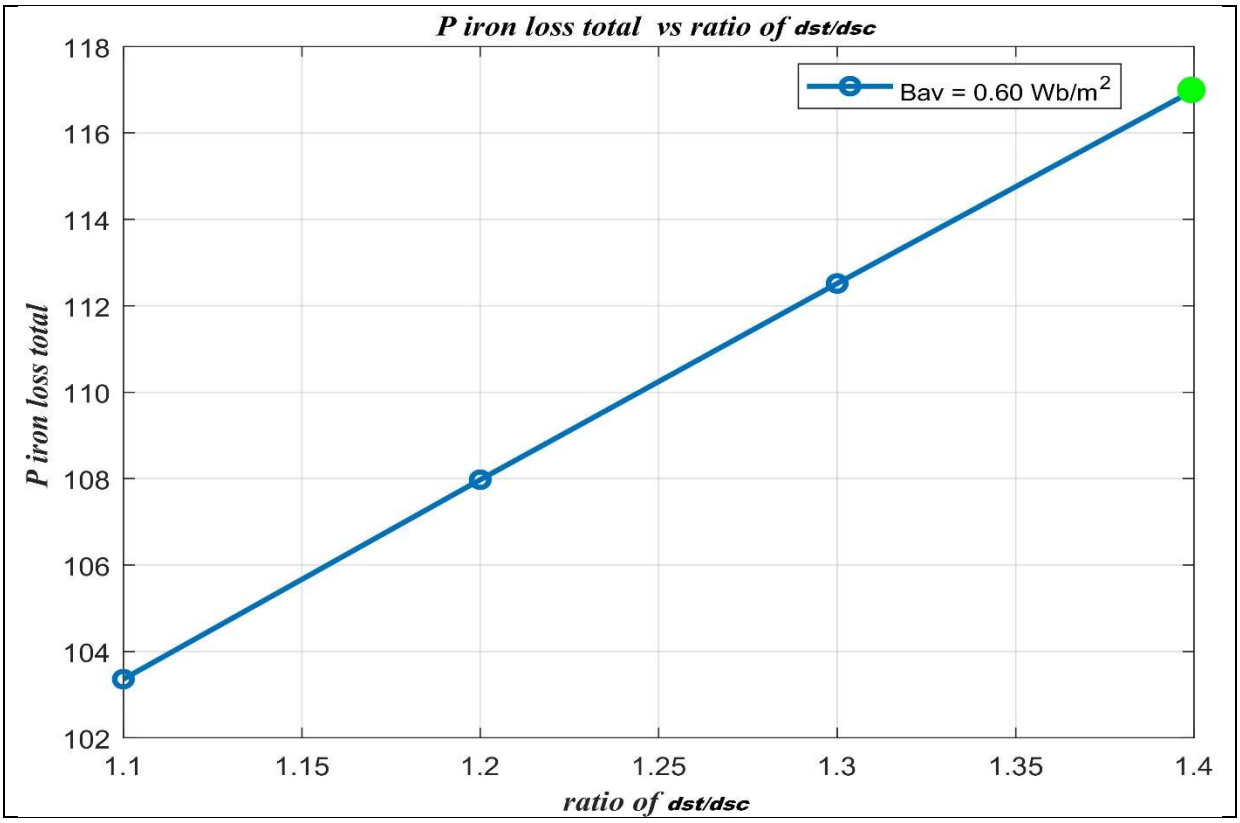
P iron loss total vs ratio of dst/dsc
Bav = 0.60 Wb/m2
P iron loss total
ratio of dst/dsc
118
116
114
112
110
108
106
104
102
1.1
1.15
1.2
1.25
1.3
1.35
1.4

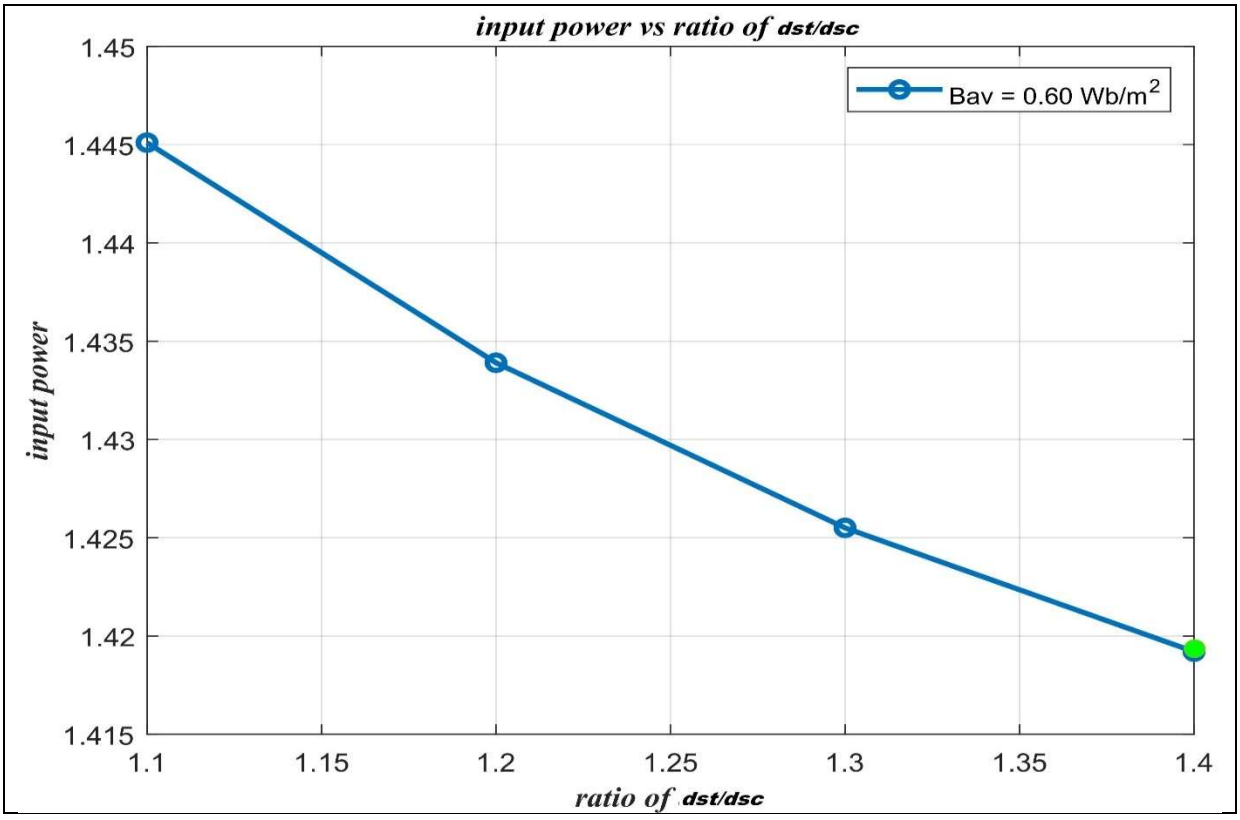
input power vs ratio of dst/dsc
Bav = 0.60 Wb/m2
input power
ratio of dst/dsc
1.45
1.445
1.44
1.435
1.43
1.425
1.42
1.415
1.1
1.15
1.2
1.25
1.3
1.35
1.4

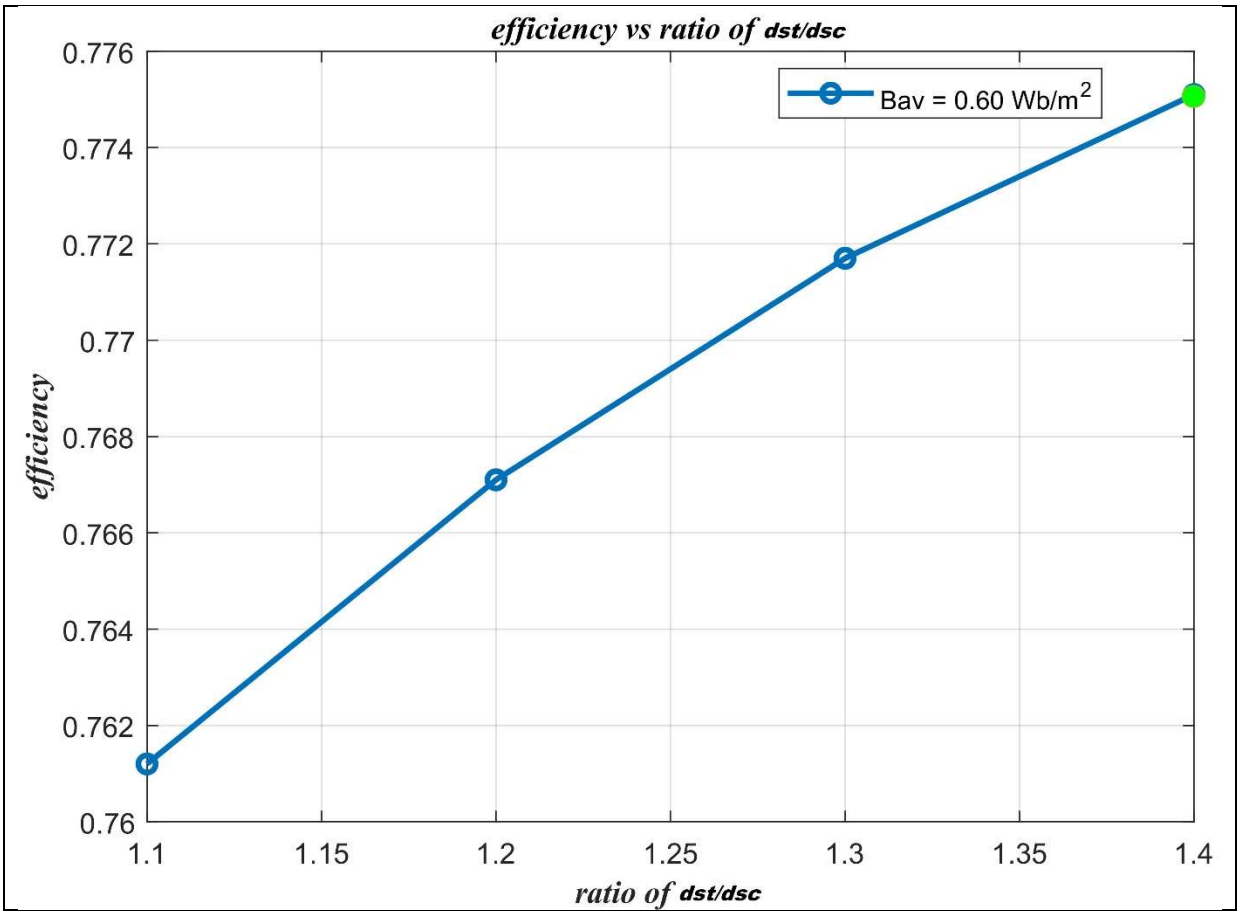

4.4 OBSERVATION

It is clear from the above figures and Table 3.2 that for a value of $\mathbf{B_{av}}$ if we change the $\mathbf{d_{st}/d_{sc}}$ ratio, the available space for slot increases and the depth of core decreases for a fixed frame size. Thus, the stator current density decreases and stator core flux density increases, resulting in increases in core loss and decrease in stator copper loss. The total loss of the machine changes affecting the efficiency.

Assuming that the machine has been designed to obtain maximum output from the frame size, the temperature rise of the motor was determined by using thermal model described in **Chapter 2** for the design with $\mathbf{B_{av}}$= 0.55 and $\mathbf{d_{st}/d_{sc}}$ = 1.6, for which the calculated efficiency is maximum. The curves obtained are plotted below.

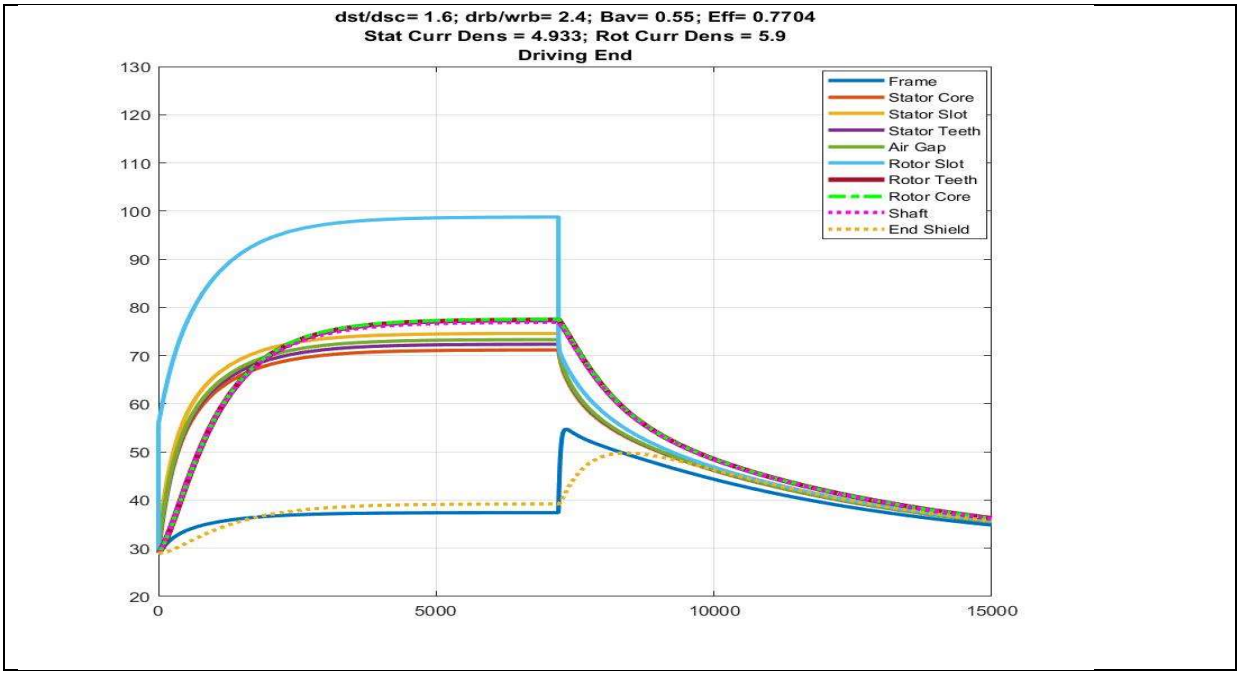

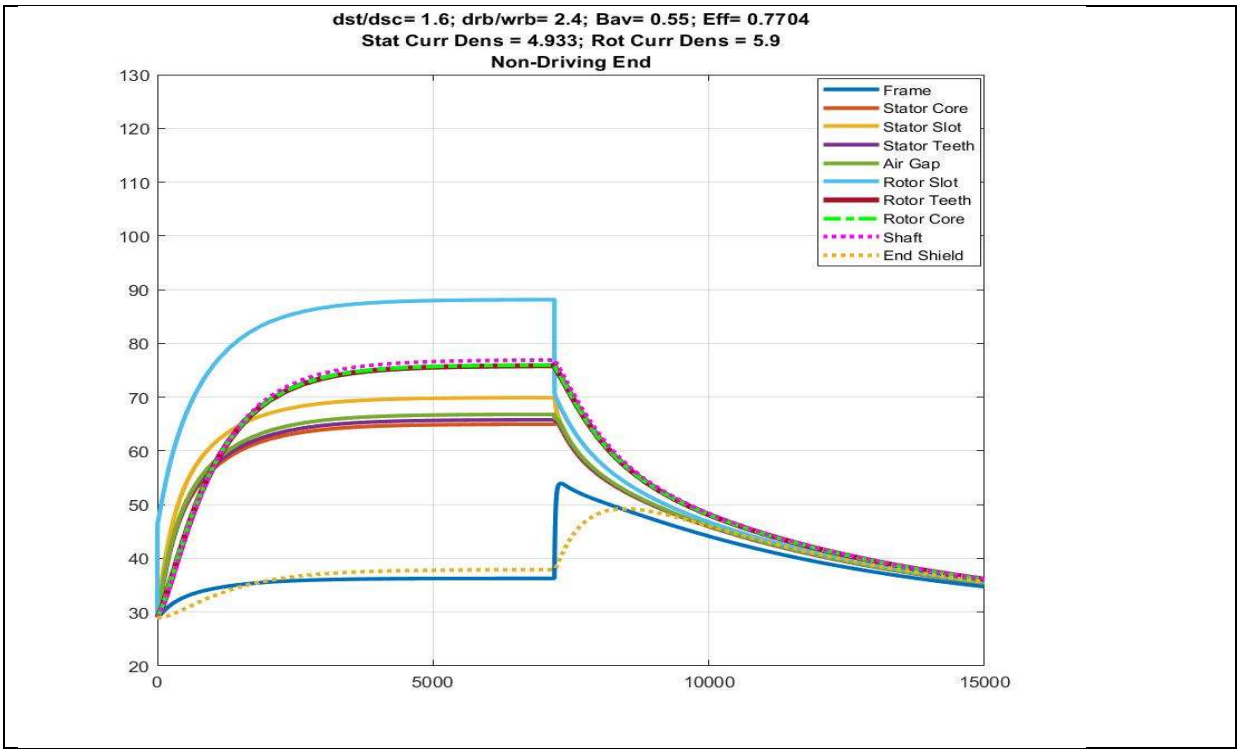

The natures of the temperature rise curves are similar to the nature of temperature rise curves of an induction motor. The maximum temperature of different parts of motor are well within limit. The surface temperature was measured and the measured value is in agreement with the value obtained from the curves. However, we did not have sufficient time to perform experiments and were not able to verify the internal temperature.

4.5 Conclusion And Scope of Future Work

Development of a formulation package for determination of the steady state thermal model of 3- phase Induction Motor has been described in this study. It provides knowledge of the possible Temperature distribution of stator and rotor core, stator surface, stator frame, stator and rotor teeth, shaft, end shield, etc. It's very useful to estimate the temperature of the motor at the design stage.

Due to short of time period and Covid scenario, the machine data was taken only on the physical stage. So, for future, if the machine run on different loads e.g. half load, full load and no load. The data is more closely to found accurate temperature rise internally.

Optimization Techniques and programmes can also be run by the different data. Which are calculated on Table 3.2-A, B, C, D and 3.2-E.

References

[1] R.L.Kotnik, "An equivalent thermal circuit for non-ventilated induction motors", AIEEE Transactions, February, 1955, p 1600

[2] P.R. Mellor and D. R. Tumner, "Lumped parameter thermal model for electrical machines of TEFC design", IEEE Proceedings B, vol.138, no.5, September, 1991, pp. 205.

[3] Dr. S. Kar Chowdhury, Dr. S. Chowdhury, Dr. S. P. Chowdhury, Dr. S.K. Pal, "Performance Prediction of Single-Phase Induction Motors Using Field and Thermal Models", IEEE PEDS 2003.

[4] NR Namburi and T.H. Barton, "THERMAL MODELLING OF AN INDUCTION MOTOR", IEEE Transactions on Power Apparatus Systems, Vol. PAS -102, No. 8, August 1983

[5] Stanley E. Zocholl et al, Dr. Edmund 0. Schweitzer III and Antenor Aliaga-Zegarra, "THERMAL PROTECTION OF INDUCTION MOTORS ENHANCED BY INTERACTIVE ELECTRICAL AND THERMAL MODELS", IEEE Trans. Power Apparatus Systems, WI. PXS-103, no. 7, July 1984.

[6] A. L. Shenkman, and M. Chertkov, "Experimental Methods for Synthesis of generalized Thermal Circuit of Polyphase induction Motors", IEEE Trans. on EC, vol. 15, no. 3, Sept. 2000, pp. 264-268.

[7] S.K. Chowdhury, P.K. Baski, 'A Simple Lumped Parameter Thermal Model for Electrical Machines of TEFC Design' IEEE PEDES-2010, pp-1-7, 2010.

[8] 0. L. Okoro, "Dynamic and thermal modelling of induction machine with non-linear Effects," Ph.D. dissertation, Dept. of Electrical Engineering., Univ. Kassel, Kassel, Gemmy, 2002.

[9] Ujjwal Sinha, “A Design and Optimization Assistant for Induction Motors and Generators” Ph.D. dissertation, Dept. of Electrical Engineering., Department of Mechanical Engineering, Massachusetts Institute of Technology, Feb 18, 1998.

[10] ‘Eugene O AGBACHI, James G AMBAFI, Omokhafe J TOLA, Henry O OHIZE’ “Design and Analysis of Three Phase Induction Motor using Computer Program”, World J of Engineering and Pure and Applied Sci. 2012; 2(4):118 ISSN 2249-0582.,